THE ROLE OF SEPT9_V1 IN BREAST CANCER: INSIGHTS INTO THE DEVELOPMENT OF PRO-ONCOGENIC PHENOTYPES AND GENOMIC INSTABILITY

by

Esther A. Peterson

A dissertation submitted in partial fulfillment
of the requirements for the degree of
Doctor of Philosophy
(Human Genetics)
in The University of Michigan
2009

Doctoral Committee:

Professor Elizabeth M. Petty, Chair
Professor David T. Burke
Professor Miriam H. Meisler
Associate Professor Theodora S. Ross
Assistant Professor JoAnn Sekiguchi

DEDICATION

Dedicated to:
My mom and inspiration, Lady Esther Peguero

ACKNOWLEDGEMENTS

First, I am extremely appreciative to my mentor Dr. Elizabeth M. Petty for always believing in my potential as a graduate student and research scientist. Through her professional guidance and support she gave me the courage and inspiration to explore new and exciting ideas to move my research project forward. She taught me to never give up and always hope for the best, which in research is extremely valuable advice.

I would like to thank my thesis committee for providing interesting and intellectual scientific discussions. They always helped me to stay focused and provided a great diversity of exciting ideas and insightful direction, as well as the freedom to explore my research interests without losing my specific research goals.

Thank you to past and present members of the Petty lab (Lisa, Lezlie, Maria, Linda, Roma, Amy, Janice, Ming, Lesley, Christina, Jenny, Laura, Serina, Hande, Natasha, Jake, Olga, Tess, and Joanie) for all their support, help, intellectual discussions and mostly for making the lab a wonderful place to be. Special thanks to Jennifer Keller for her friendship, especially for all her support when I was writing my dissertation and for being there for me in the most stressful moments. I especially want to thank Maria E. González for teaching me so much in lab and about septins when I was new in the field. I also thank for her unconditional friendship and for always rooting for me.

I am deeply grateful to Lisa M. Privette-Vinnedge for being my role model as a graduate student, and also for her friendship. I truly appreciate all her support and the long hours she spent proofreading all my work. She made the lab a fun and intellectual place to be. Her company made the long hours less stressful. Mostly, I truly appreciate all the things that she taught me as a scientist.

I would like to give special thanks to my first friends in Ann Arbor, Devin Horton and Fawn Cothran. I will always remember the first time we talked and how we became friends instantly. Many thanks to Devin for her support and friendship that thankfully survived her move to Boston. I am extremely blessed with the unbreakable friendship of Eneida Villanueva, Gisselle Vélez, and Marta González, the Puerto Ricans. They keep me sane and make my life in Ann Arbor fun, exciting and beautiful. I am truly thankful for all their unconditional support and for being loyal not only in the good times but also in the bad ones.

I would also like to thank my lifetime friends, Rosie Albarrán, Rosa Hernández, Lorena Maldonado, Oscar Rivera and Jose Javier Flores for always being there for me, for their constant encouragement and unconditional love. They are the constant reminders that a real friendship can survive anything, even long distances.

Finally, words can't express how blessed I am to have my family. I will always be grateful for their constant encouragement, and also for understanding the sacrifice of being so far away from them. Special thanks to my dad, Anibal Peterson, for his constant and unconditional support, especially when I decided to move thousands of miles away to pursue a

career in research. I would like to thank my best friend, my sister Anibelle Peterson, for all the daily phone calls, her love, understanding of my career choices, and especially, for visiting me even though she doesn't like to travel this far. I would also like to thank my stepmother, Lourdes, for taking care of my dad and for giving me a beautiful extended family, which includes my four nephews and nieces. I will also like to thank the rest of my family in Puerto Rico and Dominican Republic for always waiting patiently for my visits and always loving me. They all know who they are and I thank them from the bottom of my heart for all their love and prayers. I would like to give special thanks to family Nazario-Montalvo, especially to my godmother Carmen Montalvo for her support, love and for being a second mom to me. Also, I would like to thank J.E.P for patiently waiting for me and loving me all these years. He taught me that love can survive anything.

Lastly, even though they are not physically with me, I would like to acknowledge my mother and my grandmother for being my inspiration to do great in life and for raising me as an independent and strong woman. They were always by my side every step of the way and when things got tough, thinking of them made everything worth it.

TABLE OF CONTENTS

LIST OF FIGURES

Figure

LIST OF TABLES

Table

ABSTRACT

THE ROLE OF SEPT9_V1 IN BREAST CANCER: INSIGHTS INTO THE DEVELOPMENT OF PRO-ONCOGENIC PHENOTYPES AND GENOMIC INSTABILITY

by

Esther A. Peterson

Chair: Elizabeth M. Petty

Breast cancer is a complex heterogeneous disease stemming from alterations in the function and/or expression of multiple oncogenes and tumor suppressor genes. *SEPT9*, a member of a family of genes encoding cytoskeletal GTPases important in cell division, encodes multiple SEPT9 splicing isoforms, SEPT9_v1-SEPT9_v7. *SEPT9* maps to a region of allelic imbalance in breast cancers and SEPT9 isoforms are differentially expressed in breast cancer. One isoform, SEPT9_v1, is over-expressed in more than 50% of breast cancer cell lines and primary breast cancer samples, suggesting an important role in tumorigenesis.

To examine the role of *SEPT9_v1* in mammary tumorigenesis, we established expression models in immortalized human mammary epithelial cells (IHMECs) and analyzed SEPT9_v1 expression in a human breast cancer tumor microarray with clinicopathological variables. High SEPT9_v1 was observed with more than 50% of hormone receptor positive tumors. Retroviral expression of *SEPT9_v1* in IHEMCs resulted in the development of pro-oncogenic phenotypes such as increased cell proliferation, decreased apoptosis, enhanced motility and invasiveness,

epithelial to mesenchymal transition and increased aneuploidy. Conversely, ablation of *SEPT9_v1* in breast cancer cells reduced proliferation and decreased motility and invasiveness.

To explore the impact of SEPT9_v1 on genomic stability, IHMEC models expressing SEPT9_v1 were analyzed for mitotic spindle checkpoint function, chromosome segregation and cytokinesis. SEPT9_v1 promoted both mitotic spindle defects and cytokinesis failure. SEPT9_v1 was found to interact with two major components of the mitotic spindle, α-tubulin and γ-tubulin, promoting α-tubulin filament formation defects and centrosome amplification. In addition, transient expression of *SEPT9_v1* was sufficient to drive chromosome instability independent of increased cell proliferation. Subsequently, we found that SEPT9_v1 could increase cellular proliferation rates in IHMEC lines by interacting with the c-jun-N-terminal kinase (JNK). High SEPT9_v1 expression stabilized JNK and increased the transcriptional activation of target genes important in cell cycle progression such as cyclin D1.

Finally, in an effort to identify novel interacting partners of SEPT9 isoforms, we identified the newest member of the human septin family, *SEPT14*, by yeast two-hybrid analysis. SEPT14 is localized to stress fibers, is not expressed in cancer cell lines and has expression limited to testicular tissues.

Together, these novel findings indicate that *SEPT9_v1* has oncogenic potential in mammary cells and may be a biomarker for disease aggressiveness. SEPT9_v1 impacts genomic instability by affecting mitotic spindle function, chromosome segregation and cytokinesis. Its interaction with the JNK signaling pathway is relevant to understanding its diverse roles in cell

cycle regulation. This study provides novel insights into the mechanisms by which *SEPT9_v1* expression may lead to the disruption of cellular processes important in breast cancer development.

CHAPTER I

DECIPHERING THE COMPLEX WORLD OF SEPTINS: THE HUMAN SEPT9 LOCUS IN SICKNESS AND IN HEALTH

Introduction

Forty years ago, septin's pioneer researchers may have never imagined that their discovery of four novel yeast genes would open the door to a biologically complex world of cytoskeletal GTPases relevant to human disease. Septins were first characterized in *Saccharomyces cerevisiae* as a group of cytoskeletal GTP-binding proteins essential for proper cell division. Genetic screening performed by Hartwell and colleagues for budding yeast mutants lead to the discovery of the first septin genes, *CDC3, CDC10, CDC11, CDC12*, in which temperature sensitive mutations caused defects in budding morphology and cell cycle arrest (1). These genes were further characterized in *Saccharomyces pombe* in which mutations led to cytokinesis defects during mitotis. Subsequently, septins have been found to be highly conserved in all eukaryotes except plants, with an extensive pattern of alternative splicing as a common feature. Recently, phylogenetic and evolutionary analysis for septins of metazoans demonstrated that all septin proteins could be clustered into four subgroups. It has been proposed that the emergence of these four subgroups occurred prior to the divergence of vertebrates and invertebrates and that septin expansion in number was due to duplication of pre-existing genes (2). Over the past 40 years, septin research has grown impressively, from four genes identified in budding yeast to 14 members identified in humans to date. The variety

of existing septin isoforms and the diversity of their biological functions in eukaryotic cells are both intriguing and exciting. Many questions remain related to their multiple normal functions in cells and their implicated roles in the development of human diseases. Contributions to septin biology over the last few years include the first crystal structure of septin oligomers, septin protein interactions, expression profiles, associations with well known signaling pathways and involvement in human disease. These observations have set the stage for more exciting experimental strategies to further understand the role of septins in health and disease.

Human septin family conserved domains

The four human septin subgroups are characterized by sequence homology and domain composition (Fig 1.1 and Fig 1.2). All human septins share a highly conserved central region that contains a polybasic domain and the GTP-binding domain. The N- and C-terminal regions vary in length and amino acid composition. They contain a proline-rich domain and an α-helical coiled-coil domain, respectively. The relevance of the difference in the N- and C- termini of septins and their isoforms is not completely understood, but these variations may play a role in their unique cellular localizations, protein interactions and biological functions (Fig 1.2). The specific functions of these domains remain to be fully elucidated, but recent studies have begun to reveal information about the possible roles of these domains, as described later in this chapter. Several members of the human septin family also contain the less well studied proline-rich domain near the N terminal region. Even though there are no specific studies dedicated to understand the functional role of the proline-rich domain of septins, one can suggest that this domain may be essential for protein-protein interactions, including interaction with proteins containing SH3 domains, based on other proteins containing these domain (3, 4). Preceding the GTPase domain, all mammalian septins contain a highly conserved polybasic domain

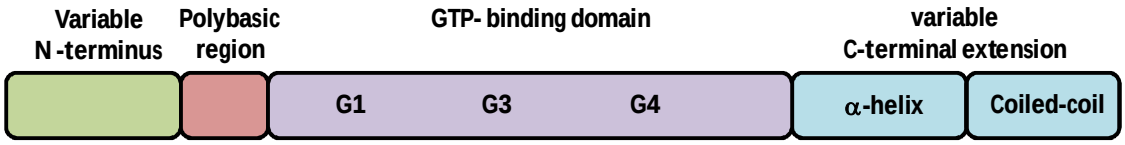

Fig 1.1: General structure of septins

N- and C- termini vary between Septin family members and their isoforms. Some septins contain a proline rich domain in their amino terminus that is involved in protein interaction. The C- terminus of some septins consists of a coiled-coil domain predicted to contain an α-helix. The polybasic domain is responsible for the association of septins with the plasma membrane. The central GTP-binding domain contains conserved motifs G1 (GxxxxGK[S/T]), G3 (DxxG) and G4 (xKxD) and is implicated in the formation of septin heteroligomers and protein interaction.

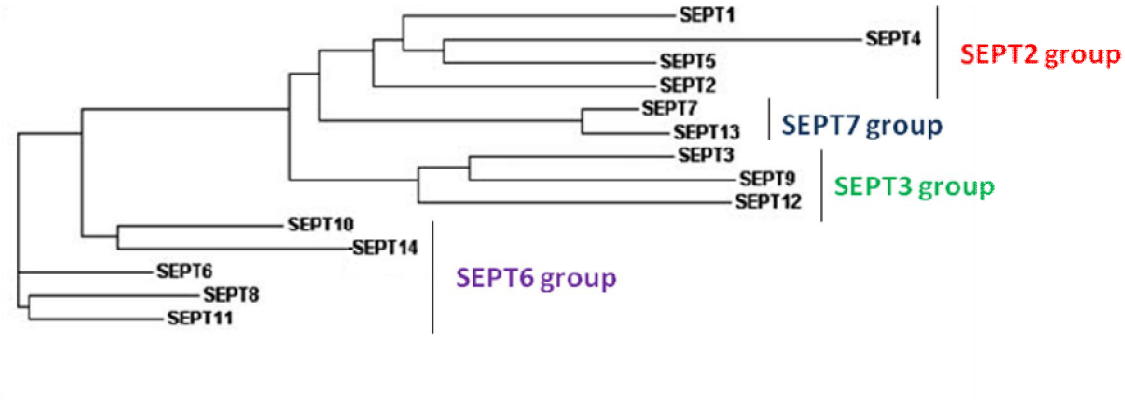

Fig 1.2: Phylogenetic tree of the human septin family

A dendrogram tree illustrates the phylogenetic relationship of the human septin family members as determined by Clustal W analysis (modified from Peterson E.A., *et al*. (2008) *Mamm Genome*).

responsible for the association of septins with cellular membranes. Studies of the polybasic domain of SEPT4 have shown that this domain binds to phosphoinositol phosphates (5). The polybasic domain might mediate the targeting of septins to membrane domains relevant for their role as diffusion barriers in yeast and mammalian cells. The Wittinghofer team studied the human septin complex composed of SEPT2, SEPT6 and SEPT7 and found that these three septins form a hexameric complex of two copies of each septin through a GTP/GDP bound interface, which is also crucial for the GTPase activity (6, 7). Future studies of these domains are necessary for comprehensive insight into septins intricate functional roles in mammalian cells.

Septins are widely subjected to functionally significant post-translational modifications. For example, sumoylation of yeast septins in G2/M-arrested cells is well described and the ubiquitin-protein ligase (E3) Siz1p is required for yeast septin sumoylation (8). Sumoylation of mammalian septins has not been reported. However, mammalian septins contain multiple phosphorylation sites and they can be phosphorylated by Ser/Thr kinases in post-mitotic neurons (9-11) and by Aurora-B kinase in mitotic cells (12). This suggests that sumoylation and/or phosphorylation of septins might modulate conformational changes that can alter their functional role.

Functional role of septins

Despite the mechanistic differences between budding yeast and dividing animal cells (13), several orthologs of yeast septins were identified in *Caenorhabditis elegans* (unc-59 and unc-61), *Drosophila melanogaster* (pnut) and mammals (Nedd5 and H5) (14-17). Similar to yeast septins, animal septins can form polymeric actin-associated filaments, hydrolyze GTP and produce multinucleated cells when mutated (18, 19). Septins can form microfilaments by interacting with each other or with cytoskeletal and filamentous proteins such as actin, myosin

and tubulin, indicative of their functional roles in cytokinesis during contractile ring formation, cell morphology changes and dynamic scaffolds (14, 20-24). Mammalian septins have many interacting partners (Table 1.1) and form complexes between family members to create filaments important in different cellular functions. The diverse functional roles of mammalian septins are intrinsically related to their physical interactions, which might explain how one septin can have multiple functions in different tissues and at different times during cell cycle and development.

In addition to their roles in cytokinesis, mammalian septins have been associated with other distinct cellular processes including vessicle trafficking, cell polarity, cytoskeletal dynamics, apoptosis, neurodegeneration and oncogenesis. The diversity and complexity of these septin-associated functions is not well understood, but it is believed that a wide range of hetero-oligomeric septin complexes are major players in these cellular processes. For example, SEPT4/ARTS, an alternative transcript of SEPT4, is translocated from the mitochondrion to the nucleus upon exposure to the apoptotic agent TGF-β, possibly providing a mechanistic link between cell division and cell death (25-27). Recent data indicate that several septins, including SEPT2, 4, 6 and 7, co-precipitate with the mammalian sec6/8 complex, suggesting an association of septins with membrane dynamics and vesicle trafficking (28-31). In addition, septins have been implicated in platelet function (SEPT4, 5 and 8) (32-35), cardiac myocyte development (36), chromosome dynamics (SEPT2) (37), cell polarity, motility and microtubule dynamics (SEPT9 and others) (20, 22-24, 38). In a very elegant study, Kremer *et al*. showed that a complex of septin proteins (SEPT2, 6 and 7) interacts with SOCS7, which is necessary to retain SOCS7 and NCK in the cytoplasm at a steady state to regulate actin organization and DNA

Table 1.1 Interacting partners and functional roles of mammalian septins

Complexes	Function	Septin Domain	Reference
SEPT1/ Aurora B	Chromosome segregation, Cytokinesis	-	Qi et al, 2005
SEPT2/F-Actin	Cytokinesis	GTP binding	Kinoshita et al. 1997
SEPT2/5/6/Anillin	Cytokinesis	-	Kinoshita et al. 2002
SEPT2/6/7	Filament formation	C- & N- termini	Low et al, 2006
SEPT2/GLAST	Neurotransmitter release	-	Kinoshita et al, 2004
SEPT2/myosin II	Cytokinesis	-	Joo et al, 2007
SEPT2/6/7/MAP4	Microtubule stability	-	Kremer et al. 2005
SEPT2/4/7/Sec6/8	Vesicle trafficking	-	Hsu, et al. 1998
SEPT3/5/7	Neuronal biology	-	Fujishuma et al, 2007
SEPT4/5/8	Vesicle Targeting/Exocytosis	N- & C- termini	Martinez et al, 2006
SEPT4/8	Platelet biology	-	Blaser et al, 2004
SEPT5/parkin	Parkinson's pathogenesis	-	Choi et al, 2003
SEPT5/11	Exocytosis in endothelial cells	GTP binding & C- termini	Blaser et al, 2006
SEPT5/SNARE complex	Vesicle Targeting/Exocytosis	GTP binding & C- terminal	Beites et al, 2005
SEPT6/12	Filament formation	-	Ding et al, 2007
SEPT7/9/11/Actin	Filament formation	N-terminal	Nagata et al, 2004
SEPT7	Chromosome segregation	-	Zhu et al, 2008
SEPT8/Vamp2	Snare complex formation Neurotransmitter release	-	Ito et al, 2009
SEPT9/Actin	Stress Fiber	-	Nagata et al, 2005 González et al, 2007
SEPT9/SA-RhoGEF/Actin	Rho Signaling	N-terminal	Nagata et al, 2005
SEPT9/HIF-1	Cell proliferation, angiogenesis, prostate Cancer	-	Amir et al. 2006
SEPT9/JNK	Cell proliferation, breast cancer	GTP binding	Gonzalez et al, 2008
SEPT9/Tubulins	Filament formation, microtubules, spindle formation,	GTP binding	Surka et al, 2002 Nagata et al, 2003 González et al, 2007
SEPT11/12	Filament formation	-	Ding et al, 2008
SEPT14/SEPT 1-7/9/11-12	Testicular biology	-	Peterson et al, 2008

damage response. The SOCS7/NCK complex accumulates in the nucleus to activate CHK2 and p53 mediated cell cycle arrest upon DNA damage. This action is potentiated by the depletion of the septin complex by siRNA. The spatial distribution of NCK as mediated by septin complex is important in the reorganization of the actin cytoskeleton, cell polarity and the DNA damage response. One can predict that *in vivo* the distribution of septins in the cytoplasm is an important mechanism that regulates the localization of many proteins and their site of action in the cell (39).

SEPT2 and SEPT11 are required for phagosome formation important for cell membrane dynamics (31). SEPT2 is also required for epithelial cell polarity by associating with tubulin networks and facilitating vesicle transport by preventing polyGlu microtubule tracts from binding to MAP4 (38). SEPT12 has been implicated in mammalian spermatogenesis (40, 41). In addition, SEPT4 and SEPT7 serve as diagnostic markers for human male asthonozoospermia, since healthy individuals showed septin expression in the annuli of spermatozoa while infertile patients do not(42). Ihara *et al.* demonstrated that expression of murine Sept4 is important for the cortical organization required for morphology and motility of the sperm flagellum (43). SEPT2 and SEPT11 are modulators of InlB-mediated invasion by *Listeria monocytogenes*. SEPT2 is essential for the entry of Listeria to the cells, but SEPT11 expression restricts the efficacy of Listeria invasion to the cells. Overall, these findings demonstrate the diverse roles of septins despite their high structural conservation (44-46).

Septins as microtubule associated proteins

Several studies suggest that septins might be involved in microtubule dynamics and chromosome segregation. Two groups showed that mammalian SEPT2 and SEPT7 may form a mitotic scaffold for CENP-E and other effectors to coordinate chromosome segregation and

cytokinesis (37, 47). Kremer *et al.* proposed a novel molecular function for septins in mammalian cells through the modulation of microtubule dynamics via an interaction with MAP4 (22). Looking specifically at SEPT9 isoforms, SEPT9_v1 (MSFA) was found to localize specifically with microtubules. This localization was required for the completion of cytokinesis and it could be disrupted by nocodazole treatment (24). Interaction of SEPT9_v1 with microtubule networks was found to be essential for septin filament formation (23). We propose that there is a tight regulation between tubulin filaments, microtubules and septins filaments. How this regulation is mediated and what other proteins are involved remains unclear. Fluorescence microscopy and further characterization of protein interactions might give better insight into septin-tubulin interaction and its regulation chromosome segregation during mitosis.

Septins and neurological disorders

Possible roles for septins in neurological disorders have emerged based on the brain-specific expression of some septins (Table 1.2). SEPT2/NEDD5, SEPT1/DIFF6 and SEPT4/H5 have been found to associate with Alzheimer-specific neurofibrillary tangles (5, 48). The SEPT5/CDCREL-1 interaction with Parkin, a pathogenic protein in Parkinson's disease (49, 50), provides evidence for the involvement of another subset of septins in neuronal development and disease. SEPT4 has also been implicated in brain pathogenesis by its association with cytoplasmic inclusions in Parkinson's disease and other synocleinopathies (51). The SEPT3/5/7 complex was identified in the mammalian brain and SEPT3 specifically is developmentally regulated and enriched in presynaptic nerve terminals, suggesting a role for these septins in neuronal biology (52, 53). SEPT2 and SEPT8 are associated with neurotransmitter release due to their interaction with the glutamate transporter (Glast) and the synaptic vesicle protein synaptobrevin 2 (Vamp2), respectively (54, 55). Other septin complexes have been associated

with myelin formation in the peripheral nervous system (56). Recently, SEPT9 point mutations and a duplication within the gene have been identified in patients with the autosomal dominant neuropathy Hereditary Neuralgic Amyotrophy (HNA) (57-59), further supporting a role for septins in neurological disease. The mechanism by which these mutations are pathogenic in HNA is still not fully elucidated, but McDade *et al.* showed that isoforms v4 and v4* have distinct 5' ends encoded by exons where germline mutations of HNA are found. The two mRNAs are translated with different efficiencies and cellular stress can alter this pattern (60). These mutations dramatically enhance the translational efficiency of the v4 5'-UTR, leading to elevated SEPT9_v4 protein under hypoxic conditions (60). These data provide mechanistic insight into the effect of HNA mutations on fine control of SEPT9_v4 protein and its regulation under physiologically relevant conditions. The data are consistent with the episodic and stress-induced nature of the clinical features of HNA (60).

Septins in cancer

The first evidence that septins may contribute to neoplasia occurred with the discovery of septin SEPT5/CDCREL-1 as a carboxy-terminus fusion partner with mixed lineage leukemia (MLL) in an acute myeloid leukemia (AML) patient with a t(11;22)(q23;q11.2) translocation (61). Subsequently, SEPT9/MSF, SEPT6, SEPT2, and SEPT11 were also identified as fusion partners with MLL in human leukemic cells (62-65). MLL, the human homolog of Drosophila trithorax, is a common translocation partner in leukemias with more than 80 rearrangements with 50 fusion partners identified (66). The well-characterized MLL fusion products produce in-frame translated chimeric proteins associated with phenotypic disease variability such as leukemia type and prognostic outcome. These carboxy partners, in addition to MLL, appear to be essential contributors to the pathogenesis of leukemia (67).

Table 1.2 Characteristics of the human septins loci and disease association

Septin	Location	Expression	Disease Association
SEPT1	16p11.1	brain, lymphocytes, others	Alzheimer's, leukemia, lymphoma
SEPT2	2q37	brain, lymphocytes, others	brain cancer, liver cancer, renal cancer, VHL
SEPT3	22q13.2	brain-specific	brain cancer, Alzheimer's
SEPT4	17q22	brain, testes, eye, lymphocytes	Alzheimer's, urogenital and colon cancer, leukemia , infertility
SEPT5	22q11.21	brain, eye, platelets	Parkinson's, pancreatic cancer, leukemia
SEPT6	Xq24	ubiquitous	leukemia, Hepatitis C
SEPT7	7q36.1	brain	-
SEPT8	5q31	brain, various others	-
SEPT9	17q25	ubiquitous	leukemia, breast, ovarian and colorectal cancers, Hereditary Neuralgic Amyotrophy
SEPT10	2q13	ubiquitous	-
SEPT11	4q21.1	ubiquitous	leukemia
SEPT12	16p13.3	Lymphocytes, testes	infertility
SEPT13	7p13	ubiquitous	-
SEPT14	7q11	testes	infertility?

Other septins have also been implicated in other types of cancer including SEPT2, SEPT3, SEPT4, SEPT5 and SEPT9 (25, 68, 69). In fact, SEPT4 acts as a tumor suppressor in leukemias and solid tumors. The SEPT4 gene promotes apoptosis, and is lost in 70% of leukemia patients (26), in addition to being associated with inhibition of colorectal cancer tumorigenesis (70). SEPT2 phosphorylation by casein kinase 2 was found to be important for hepatoma carcinoma cell proliferation (71). SEPT2 and SEPT3 were abundantly expressed in several brain tumors and brain tumor cell lines, suggesting that these family members are potential oncogenes (69). SEPT9 seems to be important not only in leukemias but also in solid tumor cancers (72-77).

Overall, these studies show that human septins are important in many cellular and molecular functions, as summarized in Fig 1.3. It seems that their expression needs to be highly regulated and the dynamics with their interaction partners are crucial for their function as either scaffolds for cytoskeletal proteins or signaling GTPases. Mutations or altered expression of these genes can arise by multiple mechanisms that are not well understood. Septins are strikingly associated with multiple human diseases, primarily cancers and neurological disorders (Table 1.2 and Fig 1.3). This thesis is focused on the role of SEPT9 in normal cellular functions, and the importance of specific isoforms in mammary tumorigenesis.

Human *SEPT9* locus

Human SEPT9 became of great interest to the septin scientific community after it was mapped to chromosome 17q25, a region linked to breast and ovarian cancer, by positional cloning to a region of allelic imbalance in breast and ovarian cancers in our laboratory (74, 78-80), suggesting that alterations of this novel septin gene may be important in breast and ovarian cancer. Subsequently, it was shown that the SEPT9 locus gives rise to multiple alternative transcripts encoding at least seven annotated isoforms (SEPT9_v1-SEPT9_v7) (74). The SEPT9

locus contains 13 exons and shows complex 5' and 3' alternative splicing. The variable exons 1-3 and 12-13 encode alternative translational start and stop sequences and are spliced on to a core of 8 coding exons (Fig 1.4) (74). These isoforms maintain the general structure of septins with a highly conserved central region containing the polybasic domain and GTP-binding domain (Fig 1.1). They vary in the 5'- and 3'- untranslated regions (UTR) and at the N- and C- terminus of the protein. Interestingly, the SEPT9_v4 and SEPT9_v4* isoforms encode for the exact same protein, but they differ at their 5' UTRs, suggesting that these transcripts might be differentially regulated in time or tissue of expression (73, 76, 77). SEPT9_v1 and SEPT9_v3, the longest transcripts, are highly similar except for 25 distinct amino acids at the N- terminus of SEPT9_v1. The biological reason for the presence of multiple SEPT9 transcripts is still not elucidated, but many studies, including expression analyses, show that these isoforms are differentially expressed and may have distinct functional roles in mammalian cells.

SEPT9 is widely expressed based on ubiquitous adult and fetal transcript expression, although individual isoforms may have tissue specific expression (74). The cellular localization of SEPT9 isoforms is largely cytoplasmic in interphase cells, but the SEPT9_v1 isoform has a bipartite nuclear localization signal that may direct the shuttling of SEPT9_v1 between the nucleus and the cytoplasm. In mitotic cells SEPT9 exhibits a punctuate staining pattern located between the separating chromosomes and at the cleavage furrow during telophase (24). SEPT9_v1 is localized to microtubule networks in interphase cells and in mitotic cells it is localized at the mitotic spindle and the bundle of microtubules at the midzone (23). Both studies showed that when SEPT9 is ablated, cells become binucleated, suggesting a role for SEPT9 in cell division via interaction with components of the cytoskeleton such as tubulins.

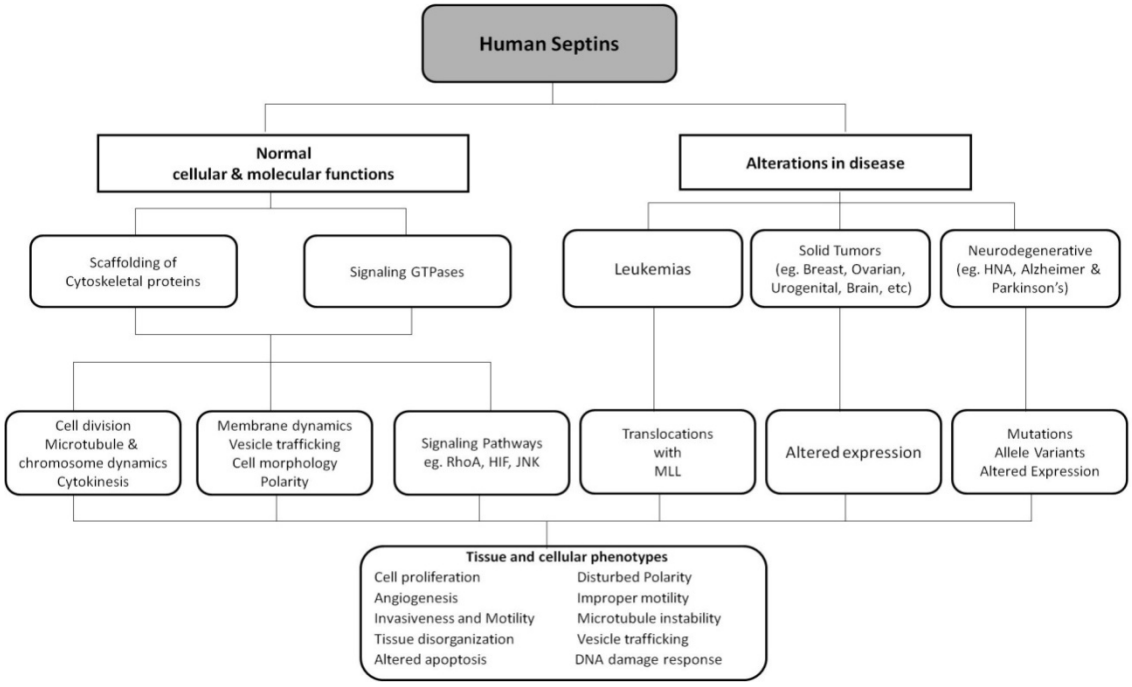

Fig 1.3: Human septins in health and disease

Human septins are involved in multiple tissue and cellular phenotypes. Alterations in their expression or gene mutations affect these phenotypes, which are mechanistically important in the pathogenesis of many diseases such neurological diseases and cancer.

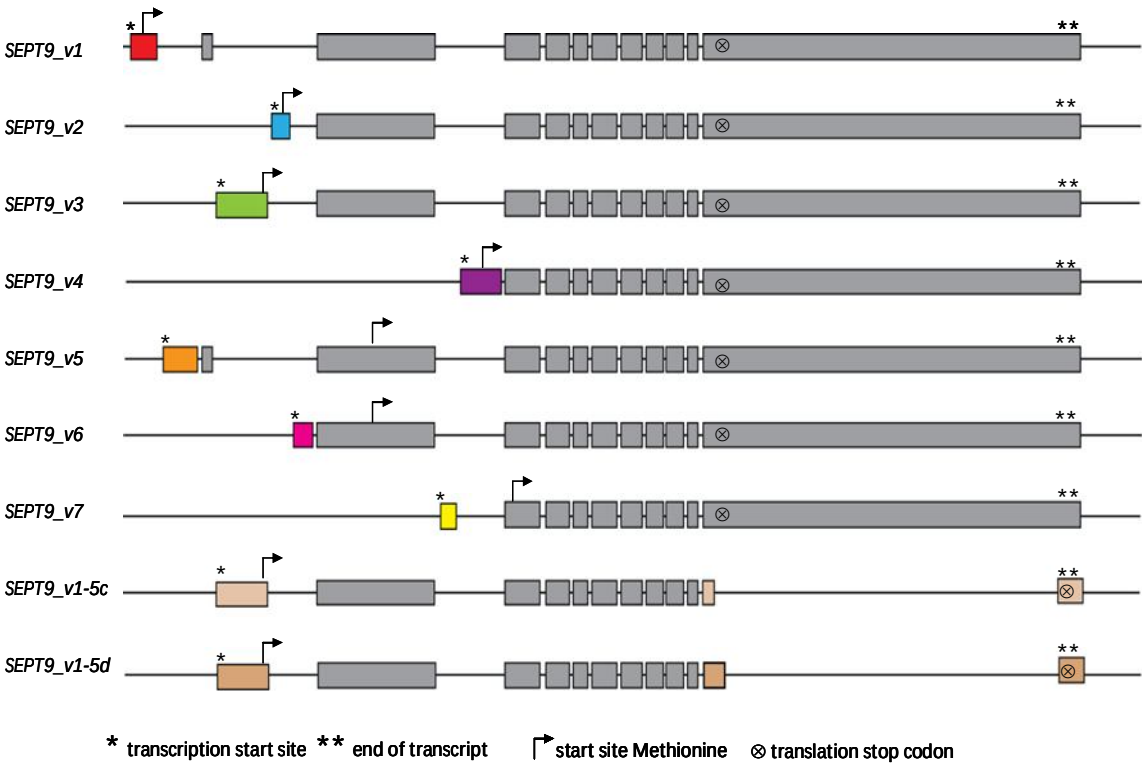

Fig 1.4: SEPT9 genomic structure

Genomic structure of SEPT9 alternatively spliced transcripts and variants. *SEPT9* exhibits 5' and 3' alternative spliced and variable exons and is composed of 13 exons in total. Gray boxes indicate common exons and colored boxes indicate variant-specific exons, all drawn to scale. Transcriptional start sites are indicated by (*) and the end of each transcript by (**). The variable exons (colored boxes) encode different translational start (arrow) and stop (⊗) and are spliced into a core of common coding exons shared between variants (gray boxes).

Since they were discovered, septins had been characterized as cytoskeletal GTPases important in cell division. Mutations of this family of genes in yeast lead to budding defects, cell cycle arrest and cytokinesis defects. In mammals, several septins (eg. SEPT2, SEPT5, SEPT7) also have been implicated in mitosis, specifically in chromosome segregation dynamics and cytokinesis (Table 1.1). SEPT9 is not an exception. Its localization to microtubules, the cleavage furrow and midbody at different stages in mitosis suggests a possible specific role of SEPT9 isoforms in chromosome segregation and/or completion of cell division by affecting the mitotic spindle assembly, disassembly or dynamics and the cytokinesis process (Fig 1.5).

Intricate human SEPT9 nomenclature

Ten years ago, the SEPT9 locus was called MLL septin-like fusion (MSF) due to the fact that it was identified as a fusion partner of MLL in leukemias (65). In 2002, a committee of septin researchers developed an official nomenclature system for SEPT9 transcripts (81). This new name was derived from the functional role of these genes in septae formation in yeast. Some research groups published with the old nomenclature while others used their own versions, making progress in SEPT9 research hard to reconcile. New nomenclature was established by the National Center for Biotechnology Information (NCBI) and HUGO Gene Nomenclature Committee (HGNC), but it has not been universally accepted by the septin community. These nomenclature changes are depicted in Table 1.3 by group and year. Throughout this study I will refer to the nomenclature used in current publications, which was established in 2005 by Scott *et al.* and endorsed at the 2009 International Septin Meeting (76).

SEPT9 model of oncogenesis in solid tumors

A compelling example of the role of septins in the oncogenesis of solid tumors was the identification of the MSF/SEPT9 murine ortholog Sint1/Sept9 at a provirus insertion site in SL3-3

Table 1.3: SEPT9 nomenclature

Kalikin LM, *et al.*	McIlhatton MA, *et al.*	Macara IG., *et al.*	Inagaki M., *et al.*	Scott M., *et al.*	NCBI	HGNC	NCBI Accession Numbers
2000	2001	2002	2004	2005[β]	2008	2008	
					variant/isoform	isoform	transcript/protein
MSF-A	epsilon	SEPT9_v1	SEPT9a	SEPT9_v1a	SEPT9_v1/SEPT9a	SEPT9_i1	NM_001113491/NP_001106963
-	gamma	-	-	SEPT9_v2a	SEPT9_v2/SEPT9b	SEPT9_i2	NM_001113493/NP_001106965
MSF	alpha	SEPT9	SEPT9b	SEPT9_v3a	SEPT9_v3/SEPT9c	SEPT9_i3	NM_006640/NP_006631
-	-	-	-	-	SEPT9_v4/SEPT9d	SEPT9_i4	NM_001113495/NP_001106967
MSF-B	zeta	SEPT9_v2	SEPT9c	SEPT9_v4*a	SEPT9_v5/SEPT9e[a]	SEPT9_i5	NM_001113492/NP_001106966
MSF-C	beta	SEPT9_v3	SEPT9c	SEPT9_v4a	SEPT9_v6/SEPT9e[a]	SEPT9_i6	NM_001113494/NP_001106966
-	delta	SEPT9_v4	-	SEPT9_v5a	SEPT9_v7/SEPT9[f]	SEPT9_i7	NM_001113496/NP_001106968
-	-	SEPT9_v5	-	SEPT9_v1-5b-c*	-	-	-

[a] SEPT9 variant 5 and 6 differ in their 5' UTR but encode the same protein isoform.

*SEPT9_v1-5b-c variants differ at the 3' UTR. No well characterized.

[β] Current nomenclature in this thesis and peer reviewed publications

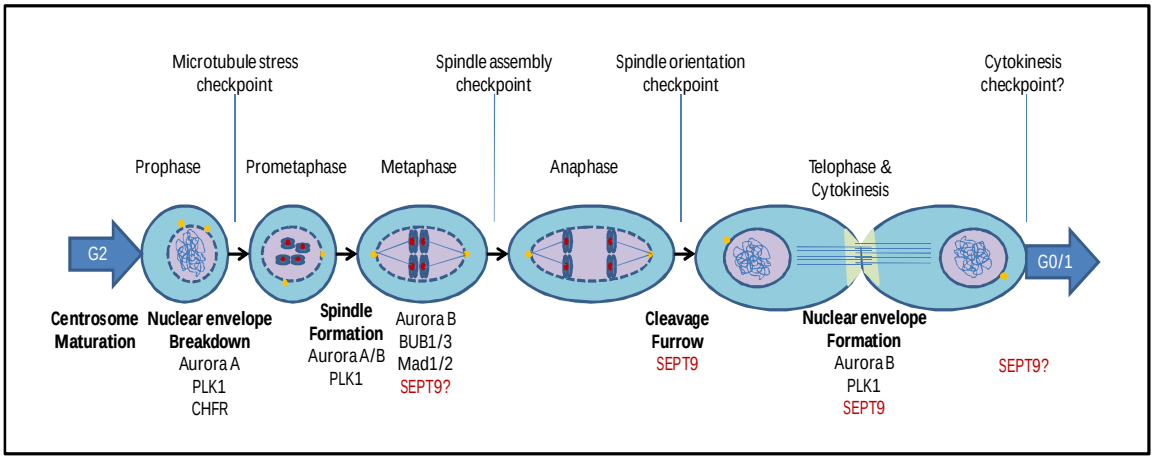

Fig. 1.5: SEPT9 functional role in mitosis

Diagram showing the phases in mitosis in which SEPT9 expression is present. SEPT9 is localized to the microtubules at the midzone during anaphase and at the cleavage furrow in telophase. Its particular localization during mitosis suggests a role in chromosome segregation and cytokinesis.

MLV-induced lymphomas (82), which demonstrated that this septin locus is a site for oncogenic integration. SEPT9 also maps to a region of allelic imbalance at chromosome 17q25.3 in breast cancer (74) and sporadic ovarian cancer (80). There is differential expression of SEPT9 isoforms in tumors of various tissues (21, 77, 83, 84). SEPT9 has been characterized as a candidate gene in head and neck squamous cell carcinomas by a genome-wide screen for methylated genes (85). Circulating methylated SEPT9 DNA cDNA in plasma was recently identified as a valuable biomarker for minimally invasive detection of colorectal cancer. This lead to the development of a new methylation (m)SEPT9 assay which may prove useful in clinical research for the detection of invasive colorectal cancer in patients (86, 87).

Finally, an isoform of SEPT9, SEPT9_v1, might be important as a biomarker for therapeutic resistance of many cancers to microtubule disrupting agents. SEPT9_v1 expression was strongly correlated with susceptibility of a wide range of cancer cells to drugs such as paclitaxel (88). In general, cancer cells with high SEPT9_v1 expression were more resistant to these drugs (88).

SEPT9 isoforms have been associated with signaling pathways relevant to oncogenesis. For example, SEPT9_v1 interacts with HIF1α preventing its ubiquitination and degradation, thus activating HIF downstream survival genes to promote tumor progression and angiogenesis in prostate cancer cells (72). The SEPT9_v3 isoform binds SA-RhoGEF, functioning as a scaffold to keep it in an inactive state, thereby inhibiting SA-RhoGEF mediated Rho activation (89, 90). This finding was crucial for the study of septins in cancer because it provided a direct link between septins and signaling proteins involved in cellular functions such as actin cytoskeletal organization, transcriptional activation, tumor invasion, cell morphology, cell motility and cytokinesis.

SEPT9 is a novel cancer associated protein and a potential biomarker for diagnosis and chemotherapeutic response in some epithelial cancers. SEPT9 was identified as candidate gene in a region of allelic imbalance in breast cancer cells. Its expression is altered in many types of cancers including head and neck tumors, ovarian, prostate, colorectal, and breast cancers and it is over-expressed in a MMTV mouse model of mammary tumorigenesis (20, 72-76, 82, 86). One of its alternative transcripts, SEPT9_v1, was found to be amplified and over-expressed in breast cancer cell lines and primary tumors. These facts led to the hypothesis that high SEPT9_v1 expression specifically promotes malignant transformation in mammary epithelial cells by promoting the development of pro-oncogenic phenotypes. To test this hypothesis, the first aim of this work was to define the relevance of high SEPT9_v1 expression to breast cancer progression in an over-expression model using mammary epithelial cell cultures. The findings from these experiments are presented in Chapter 2. The second aim, described in Chapter 3, was to characterize the role of SEPT9_v1 expression in genomic stability and cell proliferation. Chapter 4 describes a novel interacting protein of SEPT9 isoforms and the newest member of the human septin family, SEPT14. Chapter 5 is a concluding chapter that discusses the significant findings of this thesis and the potential future directions for this project.

CHAPTER II

HIGH SEPT9_v1 ECTOPIC EXPRESION PROMOTES PRO-ONCOGENIC PHENOTYPES IN MAMMARY EPITHELIAL CELLS

Summary

Altered expression profiles of human septins have been observed in multiple cancers, including leukemias and solid tumors. Almost all human septin genes demonstrate complex patterns of alternative splicing as well as 5' and 3' variations. These variations give rise to multiple protein isoforms whose expression patterns may be temporal and tissue specific. Upon positional cloning of the human SEPT9 locus, several alternative transcripts were identified that encode at least seven distinct confirmed isoforms that vary primarily in their N- and C- termini. Extensive microarray analyses of normal versus tumor tissue demonstrated differential expression of specific SEPT9 isoforms in tumors when compared to normal tissue. By examining a panel of breast cancer cell lines and a panel of primary breast tumors with matched control tissues for expression of SEPT9 variants using a variety of methods (i.e. semi-quantitative RT-PCR, Q-PCR, Western blotting and immunohistochemistry), we found altered expression in breast cancers as compared to normal mammary epithelial cells. Of all the SEPT9 isoforms, SEPT9_v1 was found to be highly expressed in >50% of breast cancer cell lines tested. SEPT9_v1 also showed increased cytoplasmic staining in primary tumors as compared to matched control samples. In addition, when analyzing SEPT9_v1 staining in breast cancer patient samples with clinicopathological variables, we found that high SEPT9_v1 staining correlated with grade and

hormone receptor-positive tumors. Therefore, we established a SEPT9 high expression model in mammary epithelial cells by retroviral transduction of SEPT9 isoforms. We found that high retroviral expression of SEPT9_v1 in immortalized human mammary epithelial cell lines (IHMECs) caused these cells to acquire common cellular phenotypes that are associated with malignant cells. Additionally, knockdown of SEPT9_v1 expression in breast cancer cell lines (BCCs) caused a reduction in some malignant phenotypes such as growth kinetics, invasiveness and cell motility. These analyses demonstrated that high SEPT9_v1 expression in mammary epithelial cells can promote the development of cellular phenotypes that are markers of cancer and that alterations of SEPT9_v1 expression may impact the development of human breast cancer.

Introduction

Breast cancer results from genetic and environmental factors that lead to the accumulation of mutations in, or altered expression of, essential genes. Cancer is a complex multistep process in which mutations and/or deregulation of major oncogenes and/or tumor suppressors with large effect in the cells (c-Myc, p53, BRCA1, etc…) dictate the path to oncogenesis (91). In addition, oncogenesis can be affected by the contribution of genes with small effects that, in combination, will impact either cancer initiation and/or progression. The last decade has been highlighted by the development of clinically useful predictive, diagnostic, prognostic and therapeutic options based on knowledge about some of these genetic changes. However, the diverse molecular pathways underlying this heterogeneous disease are complex and remain poorly understood. In fact, a variety of comparative genomic and expression studies suggest that additional genes and novel pathways important in breast cancer initiation and/or progression remain to be characterized (92, 93).

In recent years there has been an increasing interest in the association of a family of human genes called "septins" with human cancers. Septin family members have been implicated in multiple cancers, from leukemias to solid tumors (94). In fact, our laboratory previously discovered a novel breast cancer associated gene, MSF (MLL Septin-like Fusion), on chromosome 17q25 by positional cloning (74). Due to its high level of homology to cytokinesis genes encoding a family of GTPases containing septins, it was later renamed SEPT9. Its high homology to other evolutionarily conserved septins important in cell division and implicated in oncogenesis, as well as its localization to a discrete region of allelic imbalance (AI) on chromosome 17q25 in breast tumors, suggested that alterations of this novel septin gene maybe important in breast cancer (74).

Upon further analysis, the SEPT9 locus exhibited, as do many other members of the septin family, extensive alternative splicing with the majority of diversity in the 5' and 3' ends of the transcripts. This resulted in the gene encoding at least 7 well-characterized isoforms, believed to be tissue-specific, spatially and/or temporally regulated (Fig 1.4; Chapter 1). For example, SEPT9_v1, the longest isoform, has unique exons 1-2 (red boxes) as compared to the SEPT9_v3 transcript which has a unique exon 1 (green box) (Fig 2.1A). The additional exons (gray boxes) are shared between the two transcripts, including those exons encoding for the proline rich domain (PRD), polybasic domain (PB) and the GTP-binding domain. SEPT9 isoforms also differ in amino acid composition at both the N-terminus and C-terminus. These two isoforms, SEPT9_v1 and SEPT9_v3, which are the main focus of this thesis, are compared by translational start sites and domain composition in Fig. 2.1B. These two isoforms, as the other SEPT9 isoforms, shared the same domains at the central region including the PRD, PB and GTP-binding domain. The difference between these two isoforms reside on their N-termini, SEPT9_v1 contains 18 additional amino acids at position 1-18 followed by 7 amino acids that differ from SEPT9_v3. These 25 specific amino acids were used as a peptide (Fig 2.1B) to design a polyclonal antibody specific for SEPT9_v1. Another antibody that recognized a peptide shared between all the isoforms was designed and used in this work (Fig 2.1). It is hypothesized that the differences in 5' and 3' untranslated (UTR) regions of these SEPT9 variants may be important for the regulation of expression of each variant at different cell stages and tissues. For example, SEPT9_v5 (SEPT9_v4*) and SEPT9_v6 (SEPT9_v4) have different 5' UTRs but encode for the same polypeptide, but are translated at different efficiencies between normal and tumor tissues (73, 76, 77). The differences in protein structure and amino acid content between SEPT9_v1 and SEPT9_v3, as well as between the other isoforms may dictate the specificity of their protein interactions and the different effects of each in many cellular processes.

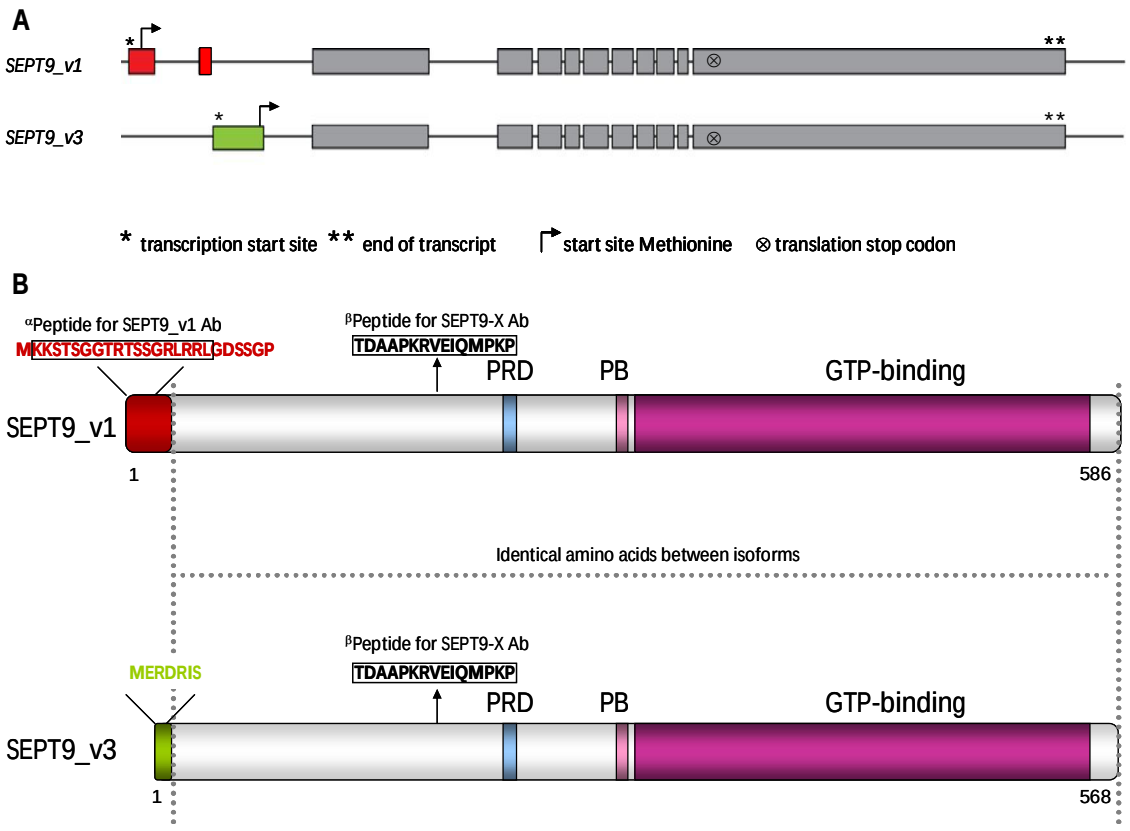

Fig 2.1: Genomic and protein structure comparison between SEPT9_v1 and SEPT9_v3 variants

(A) Genomic structure of SEPT9_v1 and SEPT9_v3 transcripts. Gray boxes indicate common exons and colored boxes indicate variant-specific exons, all drawn to scale. SEPT9_v1 specific exons are depicted by red boxes and SEPT9_v3 specific exon by a green box. Transcriptional start sites are indicated by (*) and the end of each transcript by (**). The variable exons encode different translational start (arrow) and stop sequences (⊗) and are spliced into a core of common coding exons shared between variants (gray boxes). (B) Schematic showing SEPT9_v1 (586 amino acids; 65.4 kDa) and SEPT9_v3 (568 amino acids; 63.6 kDa), which are used throughout the majority of the experiments. Red and green boxes represent specific amino acids for each isoform as shown. Shared domains are shown in colored boxes (PRD: proline rich domain, PB: polybasic domain, GTP-binding domain). Dash lines delineated identical amino acids shared between the isoforms. Boxed amino acids showed peptides used to produce SEPT9 antibodies in which (a) denotes the peptide used to produce a rabbit polyclonal SEPT9_v1-specific antibody and (b) denotes the peptide used to produce a rabbit polyclonal SEPT9-X antibody that recognized all the SEPT9 isoforms shown. SEPT9_v1 contains 18 additional amino acids at the N terminus that are not present in SEPT9_v3 and both isoforms differ in additional 7 subsequent amino acids, that makes a total of 25 specific amino acids for SEPT9_v1.

No pathogenic SEPT9 mutations associated with cancer have been reported to date, thus SEPT9 may belong to a class of critical regulatory genes in which altered expression profiles may underpin its role in tumorigenesis (76, 77, 94). In fact, many reported expression analyses of SEPT9 variants showed differential expression between different tissues, and most importantly altered expression in cancer tissues such as breast, ovarian and prostate among others (73, 76, 77, 85, 86, 88, 94, 95). Previous studies in our laboratory showed that SEPT9 was amplified and over-expressed in more than 50% of breast cancer cell lines by Southern blot and RT-PCR (Table 2.1). Additional expression analyses of each specific SEPT9 isoform by RT-PCR, quantitative real time PCR, and Western blotting showed high expression of SEPT9_v1 in more than 60% of BCCs as compared to IHMECs (Table 2.1). Preliminary immunohistochemistry analysis of primary breast tumors showed increased SEPT9_v1 cytoplasmic staining as compared to matched controls (Table 2.1). Therefore, my primary goal was to determine the role of SEPT9_v1 expression in breast tumorigenesis. We hypothesized that high SEPT9_v1 retroviral expression promotes malignant transformation in immortalized human mammary epithelial cells by promoting the development of pro-oncogenic phenotypes. To test this, we designed a high SEPT9 expression model in mammary epithelium by establishing several IHMECs and breast cancer cell lines with stable expression of two SEPT9 isoforms (SEPT9_v1 and_v3,) using retroviral transduction.

Part of our goal is to characterize the specific role of SEPT9_v1 in mammary tumorigenesis as either a “large effect” or a “small effect” oncogene by testing its effect on essential processes in cells that collectively drive malignant growth. Some phenotypes that are considered to be the hallmarks of cancer include: self–sufficiency in growth signals, insensitivity to growth-inhibitory signals, evasion of apoptosis, limitless replicative potential, sustained angiogenesis, and tissue invasion and metastasis (96). In addition, many solid tumors can be

characterized by anchorage-independent growth, loss of contact-contact inhibition, and genomic, chromosomal and microsatellite instability among other phenotypes. Our retroviral expression model showed that SEPT9_v1 impacts malignant transformation and/or progression by promoting cells to acquire many of these pro-oncogenic phenotypes as measured by cell culture model that are cornerstone of cancer biology research.

Table 2.1: Summary of SEPT9 locus and SEPT9_v1 expression analyses

SEPT9 analysis	Methods	Results (Gonzalez et al, 2007)
SEPT9 locus in breast cancer cell lines (BCCs)	PCR Southern blot	Amplification in >60% of BCCs $p<0.025$
SEPT9_v1 transcript and protein expression in BCCs	Northern blot Semi-quantitative RT-PCR Quantitative real time RT-PCR Western blot	Over-expression in >50% of BCCs $p<0.025$ correlation $R^2=0.7$
SEPT9_v1 protein expression in primary breast tumors and matched normal tissue	Immunohistochemistry	Increased cytoplasmic staining in 70% primary breast cancers $p<0.02$

Material and Methods

Cell lines

HPV-immortalized mammary epithelial cell lines were developed and provided by S.P. Ethier (Karmanos Cancer Institute, Wayne State University, Detroit, MI). MCF10A cells and additional BCCs and immortalized human mammary epithelial cell lines (IHMECs) were purchased from The American Type Culture Collection: The Global Bioresource Center™ and grown under recommended conditions.

Immunohistochemistry

To study SEPT9_v1 expression in primary breast cancers, 160 paraffin-embedded patient samples arrayed on a single high-density tissue microarray (TMA) were used for the analysis. Details on this TMA have been described previously (97). Immunohistochemistry was performed with a custom polyclonal anti-SEPT9_v1 specific antibody at a 1:200 dilution on previously prepared slides of paraffin-embedded or frozen sections of human breast tissue using standard methods. Primary antibody was detected following protocols described by the manufacturer (DAKO Cytomation, UK), with diaminobenzidine as a chromogen and with haematoxylin counterstain. Optimization and validation of the immunostaining dilution conditions were performed on several paraffin slices made from BCCs cell pellets, which reflected different levels of SEPT9_v1 expression corresponding to the endogenous level of expression described by other methods in this paper. Cells were visualized with an Olympus BX-51 microscope with a 10x and 40x objective lens. Samples were scored from 0 to 4 by a pathologist (C. Kleer) to indicate intensity where "0" represented no SEPT9_v1 staining and "+4" represented dark, intense staining.

Establishment of SEPT9's stable lines

Open reading frames of SEPT9_v1, SEPT9_v3 and SEPT9_v4 were cloned into the pLNCX2 and/or pLPCX retroviral vectors (BD Biosciences). Constructs were transfected into PT67 packaging cell lines using Fugene 6® transfection reagent. Supernatant containing viral particles were collected 48 hours after transfection. MCF10A cell cultures were individually infected with virions produced for each construct using polybrene (hexadimethrine bromide). Positive selection was started with either geneticin (G418) and/or puromycin 48 hours after infection. Polyclonal lines for each construct were established after 10 days under selection.

Western blot

Western blot analysis was performed as previously described (98) using 50.0 μg of whole cell lysates. The following antibodies were used: a custom-made rabbit polyclonal anti-SEPT9_v1 (N-terminal epitope: KKSYSGGTRTSSGRLRR, BioCarta, San Diego CA) at a 1:1000 dilution, a rabbit polyclonal anti-SEPT9 kindly provided by W.S. Trimble (24) at a 1:1000 dilution (Fig 2.1B), mouse ascites anti-βActin at a 1:10,000 dilution, mouse anti-vimentin at a 1:1000 dilution, goat anti-rabbit:HRP secondary antibody at a 1:10,000 and goat anti-mouse HRP also at a 1:10,000 dilution (or 1:20,000 when used with anti-βActin primary antibody). Antibodies were purchased from Sigma, unless otherwise noted, and diluted in 5% milk, 3% BSA and 0.05% Tween-20 in 1x TBS. The Super Signal West Pico Chemiluminescent kit (Pierce Biotechnology, Rockford, IL) was used for detection, prior to exposure to Kodak XAR-5 film. Relative to the loading control, semi-quantitative protein expression level was determined by densitometry (Alpha Innotech IS-1000 Digital Imaging System, version 2.00).

Cell proliferation assays

Two methods were conducted to examine cell proliferation. For one, cells were plated in triplicate at the same density and counted at different time points, according to their doubling time, over the course of several days. For the other, cells were plated at the same density and cultured for 24 h in a 96-well microplate. WST-1 reagent was added and absorbance at 450 nm was measured after 3 hours of incubation following manufacturer's instructions (Roche Molecular Systems).

Apoptosis assay

Subconfluent cultures of HPV4-12, MCF10A and transductants were treated with 10 μM camptothecin for 24 hours to induce apoptosis; untreated cells were used as controls. AnnexinV antibody conjugated to Alexafluor488 was hybridized to the cells, which were then counted by flow cytometry, following the manufacturer's instructions (Vybrant Apoptosis Assay #2, Molecular Probes, Invitrogen, Carlsbad, CA). Propidium iodide was used as a counter-stain to distinguish between apoptotic cells and dead/necrotic cells.

Mitotic Index

HPV4-12, MCF10A, empty vector, and SEPT9 transductants were prepared as previously described (23) and stained with 0.54mg/ml Giemsa solution, and then destained in deionized water. Cells were visualized using a Leica DAS model microscope, and 1000 cells were counted per sample in triplicate. The mitotic index was calculated as the percentage of cells with condensed chromosomes and lacking a nuclear membrane out of 1000 cells.

Scrape motility assay

SEPT9-overexpressing stable transductants and empty vector controls were grown to confluency on 6-well plates in triplicate. The cell monolayer was scraped using a pipette tip and visualized for movement into the wound 22 hours later with the Leica inverted microscope (phase-contrast optics, 20x objective). The open wound areas at the initial and end points for each motility assay were calculated using Image J (http://rsbweb.nih.gov/ij/). The ratio between time 0 and 22 h later (0 h/22 h) represented the motility for each cell line through the wound.

Matrigel invasion assay

Transwell membranes coated with Matrigel were used to assay invasion in vitro. A suspension of MCF10A cells stably transduced with SEPT9_v1, SEPT9_v3 or empty vector was added to 24-well BD BioCoat Matrigel invasion chambers at 5 x 10^4 cells/ml in triplicate (BD Biosciences Discovery Labware). The invading cells were fixed and stained using the Protocol Hema stain set (Fisher Diagnostics).

Foci formation assay

Hs578T transductants and parental cells were plated in 100mm dishes at 80% confluence. Medium was changed every three to four days over 30 days. Cells were stained with methylene blue, and colonies were photographed.

Immunofluorescence

For immunofluorescence analysis, stable transductants and parental cell lines were grown on two-chambered glass slides and fixed with 4% paraformaldehyde for 40 min at room temperature. Slides were then washed thrice in 1X PBS for 10 min, blocked for 1 h in blocking solution (5% dry milk, 1% BSA, and 0.025% Triton X-100 in 1X PBS)and incubated overnight at

4°C in polyclonal rabbit anti-SEPT9_v1 or anti-vimentin (Sigma-Aldrich Corp.) antibodies at a 1:50 or 1:30 dilution, respectively, in blocking solution. Phalloidin conjugated to Alexa Fluor 568 was used to identify filamentous actin (F-actin). Alexa Fluor 488 and Alexa Fluor 633 were used as secondary antibodies (Molecular Probes, Invitrogen) at a 1:500 dilution in blocking solution for 1 hour at room temperature. Slides were prepared using mounting solution Prolong Gold® antifade reagent with Dapi (4',6-diamidino-2-phenylindole) to visualize DNA. Cells were visualized using an Olympus FV-500 confocal microscope (100X objective).

Knockdown of SEPT9_v1 expression in BCCs

Transient siRNA knockdown was used in MDA-MB-231 cells, a cell line primarily expressing the SEPT9_v1 isoform, following the manufacturer's protocol. Cells were plated in triplicate, at a density of 4.0×10^5 cells/well in a 6-well plate, and subsequently transfected with DharmaFECT2 and the MSF siRNA pool. This pool of four siRNAs targets all SEPT9 isoforms (catalog number M-006373-02, Dharmacon Research, Inc. Lafayette, CO). Target sequences for the four duplexes in the siRNA-SEPT9 (MSF) pool correspond to the following loci of the SEPT9_v1 transcript (accession number AF189713): 5'GGAGAUCACCAUCGUCAAA (546 bp to 564 bp); 5'GGUAAAUCCACCUUAAUCA (1024 bp to 1042 bp); 5'GAGAAAGGCGUCCGGAUGA (1147 bp to 1165 bp); 5'CCAACGGCAUCGACGUGUA (1496 bp to 1514 bp). Mock transfected and siCONTROL RISC-Free siRNA supplied by the manufacturer were used as negative controls. Functional studies were performed 72 hours post-transfection, which was the time point with the greatest decrease in expression.

Stable knockdown in BT-549 cells was achieved using the pRNA-H1.1/Retro vector with either a Sept9_v1-specific shRNA construct or a scrambled sequence shRNA cassette provided by the manufacturer as a negative control (GenScript Corporation, Scotch Plains, NJ). The

SEPT9_v1 shRNA construct targeted the unique 5'UTR, spanning base pairs 15 through 33 (sense strand target sequence; 5' GGCCCAGGATTAGCGCCCT 3'; Genbank accession number AF189713). Following sequence verification of the constructs, 5 μg of purified plasmid DNA were transfected into PT67 cells to produce viruses, which were then used to retrovirally transduce the BT-549 target cell line. Polyclonal stable cell lines were selected in hygromycin (40μg/ml) for one week.

Statistics Analysis

The ANOVA test was used to determine statistical significance when comparing quantitative phenotypic differences between parental, vector and SEPT9 transductants. The Wilcoxon signed-rank test and the Student's t test were done to assess statistical significance when analyzing patient data from the TMA. In some instances, Student's t test was used to confirm statistical significance between vector and SEPT9 transductants. For all tests, statistical significance was defined as P =0.05. Error bars in the graphs presented here represent the SE.

Results

High SEPT9_v1 expression correlates with clinicopathological variables

SEPT9_v1 staining by immunohistochemistry was low in the mammary gland epithelial cells from normal primary breast tissue present in the tissue microarray whereas 50% of primary invasive breast cancer tumors showed medium to high expression (Fig 2.2). We next wanted to determine if SEPT9_v1 expression correlated with clinical and pathologic patient variables. From 152 patient samples of invasive breast carcinoma present on the TMA, 152 were available to score for SEPT9_v1 staining and 136 had complete clinicopathologic data for statistical analysis. Patient samples were annotated for several clinicopathologic variables, including tumor size, ER status, PR status, HER2/neu expression, lymph node status, patient age and tumor

grade. Because there is no published evidence as to a threshold of expression that is required for proper SEPT9_v1 function, we included all positively stained samples in our analysis. Interestingly, there was a trend toward higher SEPT9_v1 staining correlating with ER and PR positive tumors (P = 0.0006 and P=0.014, respectively; Wilcoxon rank test; Fig 2.3). Surprisingly, a low SEPT9_v1 expression was associated with high grade tumors (grade 3) as compared to grade 2 (P=0.0286; ANOVA test Fig 2.3). However, there was an increase in SEPT9_v1 expression between grade 1 and grade 2 tumors.

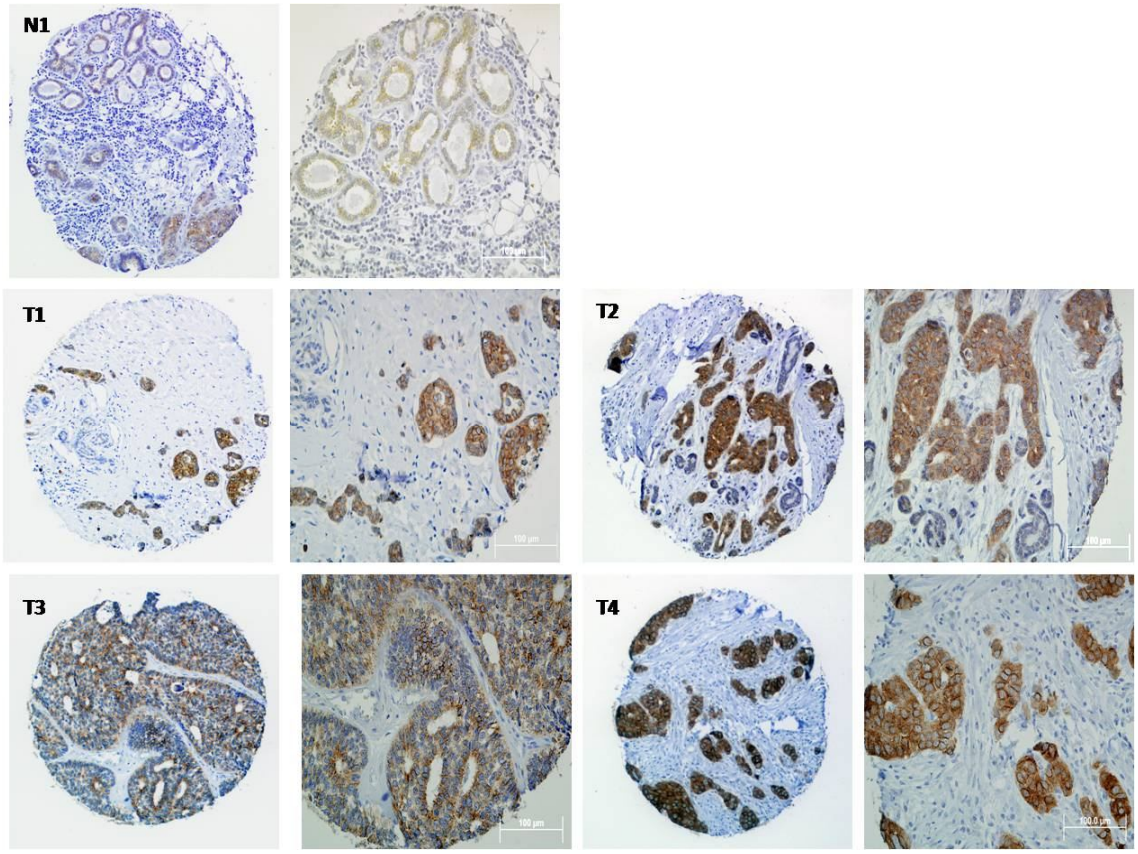

Fig 2.2: SEPT9_v1 immunohistochemistry of primary breast tumors of the breast cancer tissue microarray

Set of representative examples of primary samples of normal (N) and breast cancer tumors (T) tissues stained by immunohistochemistry for the SEPT9_v1 isoform. Note the low staining in normal mammary epithelial cells of the ducts (N1) but strong staining in the cells of the breast tumors (T1-T4). Magnifications X10 (*left*) and X40 (*right*).

Clinicopathologic variables	Patients with variable	SEPT9_v1 expression Mean ± SE	p value
Age			
<50	52	2.2404 ± 0.129	N/S
≥50	100	2.2367 ± 0.078	
Size			
< 2 cm	87	2.1628 ± 0.083	N/S
≥ 2 cm	65	2.3385 ± 0.111	
Lymph Nodes			
Positive	42	2.2262 ± 0.125	N/S
Negative	57	2.1667 ± 0.107	
ER expression			
Positive	90	2.4056±0.081	0.0006*
Negative	45	1.8926±0.133	
PR expression			
Positive	73	2.3904 ± 0.090	0.0142*
Negative	63	2.0503 ± 0.112	
Her2/*neu*			
Positive	40	2.2500 ± 0.132	N/S
Negative	96	2.2083 ± 0.087	
LVI			
Positive	47	2.1986 ± 0.124	N/S
Negative	91	2.2491 ± 0.089	
Grade			
1	13	2.1538 ± 0.205	0.0286**
2	60	2.4333 ± 0.109	
3	63	2.032 ± 0.1050	

*Wilcoxon rank test p-value ** ANOVA F test overall p-value

Fig. 2.3: High SEPT9_v1 correlates with estrogen receptor and progesterone receptor positive status breast cancer tumors

Statistical analyses of clinicopathologic characteristics from 152 primary invasive breast carcinoma (TMA 64) samples indicate that higher SEPT9_v1 mean (Mean+SE)expression correlates strongly with estrogen positive (ER+) status and have a weaker association with progesteron positive (PR+) status. Lower SEPT9_v1 mean expression was correlated with tumor grade 3 and high SEPT9_v1 expression with tumor grade 2. P values were calculated using the Wilcoxon rank test, except for tumor grade (**) for which the P value was calculated using ANOVA.

High expression of SEPT9_v1 leads to acquisition of oncogenic phenotypes

To examine the role of increased expression of SEPT9 on cellular characteristics, we retrovirally transduced several cell lines that showed no or low endogenous SEPT9_v1 expression, MCF10A, HPV 4-12 and Hs578t, with cDNA constructs of SEPT9 variants, *SEPT9_v1* and/or *SEPT9_v3*. First we analyzed the effect of ectopic expression of SEPT9 isoforms on cell proliferation by manually counting cells at different time points and by the WST-1 proliferation assay. High expression of SEPT9_v1 dramatically increased the proliferation rate of all the cell lines as compared to parental and vector controls (Fig 2.4B and Fig 2.6A). In contrast, high expression of isoform SEPT9_v3 dramatically lowered the growth rate of MCF10A cells, suggesting a potential tumor-suppressive or dominant-negative function, which needs to be characterized in future studies (Fig 2.4B; left panel). In addition, high expression of SEPT9_v1 increased the mitotic index of HPV 4-12 and MCF10A as compared to controls, confirming the high proliferative state of SEPT9_v1 transductants (Fig 2.5).

To determine if impaired apoptosis contributed to the increased growth rate, we assessed the percentage of apoptotic cells following camptothecin treatment to induce apoptosis. HPV 4-12 cells were insensitive to camptothecin-induced apoptosis, likely due to impaired p53 function as a result of the HPV E6/E7 immortalization. There was no significant difference in apoptotic response between the controls and SEPT9_v1-overexpressing cells for all cell lines without camptothecin treatment. However, overexpression of SEPT9_v1 significantly decreased the percentage of apoptotic cells in the MCF10A line following exposure to camptothecin (Fig 2.6 B).

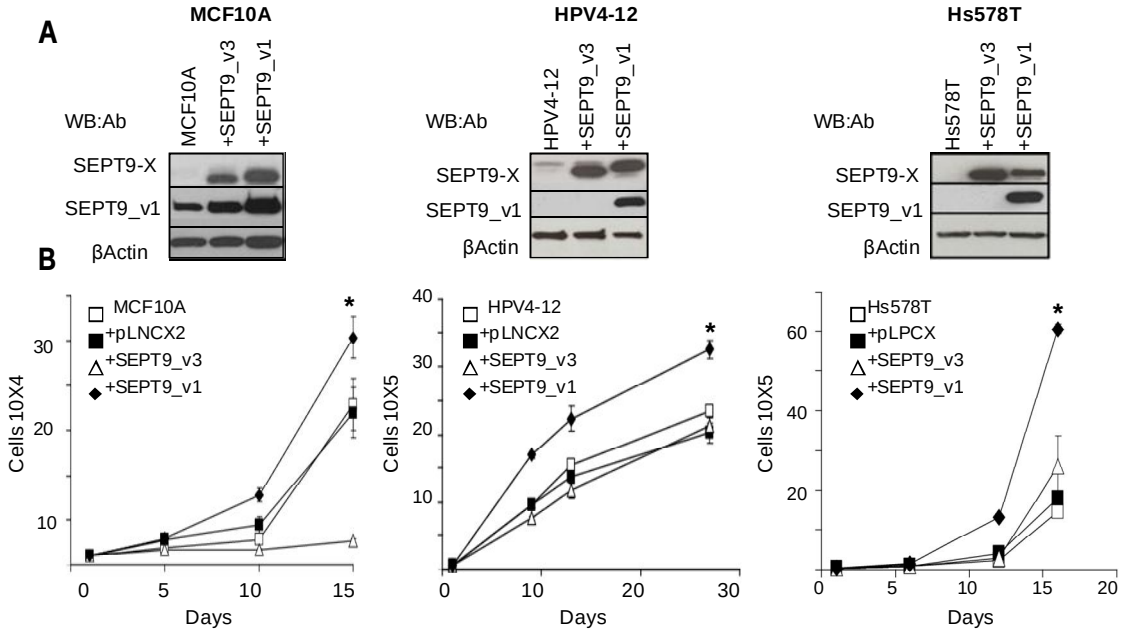

Fig 2.4: SEPT9 retroviral expression model

(A) Western blotting shows the over-expression of SEPT9_v1 and SEPT9_v3 following retroviral transduction in MCF10A (left), HPV 4-12 (middle), and Hs578t (right) cells compared with parental controls. Beta-actin was used as a loading control. (B) Growth curves showed increased growth kinetics of the polyclonal SEPT9_v1 transductants compared to empty vector, parental and SEPT9_v3 transductants in the three cell lines. Points indicate the average results of three independent experiments: bars, SE. Student t-test *p<0.05

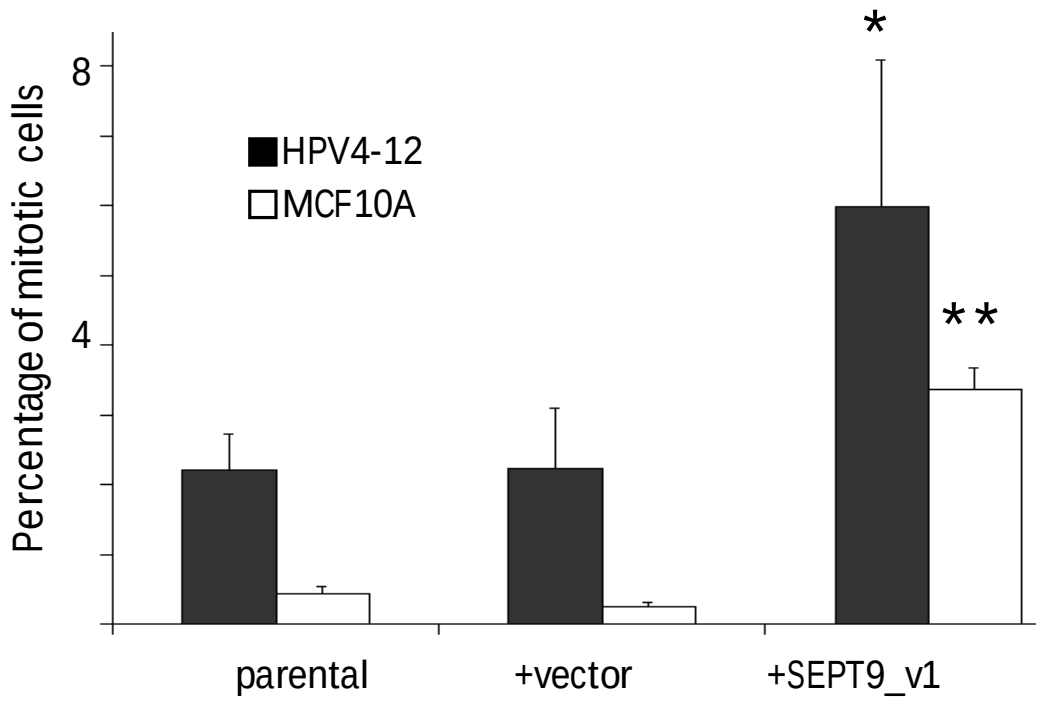

Fig 2.5: SEPT9_v1 increases mitotic index of IHMECs

SEPT9_v1 over-expression increased the mitotic index more than two-fold in HPV4-12 and more than seven-fold for MCF10A cells compared to the parental and empty vector controls. The percentage of mitotic cells in three independent experiments is shown (* denotes $p < 0.04$, ** denotes $p<0.0005$; ANOVA).

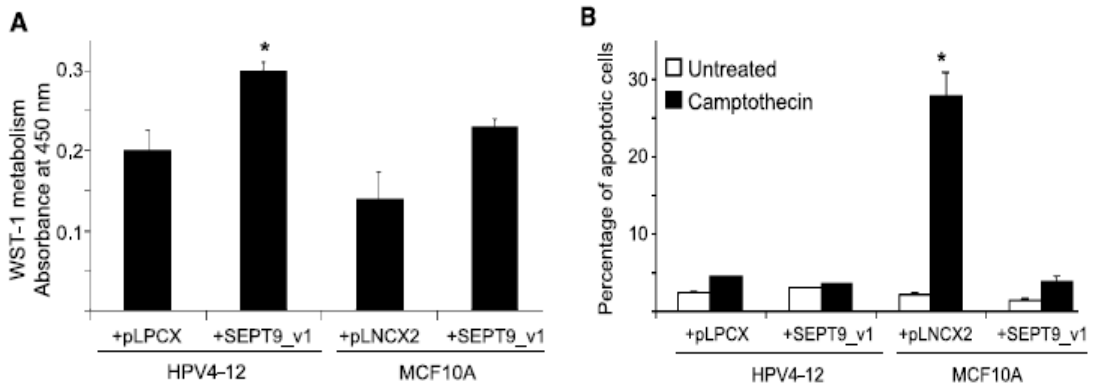

Fig 2.6: SEPT9_v1 over-expression increases cell proliferation in IHMECs and decreases apoptotic response in MCF10A

(A) This cell proliferation colorimetric assay showed that SEPT9_v1-over-expressing cells proliferated faster than the empty vector controls in IHMECs. Cells were treated for 3 h with the WST-1 substrate and absorbance was measured at 450 nm after 48 h for HPV4-12 and 24 h for MCF10A (*p<0.05). (B) SEPT9_v1 over-expression inhibits camptothecin-induced apoptosis in MCF10A cells compared with parental and empty vector controls. Cells were treated with 10 mM camptothecin for 24 h and the percentage of apoptotic cells was determined by flow cytometry using an Annexin V-Alexa Fluor 488–conjugated antibody. HPV4-12 cells were resistant to the induction, as the vector control showed no significant difference in the percentage of apoptosis between untreated and camptothecin-treated cells (*p < 0.05).

We also noted a cellular morphology change reminiscent of an epithelial to mesenchymal transition (EMT), which is characteristic of epithelial cancers, for cells with high expression of SEPT9_v1, and for some of the cells over-expressing SEPT9_v3 in MCF10A and Hs578t lines (Fig 2.7). The control cells displayed the usual organized and cuboidal appearance of epithelial cells. The cells ectopically expressing SEPT9_v1 became elongated, almost fibroblastic or mesenchymal in morphology. This morphology change was confirmed by increased vimentin expression as described below in Fig 2.12. In previous reports, similar morphology changes were associated with increased motility and invasiveness (99).

As cancer progression is often characterized by the capabilities of tumor cells to invade surrounding tissue and metastasize to distant sites, we used the Matrigel model of a basement membrane to determine if the SEPT9-transductants acquired an invasiveness phenotype. We found that ectopic expression of SEPT9_v1, but not SEPT9_v3, in MCF10A, HPV 4-12 and Hs578t cells significantly increased invasiveness as compared to controls (Fig 2.9A, B and D). Additionally, multiple polyclonal lines of MCF10A cells with high SEPT9_v1 showed increased invasion, indicating that the results were not due to a specific integration site or expression of a predominant clone (Fig 2.8 and 2.9C). Using a scrape motility assay, we also found that high SEPT9_v1 expression increased motility in MCF10A and HPV4-12 cells compared to the other variants and controls used in this assay. Additionally, the MCF10A polyclonal lines with high SEPT9_v1 expression were also tested and showed the same pattern (Fig 2.10A and B).

Next, the ability of high SEPT9_v1 ectopic expression to promote a phenotype indicative of cellular transformation was tested by analysis of a focus formation assay. Foci formation was not observed in the immortalized cell lines HPV 4-12 and MCF10A, indicating that ectopic expression of SEPT9_v1 alone is not sufficient to transform normal cells. However, the BCC

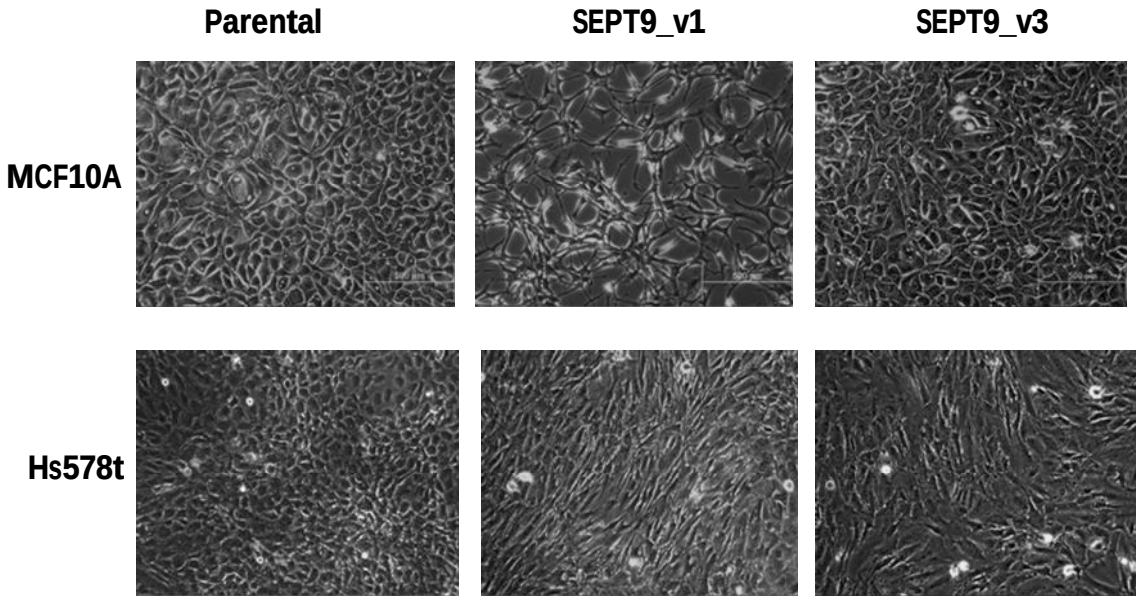

Fig 2.7: High SEPT9_v1 expression promotes an epithelial to mesenchymal transition (EMT)

Top: MCF10A SEPT9_v1 transductants showed a change in morphology from cuboidal organized epithelial cells, such as the parental control, to spindle-like elongated disorganized morphology resembling a fibroblastic or mesenchymal cell appearance. SEPT9_v3 did not have an effect when compared to controls. Bottom: Hs578t both SEPT9_v1 and SEPT9_v3 transductants showed EMT as compared to parental control.

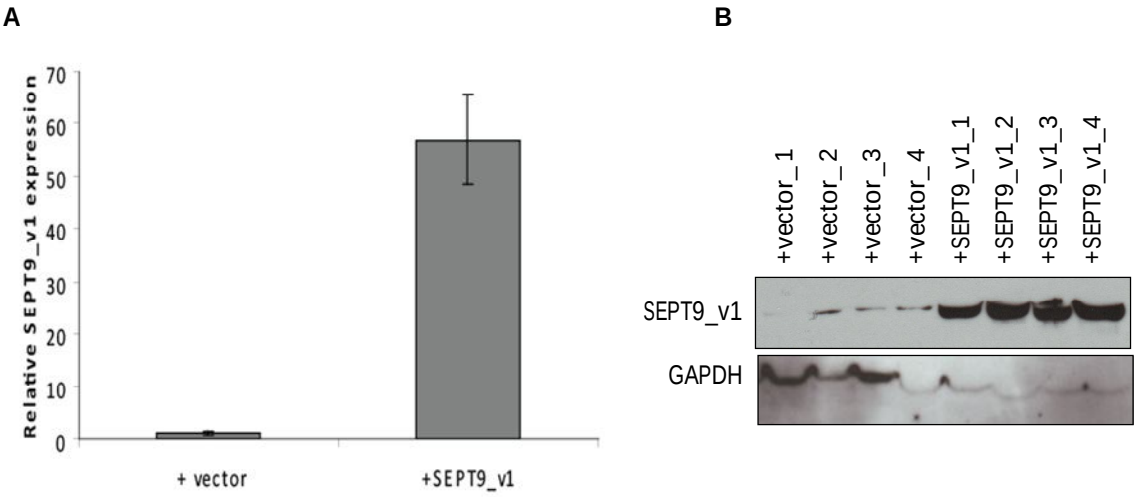

Fig 2.8: SEPT9_v1 expression of multiple polyclonal populations of MCF10A cells over-expressing SEPT9_v1

(A)Quantitative real time PCR showing the relative expression of SEPT9_v1 retroviral construct against GAPDH loading control in vector and SEPT9_v1 transductants. The average relative expression of four independent polyclonal population of MCF10A for vector and SEPT9_v1 construct is depicted. SEPT9_v1 transductants shows approximately a 6-fold increase in SEPT9_v1 expression overall. (B) Western blot analysis showing over-expression of SEPT9_v1 in each independent polyclonal population. These polyclonal lines were used in several of the subsequent experiments to eliminate the possibility that the results were due to a predominant clone.

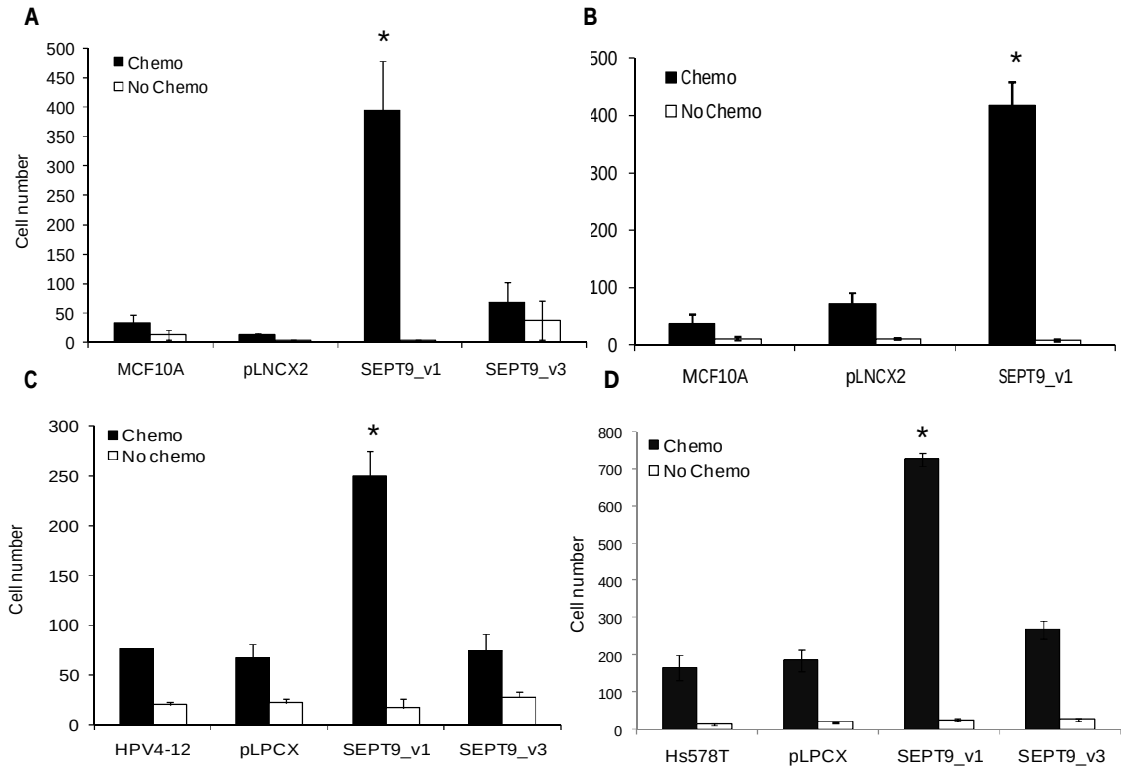

Fig 2.9: High SEPT9_v1 expression increased invasiveness

SEPT9_v1 over-expression promotes invasion in MCF10A (A) MCF10A multiple polyclonal transductants (B) HPV4-12 (C) and Hs578T (D) cells when compared with SEPT9_v3 transductants, parental, and empty vector controls. A Transwell Matrigel invasion assay was done in the presence of a chemoattractant ("chemo"), such as serum. Cells were also plated without the presence of chemoattractants as controls. Columns represent average number of invading cells of three independent experiments; bars, SE. *, $p < 0.0003$, ANOVA.

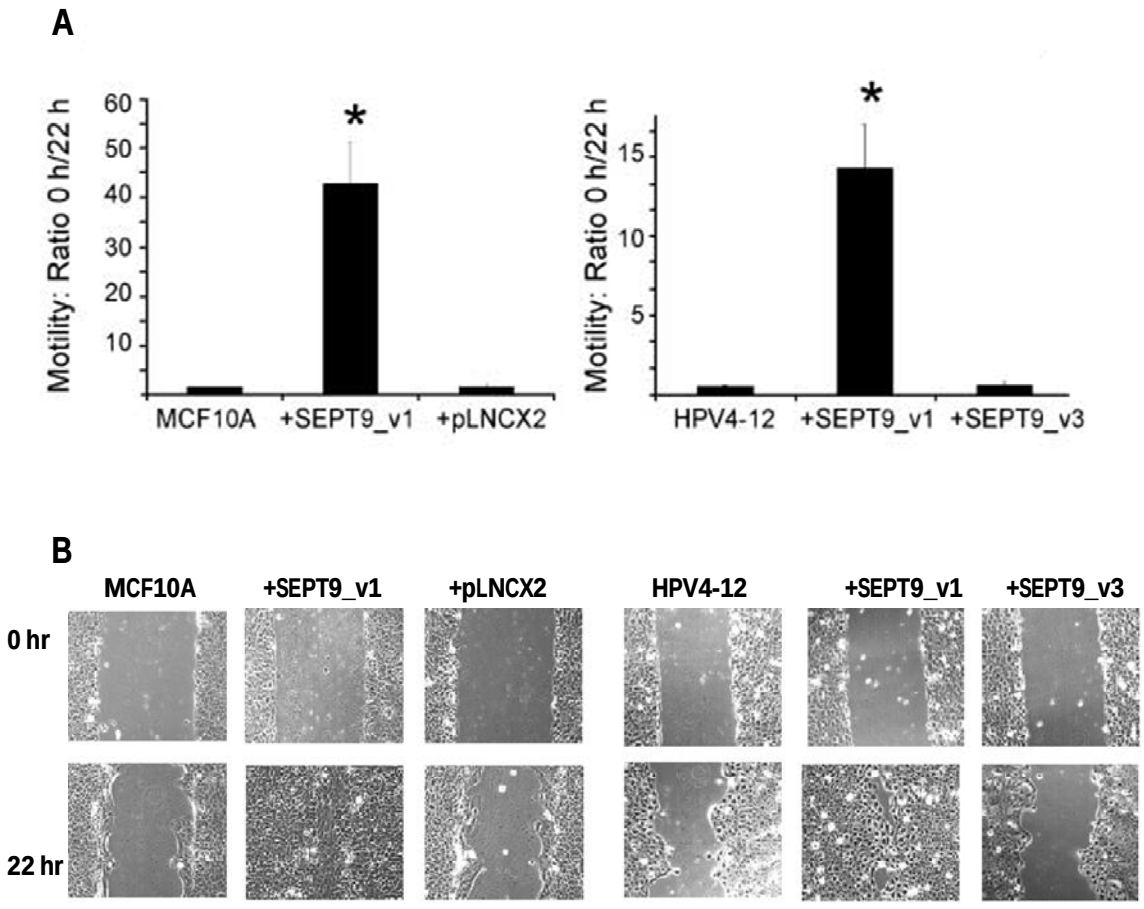

Fig 2.10: High SEPT9_v1 expression increased cellular motility

(A) A wound was created in a confluent culture and wound closure was measured after 22 h as a measure of cellular motility. SEPT9_v1 over-expression resulted in a 6- to 10-fold increase in motility compared with SEPT9_v3-over-expressing cells, empty vector, and parental cell line controls for both, HPV4-12 and MCF10A cells. The area of the wound was quantified using ImageQuant software, and the graphs depict the ratio of the area of three initial wounds to the area of the closed wounds. Average of three experiments is depicted in the graphs; *bars*, SE. *P<0.001, ANOVA. (B) Representative images of the MCF10A and HPV 4-12 scrape motility assay using a Leica inverted microscope with phase contrast optics and 20x objective.

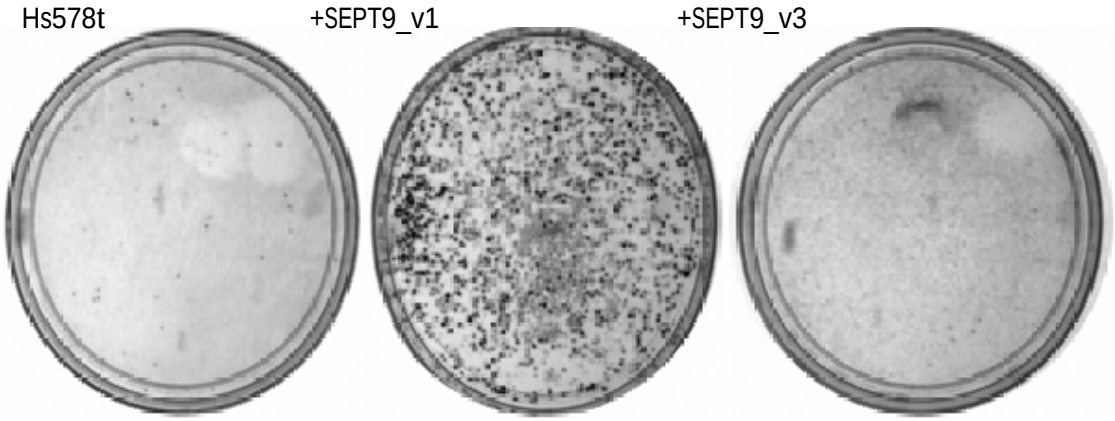

Fig 2.11: High SEPT9_v1 increases foci formation

Over-expression of SEPT9_v1 in Hs578t cells induced foci formation as compared to parental and SEPT9_v3 isoform, after prolonged culture. Cells are stained with methylene blue and colonies were photographed.

Hs578t transduced with SEPT9_v1 showed enhanced foci formation when compared with SEPT9_v3 transductants and parental cells (Fig 2.11).

High SEPT9_v1 co-localizes and increases vimentin expression in IHMECs

The breast cancer cell line Hs578T is classified in the mesenchymal-like group and expresses high levels of vimentin, a cytoskeletal protein marker for mesenchymal cells that has been shown to increase cellular motility and invasiveness in MCF7 cells (100). We hypothesized that this feature of Hs578T cells, in addition to the over-expression of SEPT9_v1, could contribute to the increased invasion and foci formation of the SEPT9_v1 transductants when compared to the IHMEC lines, which do not express high levels of vimentin. Therefore, we studied the interaction between vimentin and SEPT9_v1 by immunoprecipitation. We found co-immunoprecipitation between vimentin and SEPT9_v1 only in Hs578T cells with high SEPT9_v1 expression but not in HPV4-12 cells with high SEPT9_v1 expression or either parental cell line. This indicates that up-regulation of both vimentin and SEPT9_v1 were needed for their interaction (Fig. 2.12A). In support of this, we also noted strong co-localization of SEPT9_v1 and vimentin by immunofluorescence when SEPT9_v1 was highly expressed (Fig. 2.12B panels j and t). In addition, high expression of SEPT9_v1 in MCF10A and Hs578T cells increased vimentin expression as shown by immunofluorescence (Fig 2.12B, panels i and s versus panels d and n). This data further supports the epithelial to mesenchymal morphology change described above and is suggestive of coordination between vimentin and SEPT9_v1 for cellular transformation.

Depletion of SEPT9_v1 in BCCs reverses oncogenic phenotypes

To test further our hypothesis that the SEPT9_v1 isoform contributes to tumorigenic phenotypes, we questioned whether lowering its expression would reverse these phenotypes in breast cancer cell lines that normally showed high endogenous expression. We used two

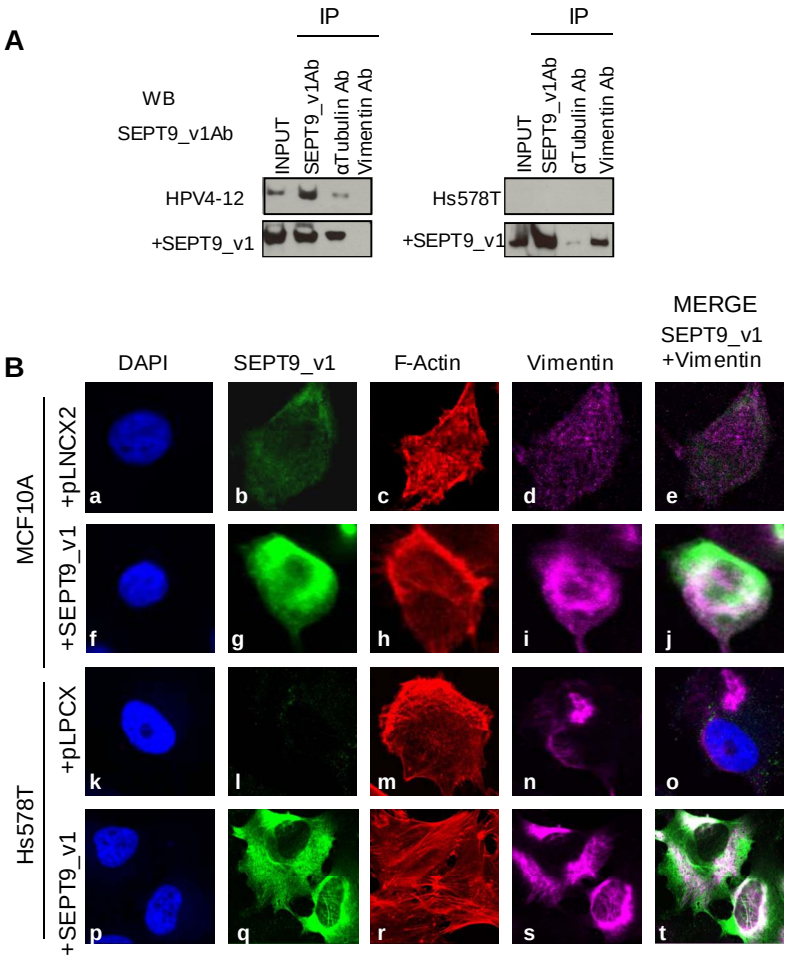

Fig 2.12: SEPT9_v1 immunoprecipitates and co-localizes with vimentin and over-expression of SEPT9_v1 causes increased vimentin expression in MCF10A and Hs578T cell lines.

(A) Vimentin co-immunoprecipitated with SEPT9_v1 in Hs578T cells, but not in HPV4-12 cells, only when both proteins were over-expressed (top blots versus bottom blots). SEPT9_v1, alpha tubulin, and vimentin antibodies were used for immunoprecipitation and the samples were subsequently immunoblotted for SEPT9_v1. Whole cell lysates from the parental cell lines were used for as shown in the blots in the top panel. Whole cell lysates from cells transduced with the SEPT9_v1 construct were used for immunoprecipitation for the blots represented in the bottom half of the image. (B) Immunofluorescence studies indicate that vimentin co-localizes with SEPT9_v1 in interphase cells, as indicated by the white areas where the green and magenta overlap, and more intense staining of vimentin is observed in SEPT9_v1-over-expressing cells, supporting the hypothesis of an epithelial to mesenchymal transition. The DNA is stained with DAPI (panels a, f, k, and p), SEPT9_v1 is green (panels b, g, l, and q), vimentin staining is shown in purple (panels d, i, n, and s) and the merged images of SEPT9_v1 and vimentin are shown in the last column (panels e, j, o, and t).

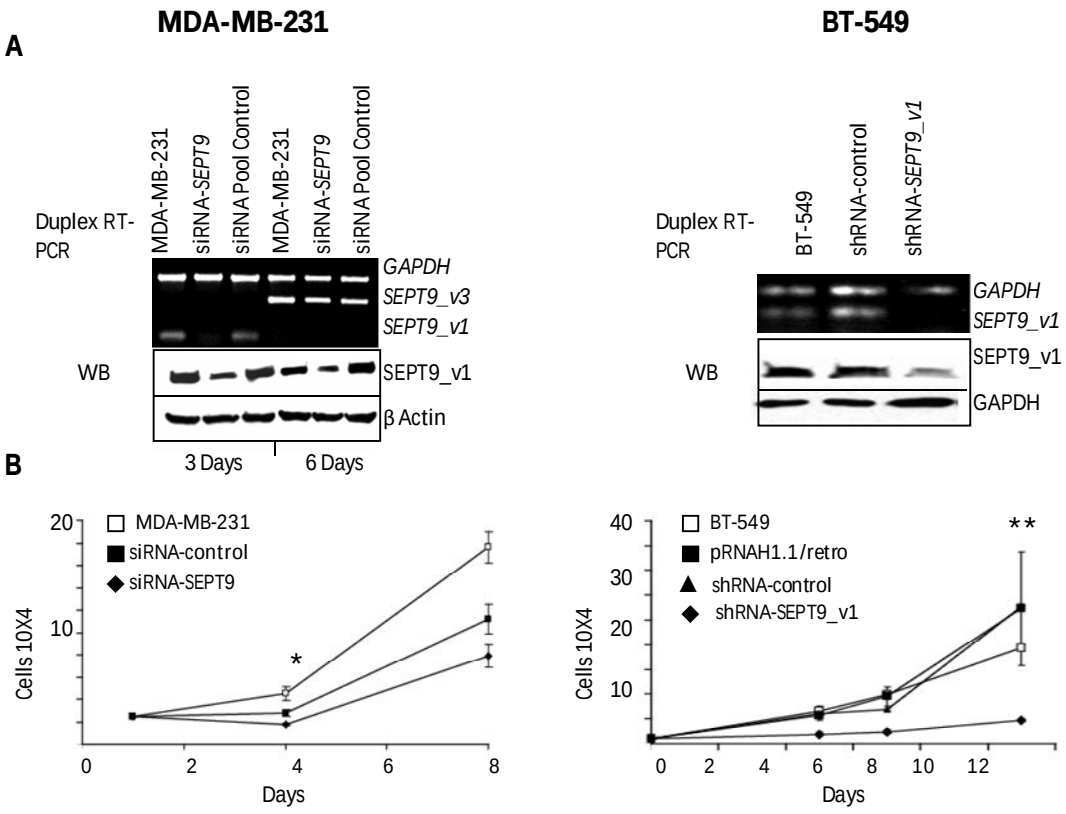

Fig. 2.13: siRNA and shRNA mediated knockdown of SEPT9_v1 in BCCs with high endogenous expression level results in the loss of tumorigenic cellular phenotypes.

(A) Transient transfection of siRNA to deplete SEPT9_v1 in MDA-MB-231 (left) was assessed 72h post-transfection by semi-quantitative duplex RT-PCR, which shows specific knockdown of SEPT9_v1 mRNA levels by > 80% compared to controls, relative to GAPDH. *Bottom left,* immunoblot to validate the specific knockdown of SEPT9_v1 protein. Densitometry showed that >60% of SEPT9_v1 protein was lost 72 hours post-transfection, and knockdown persisted for six days, compared to the parental and mock control, relative to the β-actin. Specific stable knockdown of SEPT9_v1 by shRNA in BT-549 cells (right) showed >80% depletion of SEPT9_v1 mRNA. *Bottom*, results of Western blotting, which reveals that > 70% of SEPT9_v1 protein is lost in the shRNA-expressing polyclonal cell population when compared to the parental cells and cells expressing a scrambled shRNA negative control, relative to the GAPDH. (B) Depletion of the endogenous SEPT9_v1 isoform in BCCs impaired cell growth compared to the parental and negative controls (*left***,** MDA-MB-231; *right*, BT-549). *, P<0.03; ** P<0.003.

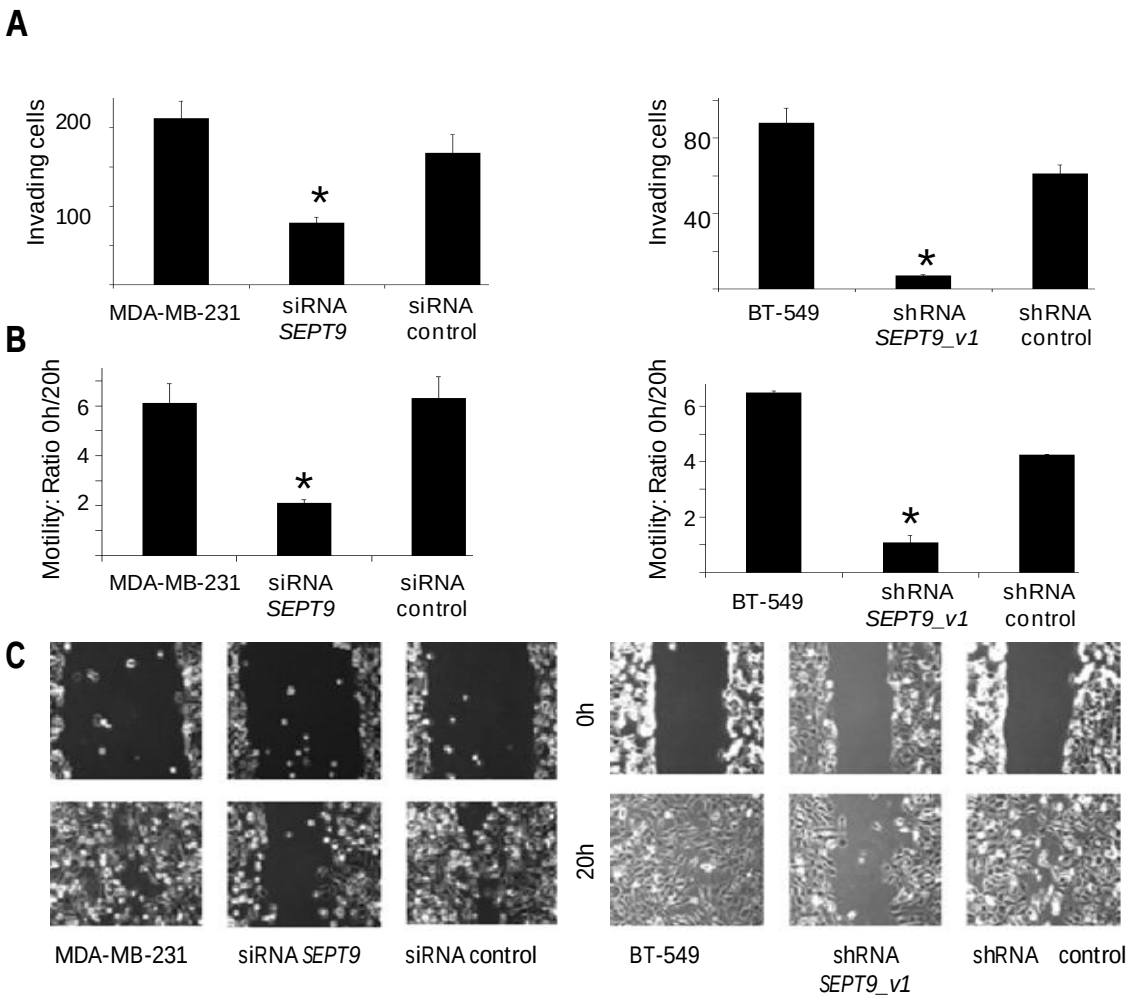

Fig 2.14: Depletion of SEPT9_v1 in BCCs reverses invasiveness and motility phenotypes

(A) Both transient and prolonged, stable knockdown of SEPT9_v1 in BCCs resulted in a decrease in the number of invading cells compared to parental and mock controls, by two-fold for MDA-MB-231 (right) and by more than seven-fold for BT-549 cells (left). *, P<0.008 by ANOVA. (B) SEPT9_v1 depletion causes a reduction in cell motility, in MDA-MB-231 (left) and BT-549 (right) cultures. Cells with decreased SEPT9_v1 were not able to close the wound in the confluent culture, when compared to parental and negative controls, after 20 h. The graphs show that SEPT9_v1 ablated cells have reduced motility by >3-fold in MDA-MB-231 cells (left) and 6-fold in BT-549 cells (right). Columns, mean ratio of the initial wound area to the final wound area, ±SEM, from triplicate experiments; *bars*, SE. *, P<0.008, as determined by the ANOVA test for statistical significance. (C) Representative images of three motility assays for MDA-MB-231 (left) and BT-549 (right) are depicted. A wound was created in a confluent culture and wound closure was measured after 20-22 hours as a measure of cellular motility.

different approaches in two breast cancer cell lines. First, we transiently transfected MDA-MB-231 cells, which predominantly over-expressed SEPT9_v1 protein compared to other isoforms, with a pool of four siRNAs that targeted the SEPT9 locus. Seventy-two hours post-transfection, there was an 80% decrease of SEPT9_v1 mRNA and a 60% decrease in SEPT9_v1 protein levels compared to the mock transfected and non-targeting (siControl) negative controls (Fig 2.13A, left panel). Other SEPT9 isoforms were not affected (Fig 2.13A, left panel and data not shown). Also, we used a stable shRNA construct to permanently and specifically decrease SEPT9_v1 expression in BT549 breast cancer cells by targeting the isoform-specific 5' UTR. This resulted in an 80% decrease in endogenous SEPT9_v1 mRNA expression and decreased protein expression by more than 70% compared to the parental and the scrambled shRNA controls (Fig 2.13, right panel).

For both lines, cells with decreased SEPT9_v1 expression showed inhibited cellular proliferation (Fig 2.13B), decreased invasion in the presence of chemoattractant (Fig 2.14A) and impaired cellular motility (Fig 2.14B and 2.14C), when compared to mock transfected and non-targeting/scrambled construct controls. In MDA-MB-231 cells in which SEPT9_v1 expression is transiently decreased by SEPT9 locus siRNA, the growth curves indicated a significant difference between the SEPT9 knockdown cells and the control cells at day four ($p=0.03$; Student's t test) while there is not a significant difference between the parental and the negative controls. However, at day eight, the difference in growth rates becomes less significant, likely due to a return of SEPT9_v1 expression since loss of expression was transient and increasing by day six, as indicated by the Western blot. As expected, the results obtained with the stable knockdown were much more striking than the transiently depleted cells, likely due to a more efficient and isoform-specific knockdown of SEPT9_v1 in these cells. These two strategies support the initial hypothesis implicating SEPT9_v1 in cell transformation in cell cultures studies.

Discussion

To further examine if altered SEPT9_v1 expression was relevant to the pathogenesis of breast cancer, we analyzed expression in an invasive breast cancer tissue microarray panel and developed SEPT9_v1 expression models in immortalized mammary epithelial cells. Previously in our laboratory, we analyzed SEPT9_v1 expression in a patient-matched normal and primary breast cancer tissue panel and found that 70% of the primary breast cancer tissue samples showed high cytoplasmic SEPT9_v1 staining as compared to absent or low staining in matched normal control tissues (20). In the present study, after analyzing SEPT9_v1 expression in a TMA of samples from patients with invasive breast carcinomas with clinicopathological variables, we found that high SEPT9_v1 expression correlated with ER+ and PR+ positive tumors. This might suggest that high SEPT9_v1 expression is relevant in hormone receptor positive tumors which account for 65% to 75% of breast cancers (101). Interestingly, SEPT9 expression was shown to be correlated to BRCA1 expression in a microarray study annotated in GEO (Gene Expression Omnibus) profiles. Most BRCA-deficient tumors tend to be estrogen (ER-) receptor negative and progesterone (PR-) negative (102). Hormone receptor positive tumors are responsive to hormone therapy such as tamoxifen, and the chance of patients to respond to therapy is generally 80% (101, 103, 104). Further studies to tease out relationships between hormone receptor status, BRCA1 status and SEPT9_v1 expression will be extremely useful to characterize SEPT9_v1 as a potential biomarker in breast cancer initiation, aggressiveness and therapy.

On the other hand, it is possible that SEPT9_v1 up-regulation is associated with cancer initiation. For example, SEPT9_v1 could modulate the development of neoplastic lesions or DCIS during breast cancer progression. The majority of breast cancer tumors started by being estrogen and progesterone receptor positive, but as the tumor progress they tend to lose

expression of these receptors (105). Future studies are crucial to determine if SEPT9_v1 will be an important biomarker for prognosis or treatment options, given that hormone-receptor positive tumors are better treated with tamoxifen while negative tumors are treated with conventional chemotherapeutic drugs, especially drugs that target cytoskeletal proteins important for cell division. In fact, recent studies support the importance of SEPT9 isoforms as biomarkers for cancer prognosis and therapy. For example, deVos *et al.* showed that circulating methylated SEPT9 DNA is a potential biomarker for colorectal cancer (86). Also, Amir *et al*., showed that high SEPT9_v1 expression is associated with resistance of cancer cells to microtubule disrupting drug such as paclitaxel (88).

We hypothesized that high SEPT9_v1 expression would be correlated with high grade tumors. It was surprising to find that while SEPT9_v1 expression did increase between grade 1 and 2 tumors it decreased between grades 2 and 3 tumors. One possible reason could be that SEPT9_v1 expression is high during the course of tumor growth which explains the increase in expression between grade 1 and 2. Then, by an unknown mechanism or an overall increase in genomic instability, SEPT9_v1 expression is gradually lost during tumor progression which could explain the low expression in grade 3 tumors. The fact that high SEPT9_v1 expression is not associated with lymph node status further supports the possibility that SEPT9_v1 expression may be important early in the pathogenesis of invasive breast cancer rather than metastatic disease. Still, additional studies, including analysis of more patient samples, are needed to confirm these results and to have a better sense of how SEPT9_v1 is modulating tumor progression in breast cancer.

We next hypothesized that increased expression of SEPT9 might contribute to malignant progression in mammary epithelial cells and wanted to examine if it contributed to the

development of invasive phenotypes. This hypothesis was supported by reports of increased expression of SEPT9 in human and murine cancers (75, 77, 83, 94). In addition SEPT9, as well as other human septins (i.e. SEPT5, SEPT6, SEPT11), are well-described MLL-fusion partners noted in acute leukemia cells (61-65, 106, 107). This evidence suggested important roles for one or more SEPT9 variants in tumorigenesis, but no compelling data supporting a role for SEPT9 in breast cancer had been reported to date. To test our hypothesis, we retrovirally transduced cDNA constructs of SEPT9 variants into IHMECs (HPV4-12 and MCF10A), which promoted the development of cellular phenotypes characteristic of malignant cells. Specifically, ectopic expression of SEPT9_v1 induced increased growth kinetics, accelerated cell proliferation, enhanced invasiveness, promoted an epithelial to mesenchymal morphology change with increased vimentin expression and increased cell motility when compared to controls. Similar results were seen, as well as enhanced foci formation, when SEPT9_v1 was ectopically expressed in a BBC line with low SEPT9-X and no SEPT9_v1 endogenous expression, Hs578T. Knockdown of SEPT9, and specifically to SEPT9_v1, in two cancer cell lines with high endogenous levels of SEPT9_v1 (MDA-MB231, BT-549) using RNAi techniques confirmed our hypothesis and substantiated our conclusions by rescuing tumorigenic phenotypes. Still, a rescue experiment expressing a SEPT9_v1 construct resistant to siRNA will be important in the future to further support the specificity of SEPT9_v1 effects on the cells. Together, our results provide compelling support that SEPT9_v1 may function as an oncoprotein in mammary epithelial cells to drive malignant progression. The association with invasiveness, motility and a mesenchymal phenotype suggests that up-regulation of SEPT9_v1 may be functionally important in progression to invasive or metastatic phenotypes.

The other abundant SEPT9 variant detected in our assays, SEPT9_v4* (SEPT9_v5), was previously noted to be up-regulated in tumor cells and showed only mild evidences of cell

transformation, suggesting that it might be a manifestation of tumorigenesis rather than a significant functional contributor to malignant progression (19). In addition, the observation that the SEPT9_v3 isoform dramatically decreased growth rates in MCF10A cells supports the idea that these isoforms of the same gene could be dynamically rearranged under the guidance of different signaling pathways to accomplish different intracellular functions. This work, combined with the data presented here, indicates that the SEPT9_v1 isoform contributes to oncogenesis when the SEPT9 locus is amplified or deregulated. However, further work to determine if the other SEPT9 isoforms are also involved in tumorigenesis, either as oncogenes or as tumor suppressors, will be necessary to clarify the role of this locus in breast cancer development.

To our knowledge, the effects of SEPT9_v1 on cell proliferation, motility and invasion in the context of cellular transformation have not been previously examined. Our studies provide compelling evidence supporting an important functional role for SEPT9_v1 in mammary tumorigenesis. Future efforts focused on mechanistic studies, to elucidate how specific SEPT9 isoforms coordinate different cellular functions, and to determine what regulates expression of one variant over another, should provide additional novel insights to the functional roles of SEPT9 in health and disease. In addition, further characterization of the SEPT9 variants in *in vivo* models should enhance our understanding of how cellular division and proliferation normally proceeds and how aberrations can lead to deleterious states such as breast cancer.

Acknowledgments

This work was supported by the NIH National Research Service Award #5-T32-GM07544 from the National Institute of General Medicine Sciences to E.A. Peterson, by the NIH National Cancer Institute grant RO1CA072877 to E.M. Petty and Department of Defense USAMRMC BC 980697 to L.M. Kalikin. We thank Hernan Roca for helpful data analysis and discussion and Donita L. Sanders for assistance with immunohistochemical protocols. We also thank Celina Kleer, M.D., for the primary normal breast tissue samples and the score of the tissue microarray, Stephen Ethier, Ph.D., for the HPV and SUM breast cell lines and Mousumi Banerjee, Ph.D for the statistical analysis of the tissue microarray.

Notes

Parts of this work were previously published as:

González, M.E., Peterson, E.A., Privette, L.M., Loffreda-Wren, J.L., Kalikin, L.M., and Petty, E.M., "High SEPT9_v1 expression in human breast cancer cells is associated with oncogenic phenotypes", *Cancer Res*. 2007 Sept 15; 67(18): 8554-8564.

CHAPTER III

SEPT9_v1 interactions with cytoskeletal proteins and JNK promote malignant progression

Summary

Septins are highly conserved cytoskeletal GTP-binding proteins implicated in numerous cellular processes from apoptosis to vesicle trafficking. Importantly, they also have been associated with human cancers and neurological disorders. We previously reported that high SEPT9_v1 expression in human mammary epithelial cell lines (HMECs) led to malignant cellular phenotypes (i.e. increased growth kinetics, invasiveness, motility, and aneuploidy), suggesting its role in oncogenesis. Our goal is to better understand how altered SEPT9_v1 expression may contribute to genomic instability and malignant progression.

To determine if SEPT9_v1 expression disrupts normal mitotic spindle formation and chromosome segregation, we analyzed SEPT9_v1 expression by immunofluorescence. SEPT9_v1 also interacted with alpha-tubulin, where its expression disrupted normal tubulin filaments. SEPT9_v1 expressing cells demonstrated striking cytokinesis defects, chromosome segregation abnormalities, and centrosome amplification, suggesting more than one molecular mechanism contributing to the development of aneuploidy or chromosomal instability. To determine if aneuploidy accelerated cell proliferation we examined flag-SEPT9_v1 transient expression in HMECs and found that increased cell proliferation may develop independently of aneuploidy. Further investigation of SEPT9_v1–associated molecular mechanisms underlying increased cell proliferation revealed that SEPT9_v1 stabilizes JNK, which can accelerate cell cycle progression.

While the roles of SEPT9 in malignant progression remain poorly understood, our work suggests that SEPT9_v1 may accelerate cell proliferation through the JNK signaling pathway and chromosomal instability through both cytokinesis and mitotic spindle defects.

Introduction

Genomic instability is a characteristic feature of carcinogenesis, especially in human tumors of epithelial origin, such as breast tumors. Genomic instability is broadly classified into two categories: microsatellite instability (MIN) associated with mutations in DNA repair genes and chromosome instability (CIN), which is recognized by numerical or structural chromosomal abnormalities (108). During normal mitosis the parent somatic cell divides to generate two daughter cells with a diploid number of chromosomes. In carcinogenesis, many tumors exhibit abnormal chromosome segregation during mitosis, which can lead to loss or gain of one or more chromosomes, also known as aneuploidy (109). These events have been associated with tumorigenesis by increasing the rate of chromosome mutations, including deletions and amplifications of critical genes involved in cell proliferation and/or survival (109). The various possible mechanisms that lead to the development of aneuploidy are described below (Fig 3.1).

Mechanisms of aneuploidy

Mitotic spindle defects

Proper mitotic spindle assembly is crucial for the subsequent segregation of chromosomes during anaphase (110). Mitotic spindle formation is orchestrated by the tight regulation of microtubule and microtubule organizing center (MTOC) proteins such as α/β–tubulin, γ–tubulin, and Aurora A kinase among others (110, 111). Mammalian cells have one MTOC, or centrosome, during interphase, usually located near the nucleus, and generally associated closely with the Golgi apparatus (111, 112). The centrosome is made of a pair of centrioles (111, 112). Microtubules are anchored with their "minus" ends in the centrosome, and because microtubules dissociate preferentially at this end, this anchoring has a stabilizing effect and MTOC-associated microtubules can grow very quickly (111, 112). During cell division, the centrosome is duplicated and each one moves to opposite poles in preparation for mitosis.

At this point, microtubule organization and dynamics are extremely important for the localization of the condensed chromosomes at the metaphase plate and their proper segregation later on in anaphase. The disruption of proper centrosome synthesis and/or organization and microtubule dynamics could lead to defects in mitotic spindle assembly and unequal distribution of chromosomes (112, 113). Chromosome mis-segregation may arise by lagging of chromosome movement, unipolar movement of chromosomes, multipolar spindles due to centrosome amplification, or the stabilization or destabilization of microtubules (109).

Defective attachment of chromatids

Each sister chromatid needs to be properly attached to the microtubules at the kinetochore before the cell enters anaphase during mitosis. In fact, cells have a complex and tightly regulated surveillance mechanism to ensure the proper attachment of each sister chromatid to microtubules called the spindle assembly checkpoint or mitotic checkpoint. This checkpoint is controlled by several proteins that serve as checkpoint sensors and signal transducers, which include BUB1, BUB3, BUBR1, MAD1, MAD2, CENP-E and the APC/CDC20 complex (113). Defective chromatid attachment to microtubules and improper separation may result in non-disjunction in which both sister chromatids may go to one daughter cell leading to the complementary gain and loss of chromosomes, thereby giving rise to aneuploidy in the daughter cells (109, 113).

Defective cytokinesis

Failure of cytokinesis may produce abnormal accumulation of chromosomes in a single cell, resulting in tetraploidy. Cytokinesis in vertebrates is governed by different core proteins including septins, which were identified by various large-scale screens in at least two distantly related animals (114). Loss or over-expression of these proteins may lead to cytokinesis failure, which may be visualized by the appearance of giant bi- or multinucleated

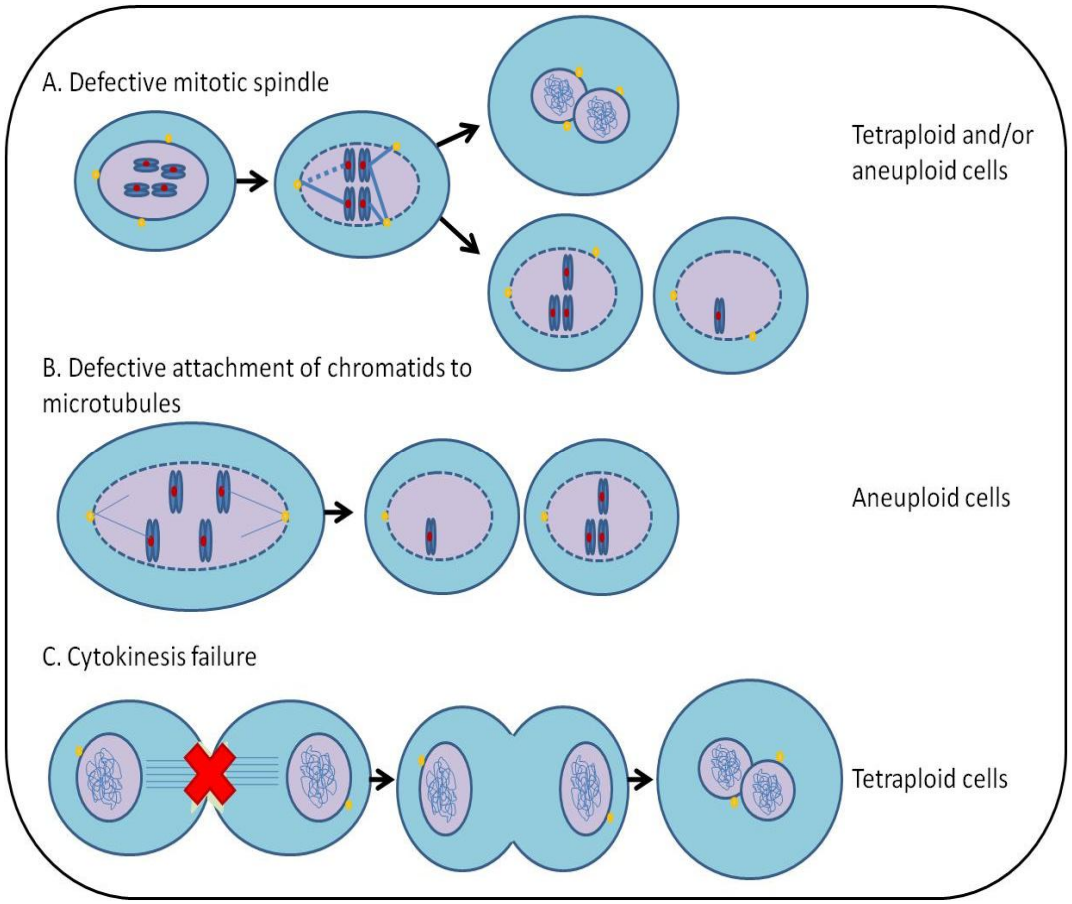

Fig 3.1: Mechanisms of aneuploidy

This diagram shows a representation of various examples of mitotic defects that can lead to aneuploidy. (A) A defective mitotic spindle which may include centrosome amplification can lead to chromosome mis-segregation or cytokinesis defects that give rise to aneuploid or tetraploid cells. (B) Defective attachment of chromatids to the spindle may occur by loss or mutations in spindle assembly proteins and/or mitotic spindle checkpoint proteins producing daughter cells with loss or gain of chromosomes. (C) Tetraploid cells can also arise from failure of the cell to complete cytokinesis. Any of these defects or a combination could lead to an increase in aneuploidy and a population of cells with genomic instability.

cells and/or cleavage furrow regression in live cells (114). Overall, this increases mitotic defects and chromosome mis-segregation in future mitoses. Currently, several lines of evidence suggest that tetraploidy is an important intermediate chromosomal state that plays a major role in the development of aneuploidy. In fact, different models demonstrate that aneuploidy may develop through chromosomal loss from a tetraploid intermediate and that this could be monitored by the appearance of micronuclei in tetraploid cells (115).

Aneuploidy and cancer

Although aneuploidy occurs frequently in malignant tumors its role in carcinogenesis is still controversial (109). It is debated whether aneuploidy is an important mechanism driving tumorigenesis or a non-specific secondary state that occurs during the process of cancer formation. There are several compelling lines of evidence that support the hypothesis that aneuploidy plays an active role in carcinogenesis. First, there is tumor specific aneuploidy such as in the progression of colon adenoma to carcinoma (116). Second, loss or gain of chromosomes in each generation of aneuploid cells is very high as compared to diploid cancer cell lines (117). Third, mutations in specific mitotic spindle checkpoint genes are strongly associated with different cancers including colon, breast and leukemias (113). Fourth, there are many pre-neoplastic lesions that show aneuploidy such as liver dysplasia and prostate intraepithelial neoplasias that subsequently progress to carcinoma (118, 119). Taken together, these observations suggest that the development of aneuploidy may drive oncogenesis. Still it is important to point out that there are a few diploid cancers in which aneuploidy cannot adequately explain the carcinogenesis process in these tumors.

Aneuploidy of cancer cells of certain types of tumors might be involved in the development of a more aggressive phenotype. Examples of possible ways in which aneuploidy could be involved in cancer progression are by creating (109):

1. Loss of heterozygosity leading to decreased or abnormal function of a mutated tumor suppressor gene
2. Gain of chromosomes or amplification of chrosmosomal regions causing the over-expression of oncogenes that drive tumorigenesis.
3. Destabilization of the structure of genes by DNA strand breaks that promote, deletion, amplification, and/or intra/interchromosomal rearrangements contributing to genomic instability.
4. Disturbance of genes that affect the balance of the spindle checkpoint apparatus or other cell cycle regulators

In summary, based on observations to date one can hypothesize that aneuploidy is one of the critical driving forces of carcinogenesis via a two-step mechanism in which cells become aneuploid, either by cytokinesis failure, mitotic spindle defects, or mutations in spindle checkpoint genes, creating a population of cells with unstable karyotypes and chromosomal instability. Those aneuploid cells that remain and are maintained by subsequent cell division create a lineage of cells with much higher overall genomic instability that may drive tumorigenesis and/or the development of more aggressive phenotypes. Thus, better understanding of aneuploidy in various cancers has important diagnostic, prognostic and therapeutic implications.

Septin cytoskeleton interactions: Implications in mitosis and cytokinesis

Since they were discovered in budding yeast, septins have been associated with cytoskeletal dynamics. Temperature sensitive mutations in yeast septins CDC3, CDC10, CDC11 and CDC12 were found to cause cell cycle arrest with major defects in budding morphology in the budding yeast *Saccharomyces cerevisiae* (1, 120, 121). Perhaps most interesting was the characterization of septin mutants which play a central role in cell cycle delays by triggering the mislocalization of

inhibitory cyclin dependent kinases (122). It was demonstrated that this mislocalization prevented the required degradation of inhibitors needed for cell cycle progression through G2/M, suggesting that septins helped regulate cell cycle progression through the association of mitosis-inducing protein kinases. Other studies in *Saccharomyces pombe* revealed that septins play a crucial role in organizing the cytoskeleton for mitosis and cytokinesis, when septins were mutated cytokinesis failure was observed (122). It was also found that septins have the ability to form microfilaments by interacting with cytoskeleton and filamentous proteins such as actin and myosin related proteins as well as the actomyosin ring in cytokinesis. These findings demonstrate that cytoskeleton organization is tightly coupled to cell cycle progression and provides compelling evidence suggesting the possibility of a critical cytokinesis related cell cycle checkpoint.

The homologies between mammalian and yeast septins can shed light on the functional role of human septins as regulators of cytoskeletal dynamics, cytokinesis and possibly chromosome dynamics, which are all crucial for proper cell division and cell cycle progression. The complexity of mammalian septins, with 14 known members that encode several alternative transcripts, makes it quite challenging to understand their functional role as cytoskeletal proteins important in cell division and cell cycle regulation. Despite this, several recent studies have elucidated the roles of mammalian septins in cytoskeletal dynamics, proper chromosome segregation, and completion of cytokinesis. In contrast to yeast septins that localized primarily on the cortical sites of the mother-bud neck, mammalian septins localize to the plasma membrane and throughout the cytoplasm along with microtubules and actin filaments.

A first indication that higher eukaryotic septins might interact with microtubules was the observation that Drosophila septins can bind to microtubules (MT) in vitro (123). In mammalian cells, SEPT1 was found to localize to spindle poles at the centrosomes and

microtubules throughout mitosis, to the midbody at telophase, and to the contractile ring during cytokinesis. SEPT1 also partially co-localized with Aurora B kinase, a mitotic protein important for chromosome segregation and cytokinesis (12).

Two independent studies showed similar results where SEPT9 demonstrated cell-cycle dependent distribution and septins were implicated in microtubule dependent functions by their interaction with α-tubulin. Surka *et al.* found that in interphase cells, mammalian septin SEPT9 (MSF) co-localized with actin, microtubules and other septins. In addition, they were able to determine that SEPT9_v1 (MSF-A) specifically localized with microtubules and this localization was disrupted by nocodazole treatment. Interestingly, when SEPT9 was depleted by siRNA or microinjection of specific anti-MSF antibody, the accumulation of bi-nucleated cells and failure cytokinesis was observed (24). Nagata *et al.* showed similar results in human mammary epithelial cells (HMECS) in which SEPT9_v1 was found to be localized at the mitotic spindle and microtubules at the midzone during mitosis. They also were able to co-purify SEPT9_v1 with α-tubulin and identified the GTP-binding domain of SEPT9 to be required for this interaction.

This association of septins with microtubules suggested a possible role in mitosis. In fact, a possible role of septins in chromosome attachment to spindle microtubules and in chromosome congression and segregation is suggested by reports delineating SEPT6 and SEPT2 localization as a network of fibrillar structures at the mitotic midzone of epithelial cells (37). Surprisingly, SEPT2 was found to be required for the proper localization of centromere-associated protein E (CENP-E) to the kinetochore for the proper attachment of chromosomes to spindle microtubules during mitosis. MDCK cells depleted of SEPT2 by siRNA showed mis-localization of CENP-E from the kinetochores and chromosomes fail to align properly and did not segregate correctly (37). SEPT7 was also found to interact with CENP-E and regulated its distribution to the kinetochores. When cells were depleted of SEPT7, CENP-E did not localize

appropriately to the kinetochores and the mitotic spindle checkpoint was activated due to misaligned chromosomes (47).

The mammalian septin heterotrimer Sept2:6:7 was found to bind to MAP4, a microtubule-binding protein. The heterotrimer was responsible for blocking the ability of MAP4 to bind to microtubules in vitro. The suppression of septin expression caused a striking increase in microtubule stability and an abnormal nuclear phenotype which was suppressed when MAP4 was also depleted (22). Together, these data identified a novel molecular function of septins in mammalian cells of modulating microtubule dynamics through the interaction with MAP4.

Most recently, it was demonstrated that SEPT9_v1 protein expression conferred resistance to microtubule-mediated HIF-1 inhibitors such as 2-methoxyestradiol and paclitaxel in various cancer cells (88). Previously, it was determined that HIF-1 transcriptional activation depends on an intact microtubule-cytoskeleton network (124, 125) and that SEPT9_v1 regulates HIF-1 stabilization and transcriptional activity (72). At the same time, SEPT9_v1 localized and interacted with microtubules (MT), therefore in this study it was concluded that cancer cells with high SEPT9_v1 expression were resistant to MT-dependent HIF-1 inhibitors specifically. Interestingly, no difference was found with MT-independent HIF-1 inhibitors such as YC-1 and 17-AAG, that had previously been shown to inhibit HIF-1 without affecting MT (88).

Mammalian septins are also required for the late stages of cytokinesis. For example, at least some septins were reported to be binding partners of Anillin, an actin-binding protein and a component of the cytokinetic ring, which recently was found to be over-expressed in diverse human tumors including breast cancer (126). Additionally, SEPT2 acted as a scaffold for myosin II and its kinases to ensure full activation of myosin II, which is necessary for the final stages of cytokinesis in mammalian cells (127). Also, SEPT2 and SEPT9 are required at the central spindle for the completion of cytokinesis, suggesting that septins play an important role coordinating

late cytokinesis events such as membrane targeting and/or fusion during abscission. Apart from cell division and cytokinesis, septins' interaction with microtubules might be involved in other cellular processes like microtubule–based vesicle transport in nervous transmission among others, which are beyond the scope of this study.

The multiple interactions that septins have with microtubules and other components of the cytoskeleton involved in mitotic events, whether by forming a regulating scaffold for mitotic proteins, and/or facilitating the interaction between microtubules and chromosomes, likely serve to regulate multiple steps of cell division, such as cytokinesis, spindle assembly and chromosome segregation. Given this, I hypothesized that high SEPT9_v1 expression increases genomic instability through its association with cytoskeletal proteins relevant to chromosome segregation and cell division. Therefore, I wanted to investigate whether or not SEPT9_v1 expression could impact tumorigenesis in mammary epithelial cells by promoting mitotic defects through its regulation of chromosome segregation and/or cytokinesis.

Materials and Methods

Cell lines

MCF10A and HCT116 were purchased from American Type Culture Collection (ATCC). HPV 4-12 was developed and provided by S.P Ethier (Karmanos Cancer Institute, Wayne State University, Detroit, MI). MCF10A was maintained in F12/DMEM 1:1 media containing L-glutamine, 15mM HEPES buffer and supplemented with 5% horse serum, 20 ng/ml of epidermal growth factor (EGF), 8 ug/ml of insulin, 500 ng/ml of hydrocortisone and 100 ng/ml of Cholera toxin (CT). HPV4-12 cells were maintained in F12 Nutrient Mixture with 5% fetal bovine serum (FBS), 10ng/ml EGF, 8 ug/ml insulin, 1 ug/ml of hydrocortisone and 100 ng/ml of CT. HCT116 cells were maintained in McCoy's 5A medium (modified) with L-glutamine and with 10% FBS.

Aneuploidy analysis

HPV4-12 and MCF10A cells retrovirally transduced with empty vectors or SEPT9 were grown to 70% confluence. Cells were treated with colcemid at 0.02 ug/ml for 18 hours to enrich for cells in metaphase. Then, cells were trypsinized and collected by centrifugation at 1000 rpm for 5 min. Cells were then washed with 1X PBS and incubated with a pre-warmed hypotonic solution (0.4 % KCL + 0.4 % sodium citrate) for 7 min at 37 °C with subsequent centrifugation. The resuspended pellet was fixed twice by dropwise addition of a 3:1 mixture of methanol and glacial acetic acid for 30 min and centrifugation between each fixation. Fresh fixative was then added, and the resuspended cell pellets were dropped onto clean microscope slides. Slides were air dried, stained in 0.54 mg/ml Giemsa solution, and destained in deionized water. After air drying, chromosomes were visualized and counted using an Olympus BX60 model microscope with a 100 X oil objective. Twenty-five metaphases were counted for aneuploidy, in triplicate, for each sample.

Immunofluorescence

For immunofluorescence analysis, cells were grown on two-chambered slides and fixed with 4% paraformaldehyde for 40 min at room temperature. Alternatively, cells were fixed 10 min with cold methanol at -20 °C followed by 1 min with acetone at -20 °C. Slides were then washed thrice in 1X PBS for 10 min, blocked for 1 h in blocking solution (5% dry milk, 1% BSA, 0.025% Triton X-100 in 1X PBS) at room temperature, and incubated overnight at 4°C with polyclonal rabbit anti-SEPT9_v1 (1:50), monoclonal mouse anti-α-tubulin (1:100), polyclonal rabbit-γ-tubulin (1:5,000), monoclonal anti- Flag (1:500) (Sigma-Aldrich Corp.) and/or polyclonal rabbit anti -Ki67 (1:50) (Abcam Inc.) primary antibodies diluted in blockinjg solution. Phalloidin conjugated to Alexa Fluor 568 was used to identify filamentous actin (F-actin). Alexa Fluor 488, Alexa Fluor 596 or Alexa Fluor 633 were used as secondary antibodies (Molecular Probes,

Invitrogen) at a 1:500 dilution in blocking solution for 1 h at room temperature. Slides were preserved in ProLong Gold mountaing media with 4',6-diamidino-2-phenylindole (DAPI) to stain the DNA. Cells were visualized using an Olympus BX60 model microscope (100 x objectives).

Transient transfection

SEPT9_v1 cDNA was subcloned into pCMV-3tag-1A (Stratagene) using Hind III and Sal I restriction sites, which encoded for SEPT9_v1 protein tagged with 3 Flag epitopes at the N terminus. MCF10A and HCT116 cells were transiently transfected with pCMV-3tag-1A or pCMV-3tag-1A-SEPT9_v1 plasmids using Fugene® HD transfection reagent following manufacturer's instruction. Briefly, 18 ul of Fugene® HD reagent was mixed with 6 ug of plasmid in Opti-MEM reduced serum media and incubated for 15 minutes at room temperature. The transfection complex was added dropwise to ~ 1.75 x 10^6 cells grown in 100 mm tissue culture plates. Cells were collected for immunofluorescence, metaphase spreads and lysates for western blot analysis at different time points after transfection dictated by the doubling time of the cells. Flag-SEPT9_v1 expression, aneuploidy analysis and cell proliferation using Ki67 staining for immunofluorescence was determined for each time point in triplicate.

Western blot

Western blot analysis was done using 50 ug of whole-cell lysates. The following antibodies were used: monoclonal mouse anti-Flag at 1:1000 dilution, monoclonal mouse anti-actin, peroxidase conjugated (Sigma-Aldrich, Inc.) at 1:10,000 dilution and/or mouse monoclonal anti-GAPDH (Abcam) at 1:10,000. Also, a custom-made rabbit polyclonal anti-SEPT9_v1 antibody at a working dilution of 1:4000; SAPK/JNK rabbit monoclonal antibody; anti-cyclin D1 mouse monoclonal antibody; anti-phospho-cyclin D1 rabbit monoclonal antibody; and an anti-phospho-c-Jun rabbit monoclonal antibody were used. All antibodies were purchased from Cell Signaling Technology and used at working dilutions of 1:1000. In addition, anti-cyclin B1 mouse

monoclonal, anti-cyclin E rabbit monoclonal and anti-JNK2 (D-2) HRP-linked antibodies were purchased from Santa Cruz Biotechnology (Santa Cruz, CA) and used at 1:200 dilution and 1:500 respectively. For secondary antibodies a goat anti-rabbit:HRP secondary antibody (1:000 dilution), and a goat anti-mouse:HRP (1:1000 dilution) antibody were both purchased from Cell Signaling Technology. All antibodies were diluted in 5% milk, 0.05% Tween 20 in 1X TBS. The SuperSignal West Pico Chemiluminescent kit (Pierce Biotechnology) was used for detection before exposure to Kodak XAR-5 film.

Immunoprecipitation

Cells were grown in 100mm dishes to 70% confluence before medium was removed, then the cells were washed twice with ice cold 1x PBS and incubated for five minutes at 4°C in M-PER lysis buffer (Pierce Biotechnology, Inc. Rockford, IL). The cells were collected and lysates were cleared by centrifugation at 13 000 rpm for 30 minutes at 4°C. Approximately 400 µg of solubilized lysate was used for each immunoprecipitation using the Protein G Immunoprecipitation kit (Sigma Aldrich, St. Louis, MO) and immunoprecipitations were performed according to manufacturer's instructions. The immunoprecipitated proteins were analyzed by SDS-PAGE and probed with the antibody described in the assay.

GST pull downs

DH5α *E. coli* cells were transformed with plasmids for either pGEX-2T empty vector or pGEX-2T-SEPT9_v1-GST and were induced for 4 h at 25 °C with 1 mM IPTG. Then, 1.0 mg of E. coli whole cell lysates were incubated for 3 h at 4 °C with glutathione sepharose 4B bead slurry (Amersham, Piscataway N.J.). Following washes, 1 mg of whole cell lysates from HPV4-12 Flag:JNK1 stably transduced cells was added and incubated overnight at 4 °C. After washing thoroughly with NTEN200 buffer (20 mM Tris–HCl, 1mMEDTA, 0.5% NP40, 25 µg/ml PMSF, 200

mM NaCl), the beads were incubated for 15 min with 10 mM glutathione at room temperature. Samples were analyzed by Western blotting.

Protein Stability Assay

Cells were plated in six-well plates and grown to 70% confluence. The cells were subjected to cycloheximide treatment as described (125). Lysates were analyzed by Western blot at different timepoints. Quantification of relative endogenous JNK1,2 expression was performed by densitometry using β-Actin as the loading control (Alpha Innotech IS-1000 Digital Imaging System, version 2.00).

UV treatment

Sub-confluent cultures of the cells were irradiated with UV as described and incubated for one hour to recover (128). Whole cell extracts were isolated as previously described and used for Western blotting (20).

Kinase Assay

In vitro: Whole cell extracts used for the evaluation of JNK were prepared by following the manufacturer's directions (SAPK/JNK Assay Kit (non-radioactive), Cell Signaling Technology Beverly, MA). Briefly, cell extracts (250 µg of protein) were incubated with glutathione beads containing 1µg of GST-c-Jun (1-79) fusion protein, centrifuged, washed, and incubated in kinase buffer with 10 µM ATP for 30 minutes at 30 °C. Phosphorylated substrate was detected by SDS-PAGE and immunoblotting using phospho-specific c-Jun antibody. Quantification of the JNK kinase activity relative to the parental and empty vector controls were performed by densitometric scanning (Alpha Innotech IS-1000 Digital Imaging System, version 2.00).

In vivo: HPV4-12 human mammary epithelial cell lines, empty vector control (pLPCX), and SEPT9_v1 and SEPT9_v3 stable transductants were transiently transfected using FuGENE 6 according to manufacturer's instructions (Roche, Nutley, NJ) (20). Cell were plated in six-well

culture plates and prepared following the manufacturer's instructions for the c-Jun TransLucent in vivo Kinase Assay Kit (Panomics Inc., Redwood City, CA). Briefly, the system is dependent upon the pTL-TAD expression vector, which contains the transcription activation domain (TAD) of cJun (amino acids 1-223), fused to the Gal4 DNA binding domain. The TAD-Gal4 fusion protein is constitutively expressed in cells and binds to the Gal4 binding domain, upstream of the luciferase gene in the pTL-Luc reporter plasmid. When TAD is phosphorylated by its specific kinase, JNK, it will activate transcription of luciferase. The cells were co-transfected with 0.5 µg of the pTL-c-Jun or the Translucent Control Vector (pTL-BD, which only has the Gal4 DNA binding domain), 1.0 µg of the pTL-Luc reporter plasmid, and 25 ng of pRL-TK (a plasmid containing Renilla luciferase reporter vector). Cells were lysed with lysis buffer from Promega Corporation. Quantification of the JNK kinase activity relative to controls was performed following the manufacturer's instructions in the Dual-Luciferase Reporter Assay System, (Promega Corporation). Luciferase activity was assessed using a 1420 multi-label counter luminometer from PerkimElmer Life and Analytical Sciences.

JNK/c-Jun Transcriptome Activation Detection in vivo: Luciferase Assay

Whole cell extracts were treated following the manufacturer's instructions for the Pathway Profiling Luciferase System 3 kit for profiling cell proliferation and differentiation signaling pathways (Clontech Laboratories). Briefly, HPV4-12 cells, the empty vectors controls (pLPCX), and SEPT9_v1 or SEPT9_v3 stable transductants were transiently transfected using FuGENE 6 (Roche) in a 6-well culture plate format. One microgram of either the pTAL-Luc vector used as a negative control or the pAP1-Luc vector (containing the cis-acting enhancer AP-1 element) and 25 ng of pRL-TK (a plasmid containing the Renilla Luciferase reporter vector) were used. The values obtained for the negative control, pTAL-Luc, were subtracted from the experimental results to normalize the data. Cells were lysed by adding lysis buffer from

Promega Corporation. Quantification of the relative fold of induction with the AP-1 enhancer to the parental and empty vector controls was performed by following the manufacturer's instructions in the Dual-Luciferase Reporter Assay System (Promega Corporation). Luciferase activity was determined on a 1420 multi-label counter luminometer from PerkimElmer Life and Analytical Sciences.

Real-time Quantitative PCR

cDNA samples from IHMEC and BCCs were amplified in triplicate from the same starting material of total RNA following the manufacturer's instructions (Omniscript RT kit, Qiagen). Samples were amplified using TaqMan MGB FAM dye-labeled probes from Applied Biosystems in an ABI7900HT model Real-Time PCR machine. The following probes were used: Hs99999905_m1 (*GAPDH)* and Hs00277039_m1 (*CCND1*).

Cell synchronization

Cells were synchronized with a double thymidine block as described previously (129). Briefly, cells were incubated in medium containing 2 mM thymidine for 12 hours, released into normal medium for 8-10 hours, and then incubated for 12 hours in medium with 2 mM thymidine. Samples were collected at regular intervals after releasing the cells from the thymidine block and the cell cycle distribution was detected by flow cytometry following staining with propidium iodide. Whole cell lysates were collected at the same timepoints and analyzed by Western blotting to look at the SEPT9_v1 expression profile through the cell cycle.

Results

High SEPT9_v1 expression increases aneuploidy in mammary epithelial cells

Due to the implication of septins, including SEPT9, in mitosis and cytokinesis, I assayed the cells with high ectopic SEPT9_v1 or SEPT9_v3 expression for aneuploidy, a characteristic of genomic instability in many cancers. Ectopic expression of *SEPT9*_v1 increased the amount of

aneuploid cells to about ~50% as compared to ~5-15% in parental and empty vector controls (Fig. 3.2A) for both immortalized mammary epithelial cells (IHMECs) MCF10A and HPV 4-12. Similar results were observed for multiple polyclonal populations of MCF10A cells with high SEPT9_v1 expression (Fig 3.2B). High ectopic SEPT9_v3-expressing MCF10A cells also showed increased aneuploidy to a lesser extent than SEPT9_v1, but the change was significant. Interestingly, high SEPT9_v1 expression gave rise to a striking bimodal distribution of cells with extra chromosomes. One population showed generalized aneuploidy with few extra chromosomes, while the second population showed a gross number of extra chromosomes closer to a tetraploid status. In contrast, the majority of SEPT9_v3 associated aneuploid cells were close to tetraploidy (Fig 3.2C). This difference suggested that these two isoforms might impact genomic instability by at least two different mechanisms including mitotic spindle defects and/or incomplete cell division.

SEPT9 isoforms have distinct cellular localizations and over-expression of SEPT9_v1, but not SEPT9_v3, disrupt tubulin filaments

To determine SEPT9_v1 and SEPT9_v3 localization in IHEMCs in relation to cytoskeletal proteins, IHEMCs over-expressing each variant were stained with either anti-SEPT9_v1 or anti-SEPT9-X (to detect SEPT9_v3) antibodies for immunofluorescence. Endogenous SEPT9_v1 localized to the cytoplasm in interphase cells with minimal nuclear staining (Figs. 3.3, panel b). However, ectopically expressed SEPT9_v1 showed this isoform was more abundant in both the nucleus and the cytoplasm, with an altered morphology of the cells (Fig. 3.3, panel n). In contrast, ectopic SEPT9_v3 showed a distinctive localization to the periphery of the cells, around

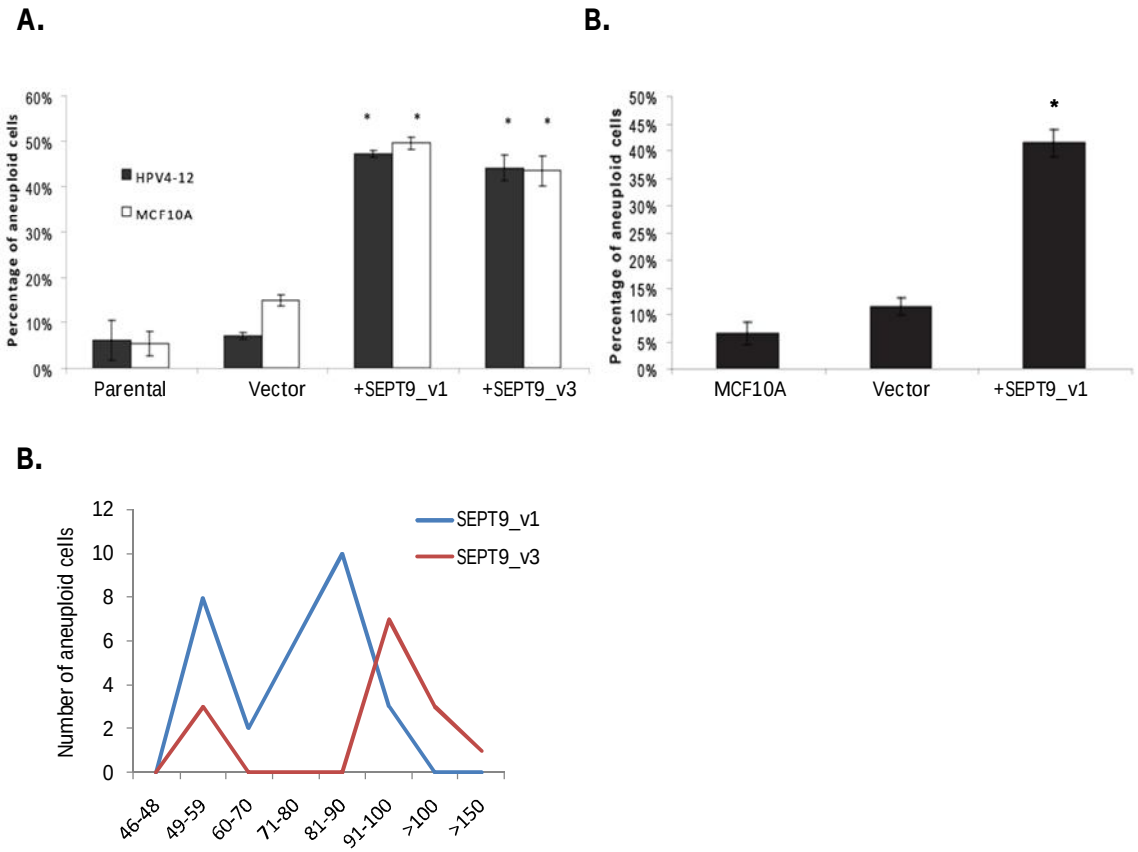

Fig 3.2: High SEPT9_v1 and SEPT9_v3 increases aneuploidy in IHMECs

(A) Ectopic expression of SEPT9_v1 and SEPT9_v3 increases genomic instability in MCF10A and HPV 4-12 cells in that ~50% of the cells in the population are aneuploid. (B) Multiple polyclonal populations of MCF10A cells over-expressing SEPT9_v1 showed similar results with ~45% of cells being aneuploid. *Columns*, percentage of aneuploid cells from 25 metaphases in each of three independent experiments; *bars*, SE. *p<0.001, ANOVA. (C) Graph showing that the majority of SEPT9_v3 cells (red line) are close to tetraploidy (81-96 chromosomes) and showing binomial distribution of SEPT9_v1 (blue line) cells; one population of cells showed aneuploidy (49-70 chromosomes) and another population showed tetraploidy (71-96 chromosomes).

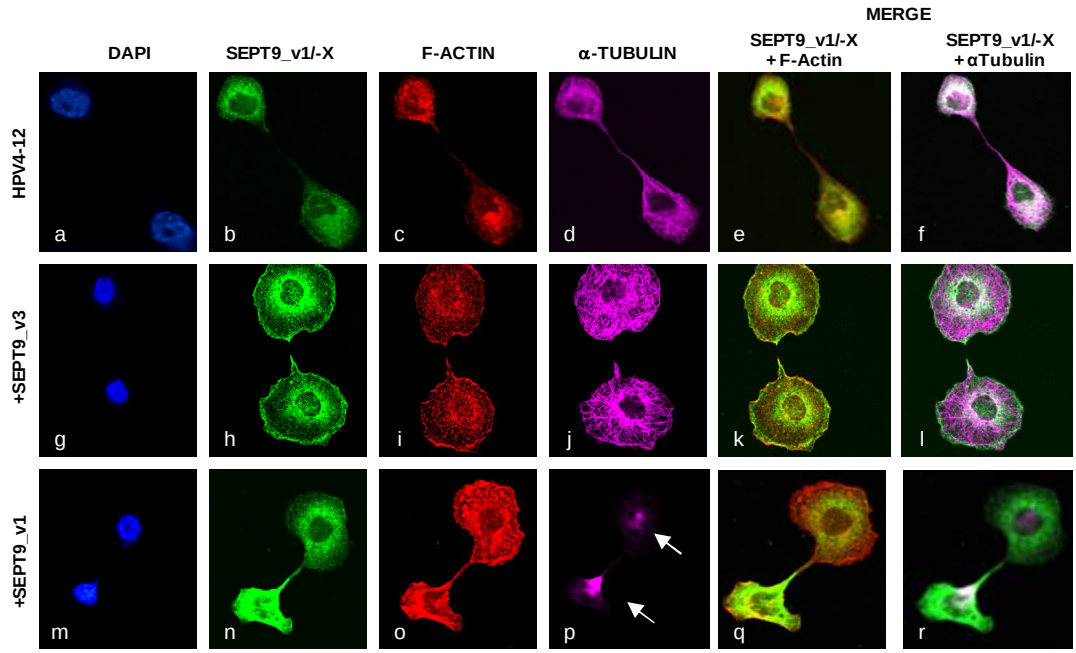

Fig 3.3: Ectopic SEPT9_v1 and SEPT9_v3 co-localize with cytoskeletal proteins but with different outcomes

Immunofluorescence studies were used to stain cells for DNA (DAPI; panels a, g, and m), SEPT9_v1 (panels b and n), SEPT9-X (panel h), phalloidin/F-Actin (panels c, i, and o), and alpha tubulin (panels d, j, and p). Ectopic expression of the SEPT9_v1 isoform in HPV4-12 cells caused the microtubule network to break down in interphase cells (panel p) compared to ectopic expression of the SEPT9_v3 isoform (panel j) or the parental cell line (panel d). The merged images of SEPT9_v1 and actin (panels e and q) show the limited co-localization of actin filaments with SEPT9_v1 and the merged image between SEPT9_v3 and actin (panel k) shows co-localization of SEPT9_v3 with actin rings in the transduced HPV4-12 cells during interphase. The merged images of SEPT9_v1 and alpha tubulin show co-localization of SEPT9_v1 and microtubule filaments in the parental cell line (panel f) and with microtubules bundles in the SEPT9_v1 over-expressing cells (panel r).

SEPT9_v1 showed limited co-localization with filamentous actin and strong localization with alpha tubulin in interphase cells (Fig. 3.3, panels e, f, q, and r). Interestingly, when SEPT9_v1 was over-expressed, there was a dramatic disorganization of the tubulin filaments in 68% of interphase cells (Fig 3.3, panel p), compared to 0% in cells over-expressing SEPT9_v3 (Fig. 3.3 panel j), and 11% of cells in the parental HPV4-12 line ($p<0.001$, ANOVA). This was in strong agreement with the differences in the subcellular localization of the two variants.

High SEPT9_v1 expression promotes mitotic spindle defects

SEPT9 transductants and empty vector control MCF10A cells were enriched in mitosis after a 10 hour release from a double thymidine block. The cells were stained for anti- α-tubulin (red), anti- γ-tubulin (green) and DAPI for DNA (Fig. 3.4). SEPT9_v1 (Fig 3.4A and Fig. 3.4B bottom panel) promotes chromosome mis-segregation showed by misaligned chromosomes (f-g), multipolar spindles (h), chromosome lagging (i) and centrosome amplification (k) in 25% of cells as compared to empty vector control (Fig 3.4A and Fig 3.4B top panel) ($p<0.005$).

High SEPT9_v1 expression promotes cytokinesis failure

To assess whether over-expression of SEPT9_v1 can affect cell division, MCF10A-SEPT9_v1, HPV 4-12-SEPT9_v1 and empty vector controls were stained with anti-α-tubulin (red) and DAPI (blue) for immunofluorescence. SEPT9_v1 over-expression had a greater effect on cell division: approximately 8-10% of SEPT9_v1 transductants were bi-nucleated as compared to empty vector control. These results suggested that over-expression of the SEPT9_v1 transcript is somehow preventing proper cell division at the end of mitosis by disrupting cytoskeleton dynamics and/or protein involved in the completion of cytokinesis (Fig 3.5).

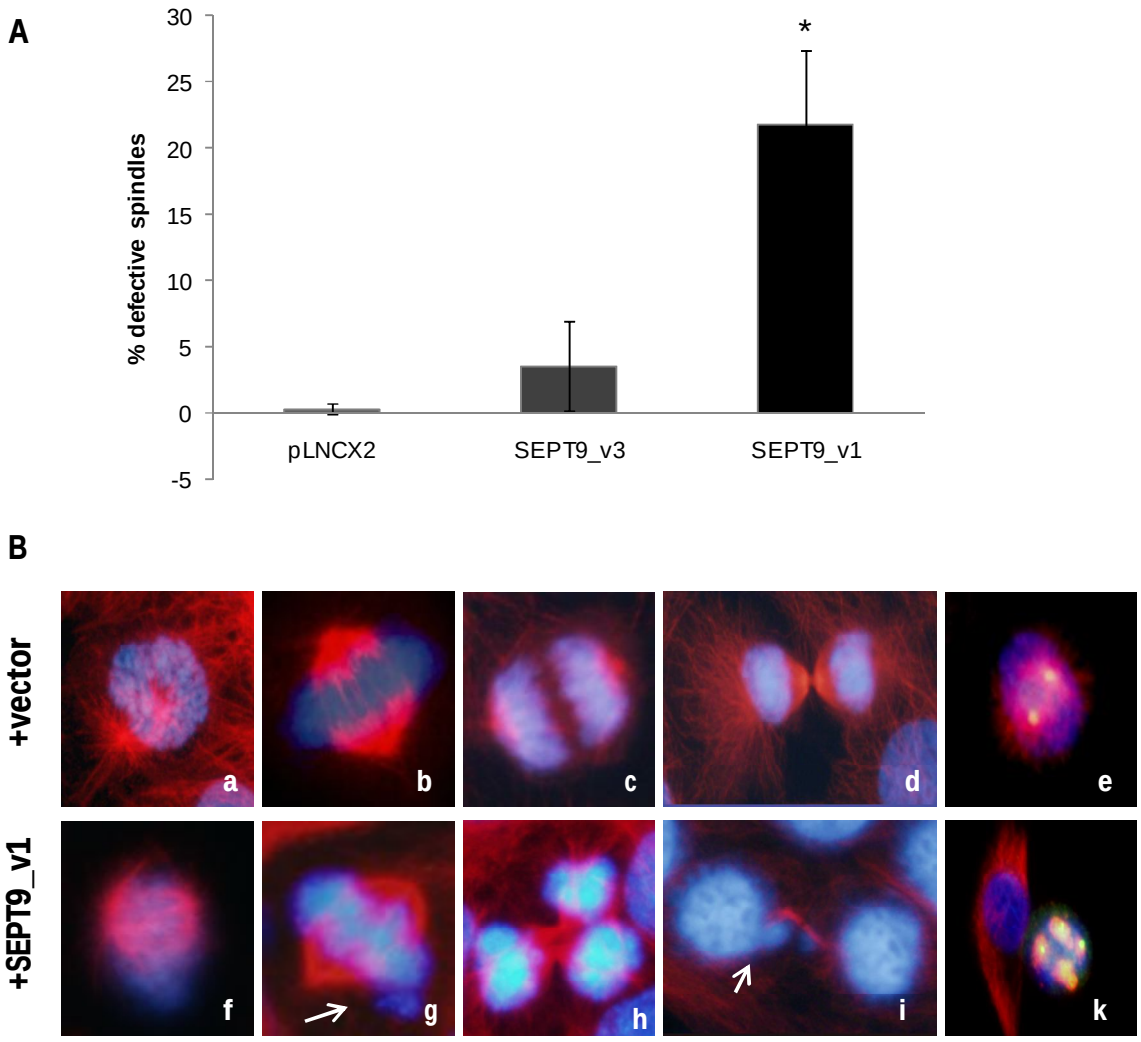

Fig 3.4: High SEPT9_v1 expression increases mitotic spindle defects

(A) Ectopic expression of SEPT9_v1 increases mitotic spindle defects in ~30% of MCF10A cells as depicted in the graph. *Columns*, percentage of cells with mitotic spindle defects in three independent experiments; *bars*, SDev. *p<0.005, Student t-test. (B) Immunofluorescence studies were used to stain cells for DNA (DAPI; blue), α-tubulin (red) and γ-tubulin (green). SEPT9_v1 over-expression promotes mitotic spindle defects as compared to vector control: disorganization of the mitotic spindle (a vs f), chromatin outside of the metaphase plate (b vs g), multipolar spindles (c vs h), lagging chromosomes at the midbody (d vs i) and centrosome amplification (e vs k).

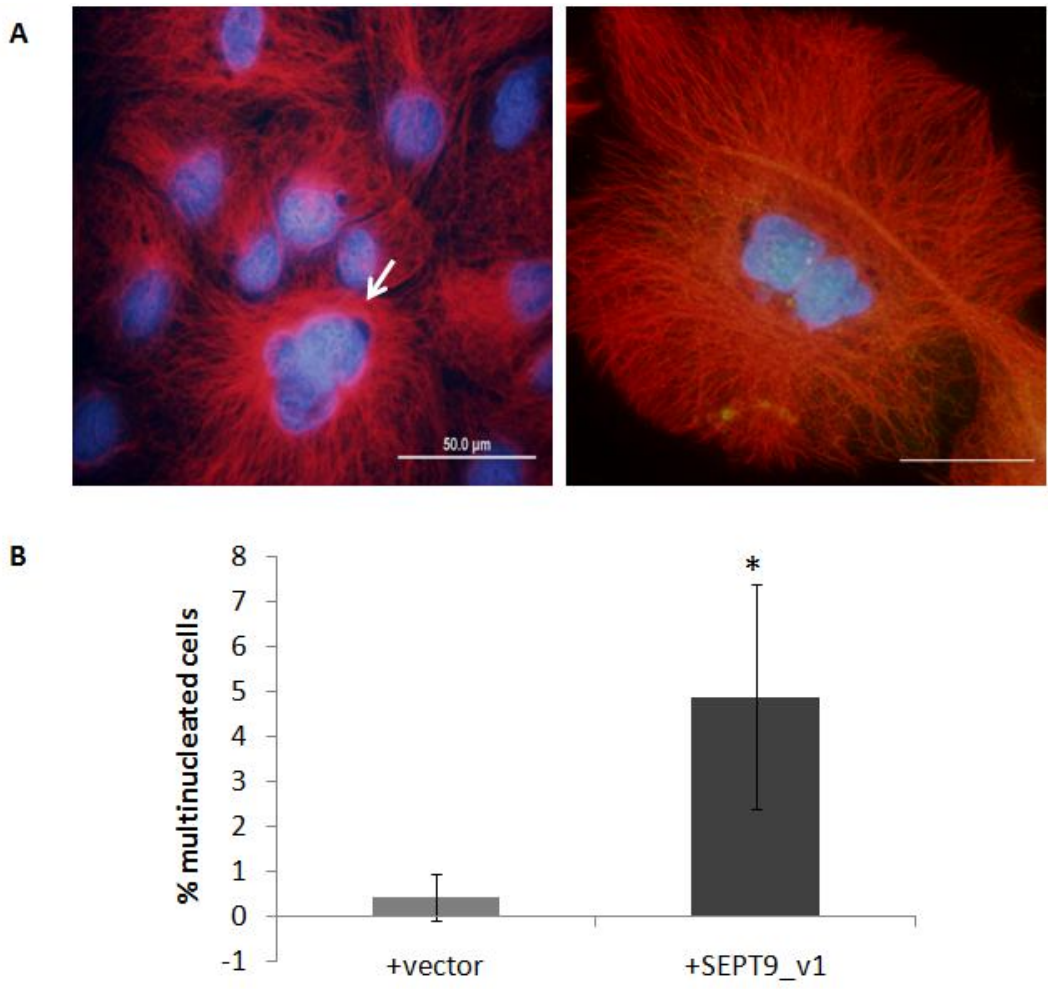

Fig 3.5: High SEPT9_v1 expression impacts cell division by increasing multinucleated cells

(A) Immunofluorescence was used to stain cells for DNA (DAPI; blue) and α-tubulin (red). Over-expression of SEPT9_v1 increases multinucleated giant cells. (B) Graph showing that ~8% of SEPT9_v1-cells become multinucleated as compared to the empty vector control. *Columns*, mean of three independent experiments; *bars*, SDev. *, $P < 0.05$, Student t-test.

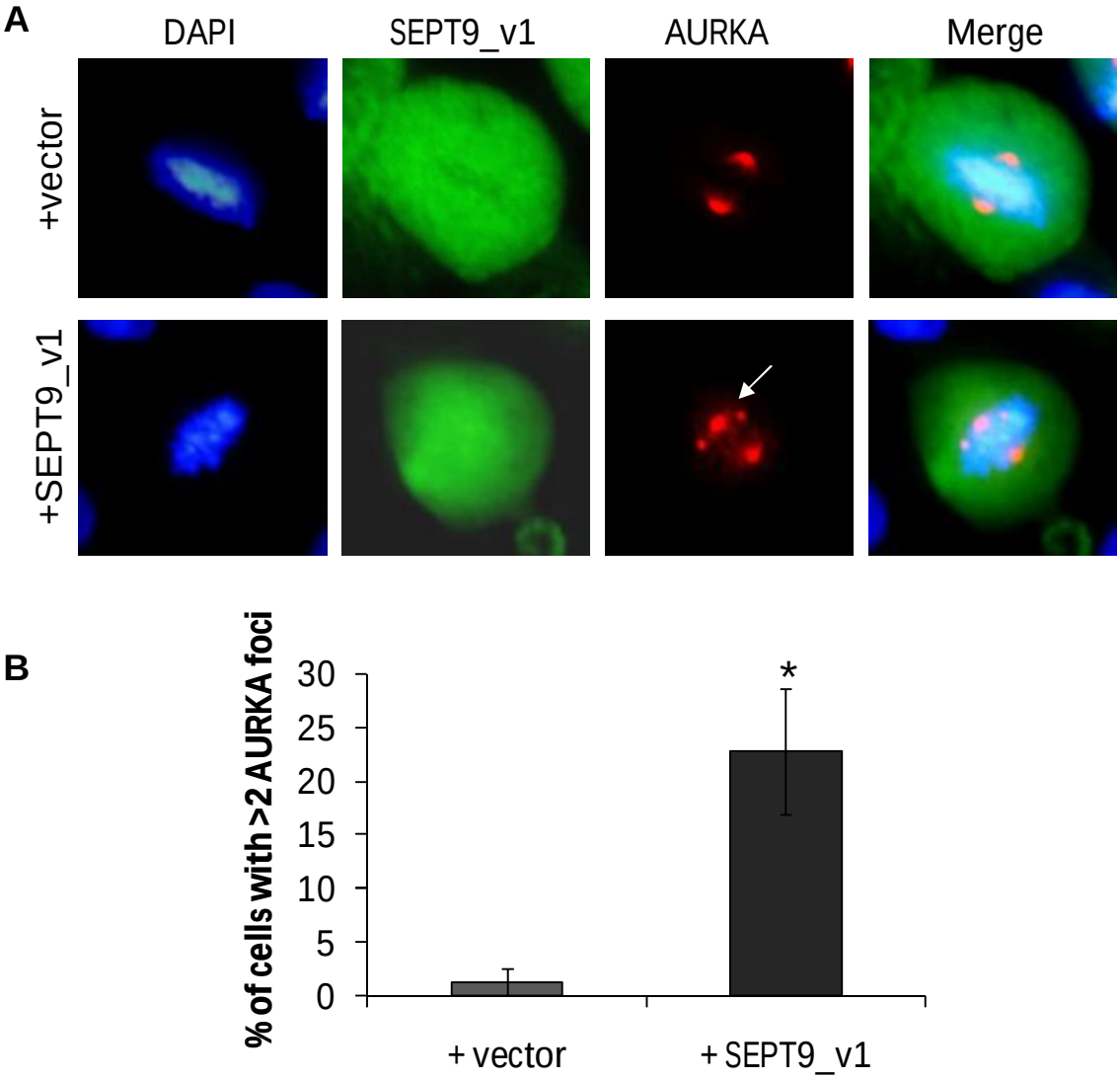

Fig 3.6: Increased SEPT9_v1 expression showed Aurora A kinase amplification

(A) MCF10A-SEPT9_v1 and vector control cells were synchronized in mitosis by a 10 hour release after a double thymidine block. Immunofluorescence was used to stain for DNA (DAPI; blue), SEPT9_v1 (green) and Aurora A kinase (red). SEPT9_v1 over-expression increased Aurora A kinase foci in mitotic cells (bottom panel) as compared to vector control (top panel). (B) SEPT9_v1 transductants show that ~30% of the cells have Aurora A kinase amplification. *Columns*, percentage of cells with >2 foci of three independent experiments; *bars*, SDev. *P<0.0001, Student t-test.

High SEPT9_v1 expression promotes increased incidence of micronuclei and nuclear fragmentation

While analyzing cells by immunofluorescence for mitotic spindle defects or evidence cytokinesis failure, novel phenotypes specific to SEPT9_v1 transductants when compared to empty vector controls were observed. MCF10A-SEPT9_v1 transductants demonstrated approximately ~4 % of cells with nuclear fragmentation (Fig 3.7A) and ~6 % with micronuclei (Fig 3.7B). Even though these phenotypes were found at low frequency, the empty vector controls did not demonstrate either of these phenotypes. The relevance of these phenotypes in term of genomic instability and cancer needs to be characterized further; however previous studies have associated the presence of micronuclei with loss of DNA material of one or both daughter cells during mitosis (115).

SEPT9_v1 interacts with proteins important in mitosis and cell division

To begin examining the mechanism by which SEPT9_v1 promotes genomic instability in breast cancer cells, potential SEPT9_v1 interactions with components of the mitotic spindle, such as tubulins, and/or proteins involve in the spindle checkpoint, such as MAD2, and centrosome specific proteins, such as Aurora A, were tested. Tubulins are key players of the mitotic machinery and cytoskeleton dynamics in mammalian cells, and MAD2 and Aurora A are key players in the organization of the spindles and proper chromosome segregation. Therefore, we hypothesized that SEPT9_v1 over-expression affected the expression and/or localization of mitotic spindle proteins, which might impact proper cell division or chromosome segregation.

Previous studies showed an interaction between septins and tubulins; therefore, to explore further the interaction of SEPT9_v1 and α-tubulin co-immunoprecipitation and immunofluorescence analyses were performed. Whole cell lysates from MCF10A-SEPT9_v1

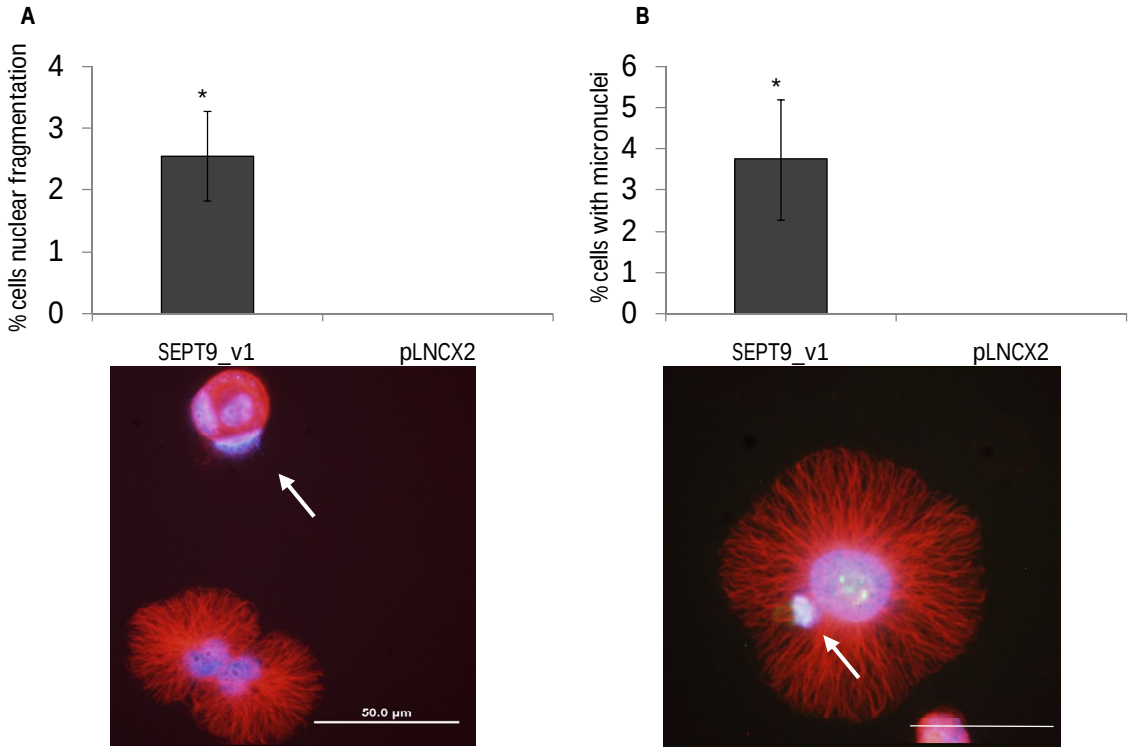

Fig 3.7: SEPT9_v1 transductants showed nuclear atypia

Immunofluorescence was used to stain cells for DNA (Dapi; blue) and α-tubulin (red). (A) SEPT9_v1 transductants showed nuclear fragmentation in ~4% of the cells as compared to the vector control. (B) SEPT9_v1 increases the presence of micronuclei in ~6% of the cells as compared to the vector control. Three hundred cells were counted per triplicate. *Columns*, mean of three independent experiments; *bars*, SDev. *p=0.01.

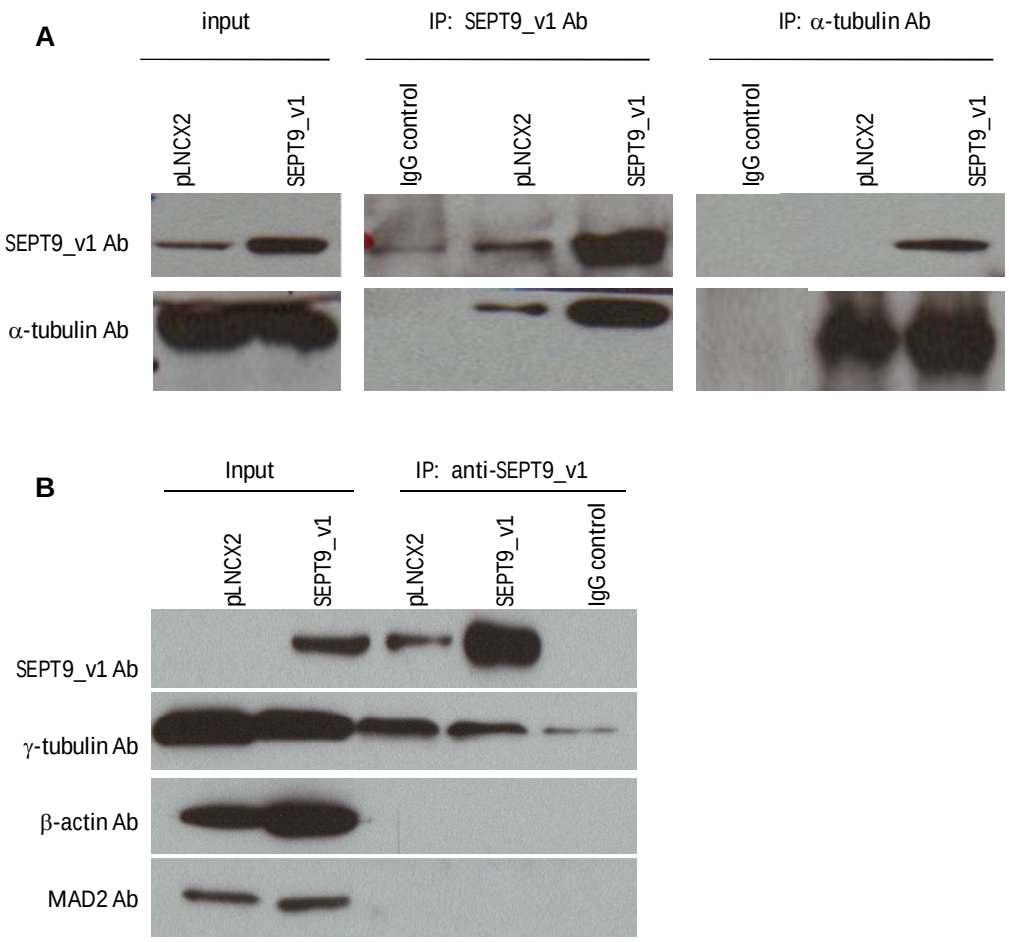

Fig 3.8: SEPT9_v1 interacts with components of the mitotic spindle

(A) SEPT9_v1 co-immunoprecipitated with α- tubulin. Whole cell lysates (left panel) from vector control (pLNCX2) and SEPT9_v1 transductants were used for immunoprecipitation. SEPT9_v1 (middle panel) and α-tubulin (right panel) antibodies were used for immunoprecipitation and the samples were subsequently immunoblotted for SEPT9_v1 or α-tubulin. (B) SEPT9_v1 co-immunoprecipitated with γ-tubulin (second panel), but not with β-actin (third panel) or MAD2 (fourth panel). Whole cell lysates from vector control (pLNCX2) and SEPT9_v1 transductants were used for immunoprecipitation. The SEPT9_v1 antibody was used for immunoprecipitation and the samples were immunoblotted for SEPT9_v1, γ-tubulin, β-actin and MAD2.

transductants and empty vector control cells were subjected to immunoprecipitation analyses with the SEPT9_v1 antibody. Co-immunoprecipitation of α-tubulin and SEPT9_v1 was confirmed in IHMECs, with a weaker band using empty vector lysates for immunoprecipitation and a stronger band with SEPT9_v1 transductant lysates (3.8A).

Immunoprecipitated proteins were then probed with anti-α-tubulin, anti-Aurora A, anti-MAD2 and anti-CDC20 independently. SEPT9_v1 did not interact with MAD2, Aurora A, CDC20 or β-Actin. A signal corresponding to γ-tubulin was found in whole cell lysates of both vector and SEPT9_v1 transductants (Fig 3.8B). These results indicated that SEPT9_v1 could interact with tubulins, suggesting a specific role of SEPT9 _v1 in mitotic spindle assembly during mitosis, but not necessarily with components of the mitotic spindle checkpoint.

Transient expression of Flag-SEPT9_v1 construct was sufficient to increase both aneuploidy and cell proliferation

Previously, increased expression of SEPT9_v1 was found to accelerate growth kinetics of IHMECs by increasing cell proliferation and decreasing apoptotic response (Gonzalez et al. 2007). Therefore, I was interested in determining the relationship between cell proliferation and aneuploidy phenotypes. With increasing genomic instability, there is a high frequency of loss and gain of chromosomes that can carry genes responsible for regulating cell cycle progression and cell proliferation. To tease apart the connection between aneuploidy and cell proliferation, MCF10A and HCT116 cells were transiently transfected with a construct expressing Flag-SEPT9_v1 and an empty vector control. SEPT9_v1 expression was assayed by Western blot at different time points post-transfection (Fig 3.9A). The timepoints were chosen by the doubling time of each cell line. At every time point, metaphases spreads were collected for aneuploidy studies and immunofluorescence for a proliferation marker, Ki67, was performed.

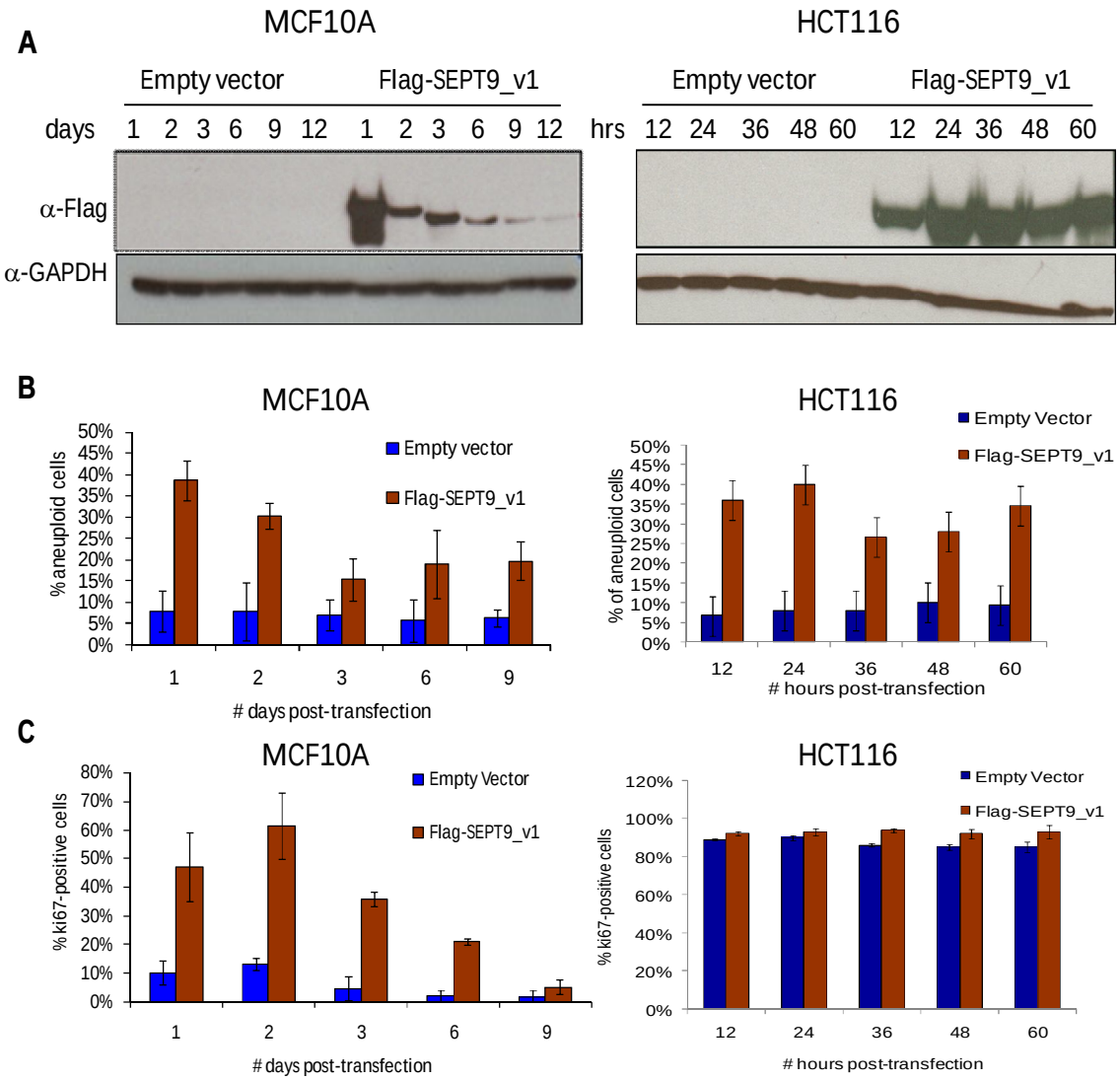

Fig 3.9: Transient transfection of SEPT9_v1 increases aneuploidy and cell proliferation

(A) Western blot analysis showing transient expression of an empty vector control and a Flag-SEPT9_v1 construct in MCF10A (left) and HCT116 (right). GAPDH was used as a loading control. (B) Metaphase spreads were counted at each time point after transfection for both cell lines, MCF10A (left) and HCT116 (right). MCF10A and HCT116 transfected with Flag-SEPT9_v1 showed an increase in aneuploidy up to ~40% of cell lines one time point after transfection. *Columns*, percentage of aneuploid cells from 25 metaphases in each of three independent experiments; *bars*, SDev. (C) Cell proliferation was assayed using ki67-positive cells. MCF10A cells showed an increase in proliferation of ~ 60% one day post-transfection as compared to the empty vector control (left). HCT116 did not show a significant increase in cell proliferation as compared to the vector control (right). *Columns*, percentage of ki-67 positive cells from 300 cells in each of three independent experiments; *bars*, SDev.

Western blot analysis showed that for MCF10A the expression of Flag-SEPT9_v1 was reduced overtime with no detectable signal on the empty vector control. Surprisingly, SEPT9_v1 transient expression increased aneuploidy to ~40% and cell proliferation to ~60% one day post-transfection (approximately one doubling time) (Fig 3.9B-C; left panel). Both phenotypes start decreasing three days after transfection, similar to the decrease of Flag-SEPT9_v1 expression over time as shown by the Western blot. These data suggested that aneuploidy and cell proliferation might be independent of each other and that aneuploidy was not necessarily driving tumorigenesis by impacting cell proliferation. HCT116 studies showed the same pattern; approximately 50% of HCT116-SEPT9_v1 cells became aneuploid 12 hours post-transfection (one doubling time) (Fig 3.9B; right panel). Interestingly, HCT116 cells did not show a significant difference in proliferation between vector and SEPT9_v1 transfectants (Fig 3.9C), further supporting the hypothesis that SEPT9_v1 increases aneuploidy and cell proliferation kinetics via different molecular mechanisms.

SEPT9_v1 impacts cell proliferation, independent of aneuploidy, through a specific c-Jun-N-Terminal kinase (JNK) interaction

SEPT9_v1 expression could impact tumorigenesis in part by its association with signaling pathways controlling cell cycle progression and/or cell proliferation. Previous studies showed that SEPT9_v1 stabilized the hypoxic inducible factor alpha (HIF-α) and increased cell proliferation rates in prostate cancer cells (72). JNK activation, a critical component of the proliferative response, was previously implicated in the induction of HIF-1 and cell cycle progression by modulating cyclin expression. Given the impact of SEPT9_v1 and JNK1, 2 on cell proliferation, and the shared ability of SEPT9_v1 and JNK1,2 to regulate HIF-1, we hypothesized that increased SEPT9_v1 expression may exert its effects on proliferation via association with the JNK signaling pathway.

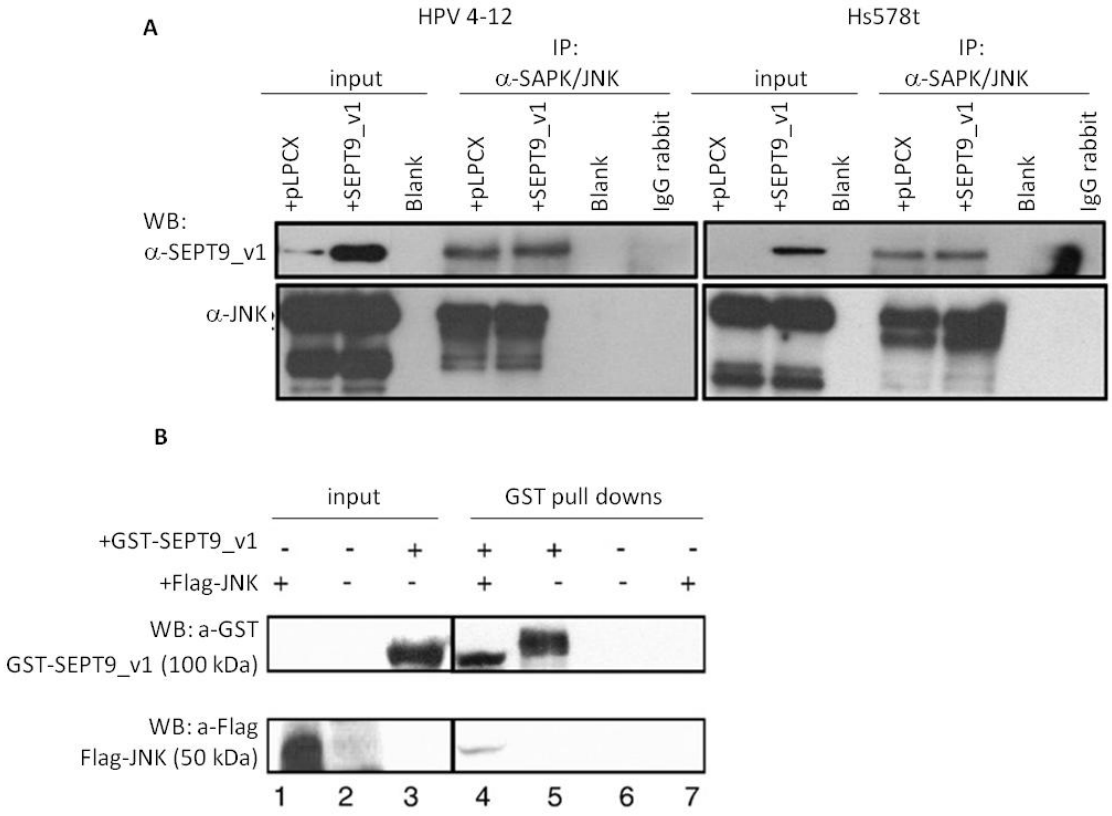

Fig 3.10: SEPT9_v1 co-immunoprecipitates with JNK1, 2

(A) Co-immunoprecipitations with a JNK1,2 antibody using whole cell lysates from HPV4-12 IHMEC cells (left side) and Hs578T breast cancer cells (right side) from both empty vector cells and SEPT9_v1 retroviral transductants. Results show that SEPT9_v1 immunoprecipitates with JNK1, 2 in both cell lines. Bottom panels: Western blotting using whole cell lysates and the indicated antibodies indicate the amount of starting material ("input") used for the immunoprecipitations. (B) A GST pull-down using a GST-SEPT9_v1 fusion protein shows an interaction between SEPT9_v1 and ectopically expressed Flag-tagged JNK. Top panel: Western blotting using a GST antibody shows the presence of the GST-SEPT9_v1 fusion protein. Lane number 3 indicates GST-SEPT9_v1 fusion protein expression in the bacterial whole cell extract (WCE) as starting material. Bottom panel: Western blotting using an anti-Flag antibody to detect Flag-JNK1 shows the interaction between GST-SEPT9_v1 and JNK (lane 4). Lane number 1 indicates the expression of Flag-JNK in whole cells extracts (WCE) from transfected HPV4-12 cells, indicating the amount of JNK in the starting material for the GST pull-down.

To test the hypothesis that altered SEPT9_v1 expression directly affects the JNK signaling pathway, we first studied the potential interaction between JNK and SEPT9_v1 by immunoprecipitation and immunofluorescence experiments. We used the immortalized human mammary epithelial cell line (IHMEC) HPV4-12, which develops tumorigenic properties after up-regulation of SEPT9_v1, and the breast cancer cell line Hs578T, which has significantly less endogenous SEPT9_v1 expression than HPV4-12, as we were specifically interested in mechanisms that may be relevant to malignant progression in breast cancer cells (20).

Whole cell lysates from HPV4-12 and Hs578T parental cells and their respective retroviral transductants stably expressing SEPT9_v1 were subjected to immunoprecipitation experiments using an anti-JNK1,2 antibody that recognizes both JNK1 and JNK2. Immunoprecipitated proteins were probed with an anti-SEPT9_v1 antibody. We found a strong specific signal corresponding to the SEPT9_v1 isoform in whole cell lysates from cells expressing exogenous and endogenous SEPT9_v1 immunoprecipitated with anti-JNK1, 2 antibodies (Fig 3.10 A). These results suggested that SEPT9_v1 could interact with JNK proteins.

To provide additional evidence of this interaction we performed GST pull-down experiments using a purified GST-SEPT9_v1 fusion protein and whole cell lysates from HPV4-12 cells transiently transfected with a construct for Flag-tagged JNK2. The results shown in Figure 3.10B demonstrated that JNK1 and SEPT9_v1 also interact in vitro.

SEPT9_v1 stabilizes JNK in mammary epithelial cells

To determine if SEPT9_v1 expression had any effect on JNK1,2 protein levels. As shown, increased SEPT9_v1 expression did not alter significantly alter the steady state JNK1,2 protein levels (Fig 3.10, input). Therefore, we hypothesized that SEPT9_v1 modified JNK1 and/or JNK2 either post-transcriptionally or posttranslationally. We studied the effects on JNK1,2 protein stability by using cycloheximide. Since cycloheximide inhibits new protein synthesis, JNK1,2

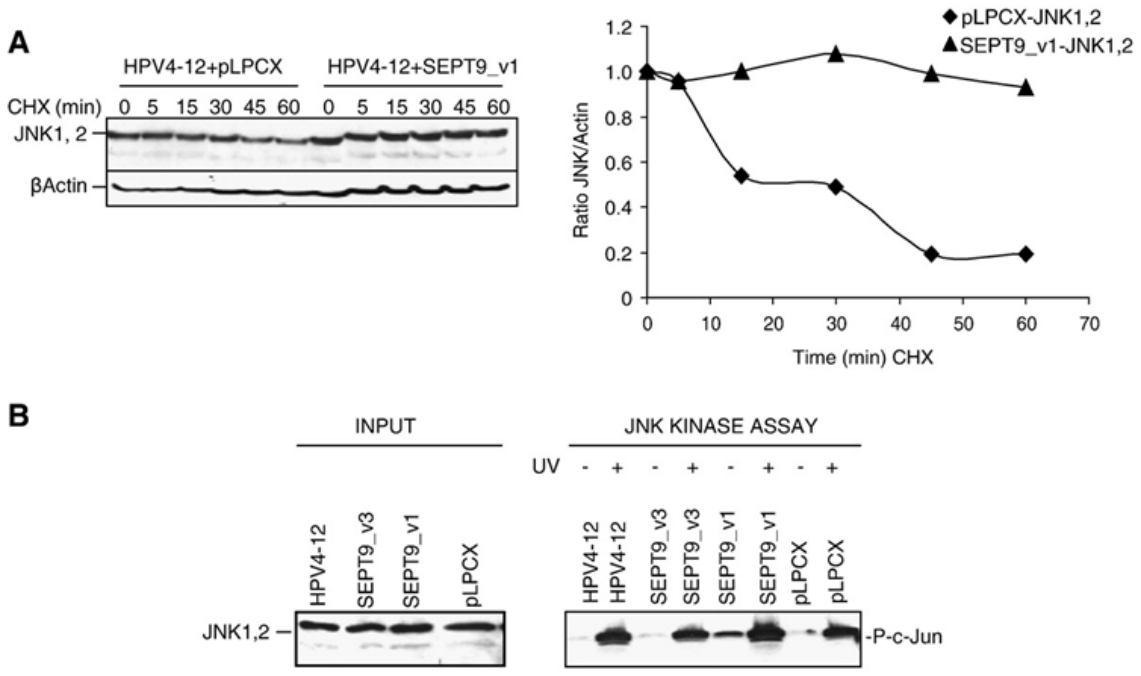

Fig 3.11: Up-regulation of SEPT9_v1 in HPV 4-12 immortalized human mammary epithelial cells, stabilizes JNK expression and increases JNK kinase activity *in vitro*

(A) Left panel: SEPT9_v1 stabilizes JNK1,2 protein levels. Western blotting for JNK1,2 protein levels at various timepoints during cycloheximide treatment in cells without (left) or with (right) stably expressed exogenous SEPT9_v1. β Actin was used as loading control. Right panel: A graphical representation of the data from the left panel, as determined by densitometry, highlights how SEPT9_v1 over-expression stabilized JNK1,2 within the cells. Within less than 30 min of exposure to cycloheximide, JNK1, 2 (♦) protein levels in HPV4-12+pLPCX cells were decreased by 50%. In cells transduced with SEPT9_v1, JNK1, 2 (▲) protein levels remained constant and did not decrease until 60 min of cycloheximide exposure (B) An in vitro kinase assay shows that SEPT9_v1 up-regulation increases JNK activity as indicated by increased levels of phosphorylated c-Jun in unstressed and UV-treated cells. Left panel: Whole cell extracts (input) show the initial endogenous JNK1, 2 levels in the cells used for the kinase assay. Right panel: Cell extracts (250 µg of protein), were incubated with glutathione beads containing 1 µg of GST-c-Jun (1–79) fusion protein. Phosphorylated substrate was detected by SDS–PAGE and immunoblotting using phospho-specific c-Jun antibody. Quantification of the JNK1,2 kinase activity was performed by densitometric scanning showing that up-regulation of SEPT9_v1 caused a 7-fold increased induction of c-Jun phosphorylation in unstressed cells compared to parental and empty vector (pLPCX) controls.

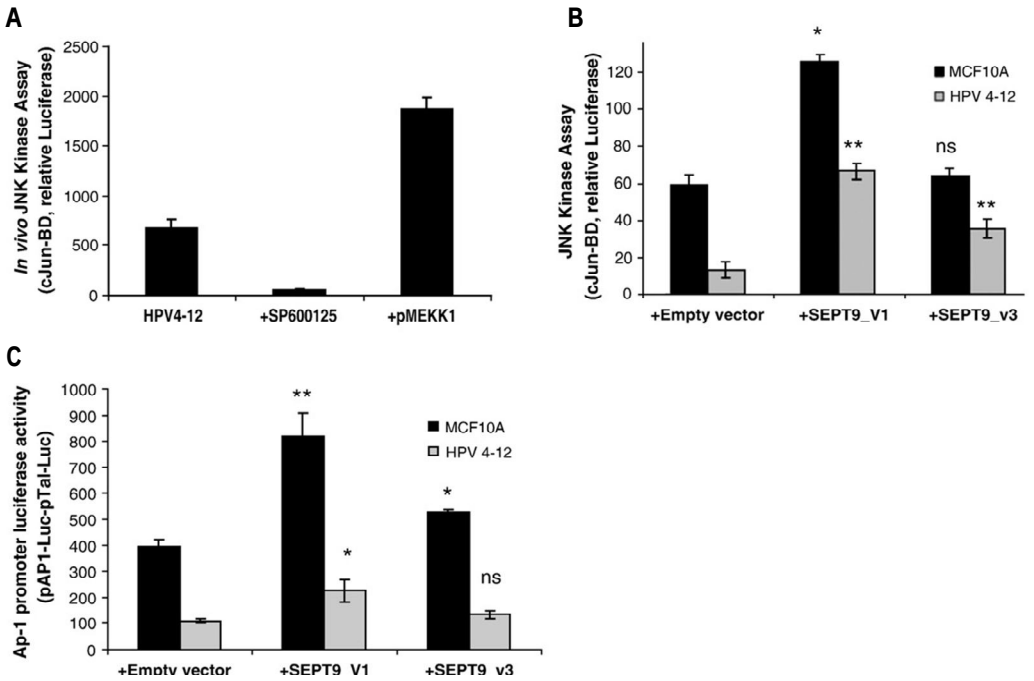

Fig 3.12: Up-regulation of SEPT9_v1 in HPV 4-12 immortalized human mammary epithelial cells increases JNK kinase activity *in vivo*

(A) The in vivo JNK kinase assay was validated for JNK specificity by transiently transfecting HPV4-12 cells with a well-characterized JNK inducer, pMEKK1 or by inhibiting JNK activity with the chemical inhibitor, SP600125. JNK kinase activity was induced by more than threefold with the pMEKK1 activator and the JNK inhibitor, SP600125, inhibited JNK kinase activity by 12 fold in HPV4-12 cells. (B) In vivo kinase assay shows SEPT9_v1 up-regulation increases JNK activity. Up-regulation of SEPT9_v1 in HPV4-12 and MCF10A IHMEC cells caused an induction of phosphorylated c-Jun-mediated reporter gene (Luciferase) expression primarily by the JNK pathway using the c-Jun Translucent in-vivo Kinase Assay Kit. The plot for this luciferase assay shows that SEPT9_v1 causes an increase of JNK1,2 kinase activity towards c-Jun by more than four-fold in HPV4-12 cells. SEPT9_v3 causes only a moderate increase in JNK1,2 kinase activity in vivo (ns: nonsignificant *p<0.001, **p<0.0001; Student's t-test). (D) SEPT9_v1 over-expression increases the expression of phosphorylated c-Jun target genes (the JNK/c-Jun signaling transcriptome) that have an AP-1 enhancer element. Cells were transiently transfected with the pTAL-Luc vector used as a negative control or the pAP1-Luc vector containing the cis acting enhancer AP1 element and pRL-TK, a plasmid containing the Renilla Luciferase reporter. Compared to the empty vector control, up-regulation of SEPT9_v1 doubled the expression of the reporter construct when compared to HPV4-12 parental and empty vector controls. SEPT9_v3 up-regulation had an insignificant effect when compared to the empty vector control. In MCF10A cells, compared to empty vector control SEPT9_v1 up-regulation doubled the expression of the reporter construct or c-Jun activated transcription and SEPT9_v3 had a milder but significant effect (ns: non significant, *p<0.05, **p<0.01; Student's t-test).

levels over time would predominantly reflect the degradation process. HPV 4-12 clones stably expressing the retrovirally transduced pLPCX empty vector or SEPT9_v1 constructs were exposed to cyclohexidimide across various time points and JNK protein levels were subsequently analyzed by Western blot. Within 30 minutes of exposure to cycloheximide, JNK1,2 protein levels in control cells were decreased by 50% as analyzed by Western blot (Fig 3.11A). However, Within in exogenously expressing SEPT9_v1 cells, JNK1,2 protein levels did not decrease to 50% levels until 60 minutes of cycloheximide exposure. This data suggested that SEPT9_v1 is likely involved in cellular processes that regulate the stability and degradation of JNK1,2 proteins.

SEPT9_v1 up-regulation increases JNK kinase activity *in vivo* and *in vitro*

To examine further the effects of SEPT9_v1 up-regulation on JNK1, 2 signaling in unstressed cells, we tested JNK1,2 kinase activity in HPV4-12 cells stably transduced with SEPT9_v1 or SEPT9_v3 isoforms, compared to the parental and empty vector controls. Strikingly, the ectopic expression of SEPT9_v1 caused an approximate seven-fold increase in c-Jun phosphorylation by JNK1,2 in unstressed cells (Fig 3.11B). Interestingly, even though SEPT9_v3 was also able to interact with JNK1,2 similar to SEPT9_v1 (data not shown) over-expression of the SEPT9_v3 isoform did not enhance JNK1,2 kinase activity (Fig. 3.11B). This indicates that SEPT9_v1's extended unique amino terminus, which consists of 25 unique amino acids when compared to the otherwise identical SEPT9_v3 isoform, is likely involved in the SEPT9 associated activation of JNK1,2. To quantify and further explore these findings, we used an *in vivo* JNK kinase assay where c-Jun binding sites are located in the promoter upstream of a Luciferase reporter. HPV4-12 cells stably expressing the empty vector, SEPT9_v1, or SEPT9_v3 isoforms were transiently co-transfected with the reporter luciferase plasmid and the *in vivo* kinase vector pTAD-cJun,

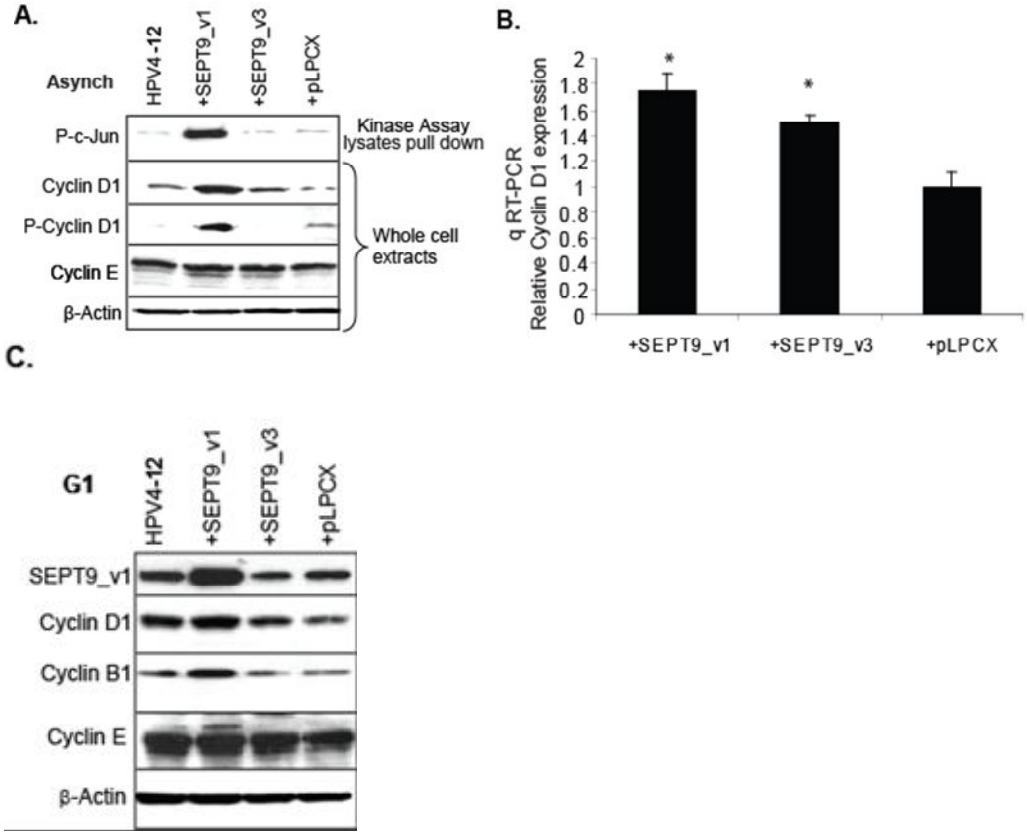

Fig 3.13: Increased SEPT9_v1 expression results in amplified expression of cyclin D1 and B1.

(A) Western blot shows that asynchronous HPV4-12 cells exogenously expressing SEPT9_v1 had higher levels of cyclin D1 expression and a 10-fold increase in phosphorylated cyclin D1 when compared to the controls. The top panel indicates the amount of phosphorylated c-Jun present in the cells, as previously shown in Figure 3B, while the remaining panels are whole cell lysates. β-Actin was used for a loading control. (B) A graphical representation of data from real-time quantitative RT-PCR shows that *CCND1* (cyclin D1) expression is approximately doubled in HPV4-12 cells exogenously expressing SEPT9_v1 when compared to controls. Relative mRNA expression of *CCND1* was determined against the *GAPDH* control (*$p<0.05$; Student's t-test). (C) SEPT9_v1 over-expression results in elevated Cyclin D1 and Cyclin B1 levels in synchronized cells. Western blot analysis was performed for cyclin expression in whole cell lysates from cells synchronized at the G1/S boundary using a double thymidine block. HPV4-12 parental, empty vector control cells and SEPT9_v1 stable transductants were analyzed for the expression profile of several cyclin proteins. SEPT9_v1 over-expressing cells had nearly double the amount of Cyclin D1 protein and a 2.5-fold increase in Cyclin B1 levels as determined by densitometry. β-Actin expression was used as a loading control.

which contains a transcriptional activator specific for the JNK signaling pathway. This *in vivo* kinase assay was validated by transiently transfecting HPV4-12 cells with pMEKK1, which induced the JNK kinase activity more than 3-fold, and also by treating the cells with a well characterized JNK inhibitor, SP600125, which inhibited JNK kinase activity by 12-fold (Fig 3.12A). Quantitative data obtained with this dual reporter Luciferase system are shown in Figure 3.12B. In one immortalized human mammary epithelial cell line, MCF10A cells, SEPT9_v3 did not significantly increase reporter expression compared to controls although SEPT9_v1 did. Up-regulation of SEPT9_v1 and SEPT9_v3 in HPV4-12 cells significantly activated the kinase activity, as determined by the endpoint of Luciferase expression, by more than 5-fold and 3-fold, respectively, when compared to the HPV 4-12 cells with empty vector control ($p<0.001$; Student's t-test).

SEPT9_v1 Expression Amplifies JNK/c-Jun Signaling

The mechanism by which SEPT9_v1 mediates its tumorigenic properties via JNK1,2 activation, leading to c-Jun induction, may include the transcriptional up-regulation of c-Jun target gene expression. Transcriptional activity was measured by transiently co-transfecting cells with pRL-TK, expressing Renilla luciferase, and either a reporter plasmid containing the luciferase gene under a cis-acting enhancer AP-1 element (pAP1-Luc) or a negative control to determine the background signals associated with the culture medium and reporter activity (pTAL-Luc). The difference between the two reporters was used to determine differences in transcription activity. SEPT9_v3 up-regulation had an insignificant effect on transcriptional activity when compared to empty vector controls. However, up-regulation of SEPT9_v1 increased the reporter gene expression, or c-jun activated transcription, more than two fold when compared to empty vector controls (Fig 3.12C, $p=0.05$; Student's t-test). This data, combined with the lack of JNK kinase activation by SEPT9_v3 in Figure 3.11B, suggest that the

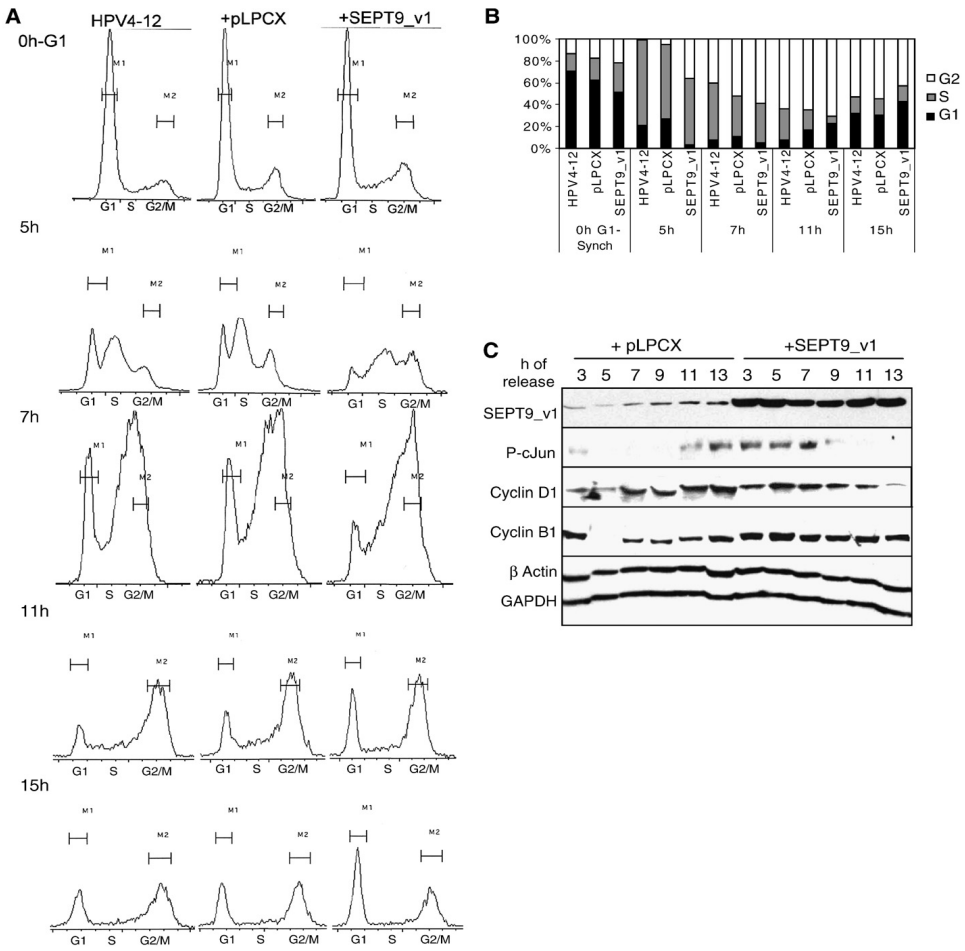

Fig 3.14: Up-regulated expression of SEPT9_v1 contributes to JNK1,2-mediated pro-proliferative effects in mammary epithelial cells.

(A) Cell cycle histograms generated by FACS analysis of parental HPV4-12 cells, the empty vector negative controls (pLPCX), and SEPT9_v1 transductants after releasing the cells from G1/S synchronization via double thymidine block. (B) Quantification of the data in panel (A) represents the percentage of cells in each phase of the cell cycle for each time point for each of the cell lines. SEPT9_v1 promotes cell cycle progression when it is up-regulated, compared to parental and vector control. HPV4-12 cells exogenously expressing SEPT9_v1 progressed to the S phase (5 hours after release), entered into G2, (7 hour post-release), and entered the next cycle (15 hours after release) faster than the controls. (C) Up-regulation of SEPT9_v1 induced higher levels of phosphorylated c-Jun, cyclin D1 and cyclin B1 at earlier stages of the cells cycle. Western blot analysis was used to determine the levels of SEPT9_v1, phosphorylated c-Jun, cyclin D1 and cyclin B1 at different time points after release from double thymidine synchronization for the empty vector controls and SEPT9_v1 transductants of HPV4-12 cells. Also note that endogenous SEPT9_v1 expression steadily increases following release from synchronization as the cells enter the G2 and M phases of the cell cycle. The samples and time points studied here were collected at the same time as those used for subpanels (A) and (B). β Actin and GAPDH were used as loading controls.

unique N-termini between the two SEPT9 isoforms have different abilities to regulate the JNK signaling pathway. For this reason, we decided to focus our remaining studies on the effects of SEPT9_v1 on JNK signaling. We decided to include SEPT9_v3 in subsequent assays as a comparison to the effects of SEPT9_v1 up-regulation in this pathway.

Up-regulation of SEPT9_v1 Increases the Expression of Cyclin D1, a c-Jun Target Gene, at the Protein and mRNA Levels

The gene encoding cyclin D1 (*CCND1*) has emerged as an important target for the JNK/c-Jun pathway in driving cell proliferation (130, 131). Ectopic expression of c-Jun induces expression of *CCND1* through an AP-1 site in the promoter, which in turn is critical in driving G0 to G1 cell cycle progression (132, 133).

We therefore investigated whether the enhanced transcriptional activity of the JNK1,2 signaling pathway, as a result of SEPT9_v1 over-expression, increases cyclin D1 levels in human mammary epithelial cells. Whole cell extracts of parental HPV4-12 cells, empty vector controls, and SEPT9_v1 over-expressing stable transductants were analyzed by Western blotting and probed with anti-cyclin D1, anti-phospho-cyclin D1 (Thr 286), and anti-cyclin E antibodies. The same lysates used in the JNK Kinase assays and immunoprecipitation experiments were used for profiling the expression of various cyclin proteins to reproduce the testing conditions in unstressed cells. Asynchronous SEPT9_v1 expressing cells showed higher levels of cyclin D1 expression and a 10-fold increase in phosphorylated cyclin D1 when compared to the controls (Fig 3.13A). As demonstrated in Fig 3.13, cells with high SEPT9_v1 expression have increased cyclin D1 levels as compared to controls, and phosphorylated cyclin D1 was also increased. Phosphorylation of cyclin D1 results in proteosomal degradation and a subsequent decline in its protein levels, which is necessary for the progression of the cell cycle from G1 to S. Through its interaction with JNK proteins, high SEPT9_v1 expression may be affecting protein kinetics, by

having more cyclin D1 molecules available, there are also more molecules to phosphorylate and target to the proteosome (134). Further studies are necessary to determine if SEPT9_v1 is directly controlling the levels of cyclin D1 phosphorylation or affecting the expression of kinases responsible for the phosphorylation. This finding agrees with the enhanced transcription from the luciferase reporter assay following SEPT9_v1 over-expression described in Figure 3.12C. Cyclin E expression was relatively unchanged in cells over-expressing SEPT9_v1. However, the high endogenous expression of cyclin E we observed in this human mammary epithelial cell line is consistent with previously described data showing that high levels of cyclin E expression is a consequence of the immortalization process, which precludes further up-regulation of this cyclin or our ability detect any subtle changes in cyclin E levels (135).

Confirmation of SEPT9_v1 activating transcription of the downstream targets of the JNK/c-Jun signaling pathway was achieved by determining the *CCNDI* mRNA relative expression compared to the GAPDH control, using quantitative RT-PCR. We found nearly a 2-fold increase in *CCNDI* expression in HPV4-12 cells expressing the SEPT9_v1 construct (Fig 3.13B).

SEPT9_v1 Up-regulation Correlates with Higher Cyclin Levels in the G1/S Phase of the Cell Cycle

Evidence to date indicates that up-regulation of cyclin D1 after the activating phosphorylation of c-Jun on residues Ser63 and Pro73 plays an important role in cell proliferation (128, 136). Cyclin D1 serves as a key sensor and integrator of cellular signals in early to mid-G1 phase (136, 137). We studied the consequences of SEPT9_v1 up-regulation in G1/S cells synchronized using a double thymidine block method. Whole cell lysates of synchronized HPV4-12 parental, empty vector controls, SEPT9_v1 and SEPT9_v3 stable transductants were analyzed by Western blotting for the expression profile of several cyclin proteins. No significant changes were noted when SEPT9_v3 was expressed. Likewise, cyclin E

expression was the same in all of the cells regardless of the SEPT9 isoform expression or the cell stage as seen earlier in asynchronous cultures (Fig. 3.13A and C). Cells exogenously expressing SEPT9_v1 had nearly double the amount of Cyclin D1 protein and a 2.5-fold increase in Cyclin B1 levels (Fig 3.13C).

Up-regulated Expression of SEPT9_v1 Contributes to JNK Pro-proliferative Effects in Mammary Epithelial Cells

We wanted to clarify the biological significance of the deregulation of SEPT9_v1 expression towards JNK kinase activity during the cell cycle. We hypothesized that increased SEPT9_v1 expression promoted cell cycle progression, possibly caused by the interaction with its binding partner, JNK1,2, thereby provoking the alteration in the JNK/c-Jun transcriptome. First, we studied the cell cycle histogram by FACS analysis of parental HPV4-12, the empty vector negative controls (pLPCX), SEPT9_v1 and SEPT9_v3 transductants after releasing the cells from G1 synchronization. We found a promotion of the cell cycle progression when SEPT9_v1 is up-regulated, compared to parental and vector control (Fig 3.14A). HPV 4-12 cells progressed to the S phase (5 hours after release), entered into G2, (7 hours post-release), and entered the next cycle (15 hours after release) faster than the controls. A quantification of these data, as shown in Figures 3.14B, represents the percentage of cells in each phase of the cell cycle for each time point.

In order to investigate the potential physiological relevance of SEPT9_v1 up-regulation in mammary epithelial cells at different cell cycle phases, we determined the levels of SEPT9_v1, phosphorylated c-Jun, cyclin D1 and cyclin B1 at different time points after release from synchronization for the empty vector controls and SEPT9_v1 transductants of HPV4-12 and Hs578T cells. Western blotting showed that up-regulation of SEPT9_v1 induced higher levels of phosphorylated c-Jun, Cyclin D1 and Cyclin B1 at earlier stages of the cells cycle (Fig 3.14C). The

time points studied here correlated with the cell cycle histogram and the percentage of cells at each cell cycle stage mentioned above.

Together, these data suggests that when SEPT9_v1 expression is up-regulated, as seen in breast cancer cell lines and primary breast cancers, SEPT9_v1 could hyper-activate the JNK signaling pathway, causing up-regulated expression of the downstream target genes, such as cyclin D1 (131). This would ultimately push the cells through the cell cycle at a faster rate.

Discussion

We explored in further detail the roles of SEPT9_v1 in tumorigenesis by describing two independent mechanisms impacting genomic instability and cell proliferation. First, SEPT9_v1 was found to increase genomic instability in mammary epithelial cells by effects on chromosome segregation defects and cytokinesis failure. In fact, when metaphase spreads of cells with high SEPT9_v1 were categorized by the number of extra chromosomes, a bimodal distribution was observed, with a population of cells with ploidy status close to tetraploidy and another population with more generalized aneuploidy. This suggested the possibility of two types of mitotic errors promoted by high SEPT9_v1 expression, mitotic spindle defects and failure to complete cell division at cytokinesis. A close look at mitotic cells showed that deregulation of SEPT9_v1 expression promotes mitotic spindle defects associated with chromosome mis-segregation including disorganization of the chromatin in respect to the mitotic spindles, multipolar spindles, and chromosome lagging during telophase. In addition, a small but significant population of SEPT9_v1 over-expressing cells became bi-nucleated demonstrating a failure of faithful division (cytokinesis) into two daughter cells. Interestingly, over-expression of SEPT9_v3, an isoform that differs from SEPT9_v1 by 25 amino acids at the N terminus, also increased genomic instability in mammary epithelial cells, but the mechanisms seemed to be more specific to defects in cytokinesis, because the ploidy status of these cells were

predominantly tetraploid. Different SEPT9 isoforms appear to have specific functional roles affecting different cellular processes by specific protein interactions, temporal-specific expression and/or cellular localization dictated possibly by the subtle differences in sequence.

Indeed, the cellular localization and protein interactions of these two SEPT9 isoforms are distinct. SEPT9_v1 cellular localization was mainly cytoplasmic with partial localization of the nucleus in mammary epithelial cells. SEPT9_v1 was found to co-localize with α-tubulin filaments in contrast with SEPT9_v3 which mainly localized to the plasma membrane and co-localized with F-actin filaments. Mitotic cells from SEPT9_v3 did not show significant gross mitotic spindle defects and/or chromosome mis-segregation, supporting the view that SEPT9_v3 impacts genomic instability by affecting cytokinesis, without major effects on the mitotic spindle machinery.

It was important to determine whether SEPT9_v1 affected general mitotic spindle assembly and function or interferes with proper regulation of the mitotic spindle checkpoint. Several candidates for protein interaction were assayed, and interactions with α-tubulin and γ-tubulin were observed by immunoprecipitation. Interactions with components of the checkpoint were negative, suggesting that SEPT9_v1 might affect mitotic spindle dynamics and/or organization by interacting with tubulins which are major components of spindle microtubules and microtubule organizer center (MTOC), or centrosomes. This is supported by previous studies that showed that SEPT9_v1 localized with microtubules at the midplane in metaphase during mitosis and in the midbody and cleavage furrow during cytokinesis (23, 24). Additional studies are needed to support these initial observations.

Previous studies have shown that knockdown of septins, including SEPT9 isoforms, resulted in cytokinesis defects and chromosome mis-segregation. In this study we presented an over-expression model of SEPT9 showing similar phenotypes, which supported the idea that the

expression and localization of septins needs to be tightly regulated in order to perform their normal functional roles in epithelial cells. When expression of septins is deregulated or the equilibrium between isoforms is altered, either by knockdown or over-expression, it could lead to the same phenotypes seen in this study. In fact a widely accepted theory in septins' research is that these proteins exert their functions by forming heterocomplexes and that the disruption of normal ratios of septins in the complex may change their functional dynamics in the cells.

Genomic instability can affect the overall equilibrium of cells between cell proliferation and apoptosis, cell cycle progression, and mitosis in general. Trying to understand the cellular context in which high expression of SEPT9_v1 impacted genomic instability and high cell proliferation in mammary epithelial cells, analysis of the effects of ectopic expression of SEPT9_v1 overtime was performed. The goal was to determine if there was a temporal relationship between the different phenotypes after SEPT9_v1 expression. Specifically, I decided to explore the possibility that cell proliferation would increase after the establishment of aneuploidy or if these phenotypes could arise independently, which would have suggested that SEPT9_v1 is associated with different cellular mechanisms and signaling pathways. As shown earlier, after transient expression of SEPT9_v1 both phenotypes arose simultaneously and as early as one doubling time after transfection. This pattern was shown more clearly with the MCF10A cell line, but even though HCT116 showed a clear increase in aneuploidy, cell proliferation did not change as much during time, which actually supports the idea that these two phenotypes are affected by SEPT9_v1 expression via two different mechanisms.

Given that SEPT9_v1 and JNK1, 2 impacted cell proliferation and they shared the ability to regulate HIF-1, which at the same time regulates cell proliferation and survival in response to oxygen levels, we hypothesized a crosstalk relevant to cell proliferation between these proteins. A potential interaction between SEPT9_v1 and JNK to try to understand better the role of

SEPT9_v1 in cell proliferation in mammary epithelial cells seemed important to explore. In trying to elucidate the mechanism by which SEPT9_v1 increased cell proliferation, a novel connection with the JNK signaling pathway was found. SEPT9_v1 interacted with c-Jun-N-terminal kinase, stabilizing it and increasing its transcriptional activation of target Ap1 promoter genes such as cyclin D1 and cyclin B1 in unstressed cells. The SEPT9_v1-JNK connection showed that SEPT9_v1 over-expression accelerated cell cycle progression and consequently cell proliferation. Interestingly, retroviral expression of the SEPT9_v1 isoform consistently had stronger affects on JNK signaling and c-Jun transcription activation when compared to retroviral expression of the SEPT9_v3 isoform, a protein identical to SEPT9_v1 except for 25 amino acids at the N-terminus. This was in agreement with previously discussed data that retroviral expression of the full-length SEPT9_v1 variant resulted in the striking development of oncogenic phenotypes when expressed in breast cells as compared to the retroviral expression of SEPT9_v3 (20). As previously mentioned, only 25 N-terminal amino acids differentiate these two isoforms; this suggests that these residues are crucial for the contrasting regulation of JNK1,2 signaling between these two isoforms. This is not the first time that a difference in SEPT9 isoforms has been noted. For example SEPT9_v4 and SEPT9_v4* differ only in their 5' untranslated regions, but only SEPT9_v4* is differentially expressed in cancers compared to normal tissue (76, 77). More relevant to the isoforms discussed in this study was the finding that SEPT9_v3, but not SEPT9_v1, interacts with a Rho-guanine nucleotide exchange factor (GEF) along with actin stress fibers and inhibits Rho signaling activation (89, 90).

Our data correlated with previous reports in which the cyclin D1 gene, *CCND1*, has emerged as an important target of the JNK/c-Jun-AP1 pathway in driving proliferation (130, 131). This suggested that the up-regulation of SEPT9_v1 induced hyper-proliferation by a signaling mechanism involving JNK stabilization, but mediators or other components upstream

of SEPT9_v1 have yet to be identified. We propose that the JNK/c-Jun/AP-1 pathway and its downstream target genes are relevant physiological targets of SEPT9_v1 as their up-regulation gave a proliferative advantage to the cells by making them cycle faster through the G1 phase of the cell cycle and altered the expression pattern of regulatory cyclin proteins, including cyclin D1 and cyclin B1.

Taken together, our data showed a novel association of SEPT9_v1 with the JNK1,2 signaling pathway, an important signaling pathway that regulates cellular proliferation among other cellular roles. This further supported the hypothesized role of SEPT9 in cell signaling pathways that regulate cellular proliferation as previously suggested by studies of SEPT9_v1 and its association with HIF-1 alpha (72). A proposed model of the mechanism by which SEPT9_v1 expression in breast cancer cells may impair cell cycle regulation, resulting in the increased transcription of key cyclins that drive progression through the cell cycle is shown in Figure 3.15.

Here it is demonstrated that deregulation of SEPT9 isoforms affects different cellular mechanisms. The resulting cellular phenotypes, or the severity of them, may vary depending on which isoform is affected. In this case, SEPT9_v1 and SEPT9_v3 both seem to increase genomic instability in mammary epithelial cells. Interestingly, SEPT9_v1 affects proper function of the mitotic spindle and the completion of cytokinesis by interacting with some important components of the cytoskeleton, but SEPT9_v3 seems to largely control the cytokinesis event during mitosis. In fact, cytoskeletal interactions between the two isoforms were somewhat different and specific. In addition, it was found that, for at least two oncogenic phenotypes, cell proliferation and genomic instability due to high SEPT9_v1 expression, the results could be explained with two distinct mechanisms involving the JNK pathway and the cytoskeleton dynamics, respectively. How SEPT9_v1 performs its diverse functions is still puzzling. There is still the possibility that septins are scaffolding proteins involved in the recruitment of other

cytoskeletal proteins to their site of action and/or their potential role as signaling GTPases. Another key factor is SEPT9_v1 localization; there is evidence of cytoplasmic and nuclear localization raising the possibility that it shuttles in and out of the nucleus. Further analysis of these observations will be important for elucidating the complex and distinct functions of SEPT9_v1 in breast tumorigenesis.

This study also demonstrated two intrinsic properties of SEPT9 isoforms. First, different isoforms seems to have specific functions and deregulation of their expression gave rise to different phenotypes such as genomic instability and cell proliferation. Second, the mechanism by which over-expression of SEPT9 isoforms, at least for SEPT9_v1 and SEPT9_v3, promoted the development of these phenotypes are discernable and probably dependent on cellular localization and cell cycle stage. Future experiments analyzing the functional domains of SEPT9_v1 and spatial and temporal expression studies are essential to understanding the specific functional role of SEPT9_v1 in mammary tumorigenesis as a promoter of cancer initiation, modulator of cancer progression and/or a marker for more aggressive breast cancers.

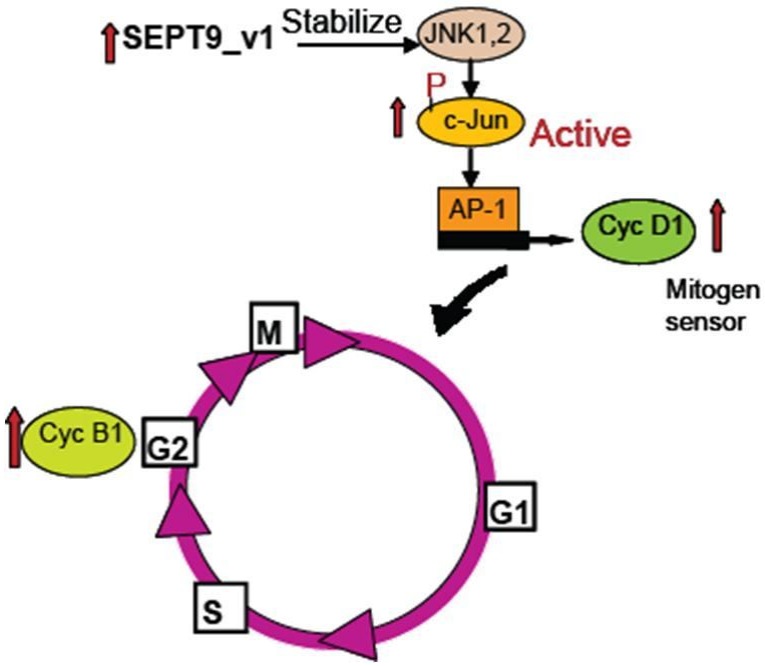

Fig 3.15: Proposed model for the mechanism by which increased SEPT9_v1 expression results in increased cell proliferation, a hallmark of cancer cells

SEPT9_v1 stabilizes JNK1,2 kinase, allowing the JNK kinases to activate c-Jun by phosphorylation. c-Jun activity thus is not properly regulated and induces AP-1 mediated transcription of cyclin D1, and other AP-1 controlled target genes, to cause increased proliferation and "faster" movement through the cell cycle. In an unidentified, or related, mechanism, cyclin B1 expression is also increased, causing the cells to prematurely enter mitosis.

Acknowledgments

This work was supported by the NIH National Research Service Award #5-T32-GM07544 from the National Institute of General Medicine Sciences and the NRSA Predoctoral Individual Fellowship to Promote Diversity in Health-Related Research # 1F31CA123639-01-A1 to E.A. Peterson and by the NIH National Cancer Institute grant RO1CA072877 to E.M. Petty. We want to thank Sam Straight from the Center for Live-Cell Imaging for helpful technical support with microscopy. We also thank Amy Silvers and Dorraya El-Ashry for helpful data analysis and discussion of the JNK signaling data.

Notes

Parts of this work were previously published as:

González, M.E., Makarova O., Peterson, E.A., Privette, L.M., and Petty, E.M., "Up-regulation of SEPT9_v1 stabilizes c-Jun-N-Terminal kinase and contributes to its pro-proliferative activity in mammary epithelial cells", *Cell Signal.* 2009 Apr; 21(4):477-87.

CHAPTER IV

CHARACTERIZATION OF A SEPT9 INTERACTING PROTEIN, SEPT14, A NOVEL TESTIS-SPECIFIC SEPTIN

Summary

Septins are a highly conserved family of GTP binding cytoskeletal proteins implicated in multiple cellular functions including membrane transport, apoptosis, cell polarity, cell cycle regulation, cytokinesis, and oncogenesis. This work describes the characterization of a novel interacting partner of the septin family, initially cloned from a human testis expression library following yeast two-hybrid isolation to identify SEPT9 binding partners. Upon further genomic characterization and bioinformatics analyses, it was determined that this novel septin-interacting partner was also a new member of the mammalian septin family, named SEPT14. SEPT14 maps to 7p11.2 in humans and includes a conserved GTPase domain and a carboxy-terminus coil-coiled domain characteristic of other septins. Three potential translational start methionines were identified by 5' RACE-PCR encoding proteins of 432, 427 and 425-residue peptides, respectively. SEPT14 shares closest homology to SEPT10, a human dendritic septin, and limited homology to SEPT9 isoforms. SEPT14 co-localized with SEPT9 when co-expressed in cell lines and epitope-tagged forms of these proteins co-immunoprecipitated. Moreover, SEPT14 was co-immunoprecipitated from rat testes using SEPT9 antibodies and yeast two-hybrid analysis suggested SEPT14 interactions with nine additional septins. Multi-tissue Northern blotting showed testis-specific expression of a single 5.0 kb SEPT14 transcript. RT-PCR

analysis revealed that SEPT14 was not detectable in normal or cancerous ovarian, breast, prostate, bladder or kidney cell lines, and was only faintly detected in fetal liver, tonsil and thymus samples. Interestingly, SEPT14 was expressed in testis but not testicular cancer cell lines by RT-PCR. Additional expression and functional analyses are essential to understand the biological role of SEPT14 in the testes.

Introduction

Unraveling the functional role of septins in mammalian cells will depend upon studying the formation of hetero-oligomers with members of their own family and other protein interactions. In fact, recent studies showed for the first time that human septins form hexamers composed of two molecules of each mediated by both GTP-GDP and Nterm-Cterm interphases as shown by the SEPT2-SEPT6-SEPT7 complex (7). These hexamers might be the structural conformation of septins while they exert their biological roles and by which they mediate dynamic interactions with other filamentous proteins. In fact, it is known that animal septins, similar to yeast septins, can form polymeric actin-associated filaments and interact with other cytoskeletal and filamentous proteins such as myosin and tubulins, supporting their roles in cytokinesis, cell morphology, cell motility and polarity, and dynamic scaffolds(138).

In humans, 13 septin genes have been characterized since 1997 (SEPT1-SEPT13) including SEPT9 which was mapped in our lab to a region of allelic imbalance in breast cancers on chromosome 17q25 (74). In an effort to further understand SEPT9's roles in normal cellular functions and oncogenesis, we sought to identify novel interacting partners. Important to mention is that finding interacting proteins of septins has been challenging due to the complexity of their oligomers and their potential redundancy in mammalian cells. One example that shows the intrinsic structural complexity and organization of mammalian septins was presented by Nagata *et al*. in which they found at least five septins, Sept2, Sept7, Sept8, Sept9b (SEPT9_v3), and Sept11, in septin complexes affinity-purified with an anti-Sept7 antibody-conjugated column from rat embryonic fibroblast REF52 cells (139). Importantly, immunofluorescence studies revealed co-localization of Sept7, Sept9b, and Sept11 along stress fibers and biochemical and immunoprecipitation analyses revealed that the three septins directly bind with each other through their N- or C-terminal divergent regions (139). These

septins formed distinct and characteristic filament structures when transiently expressed in COS7 cells. When only two of the three were co-expressed, changes in filament enlongation, bundling or disruption were observed. Taken together, these results suggest that septin filament structures may be affected by interactions with other septins included in the complex (139). In addition to this, we have to consider that the *SEPT9* locus encodes for at least 7 isofoms, which are expressed ubiquitiously in human cells.

With this in mind, I describe herein the identification of a novel septin, SEPT14, by yeast two-hybrid analysis with SEPT9. The characterization of its genomic organization, phylogenetic relationship to other human septins, expression profile, cellular localization and interaction with other septins is described in order to begin elucidating its function.

Materials and Methods

Plasmid construction

PCR products encoding full-length coding regions of MSF/SEPT9 isoforms were amplified from normal breast cDNA and TA subcloned into pCR-XL-TOPO (Invitrogen Corporation). These TA-MSF/SEPT9 constructs were subsequently used as PCR templates with primers designed to add flanking 5' *Nde*I and 3' *Xma*I sites to the MSF/SEPT9 specific sequences. Ligation of the *NdeI-XmaI* digested PCR product into yeast vectors included with the Matchmaker GAL4 Two-Hybrid System 3 (BD Biosciences, San Diego, CA) produced an in-frame MSF/SEPT9 carboxy-terminus fusion protein product with either the plasmid-encoded GAL4 binding domain or c-Myc sequences (pGBKT7). All PCR products were resolved on 1.0% agarose gels, excised, and purified through QIAquick Spin Columns (Qiagen Inc., Valencia, CA) before subcloning, and all plasmids were sequenced at The University of Michigan Sequencing Core to confirm the absence of *Taq* polymerase induced errors before proceeding.

In vitro transcription/translation

SEPT14 cDNA starting at three different potential start site methionines was subcloned into the T7 promoter plasmid pCR-XL-TOPO by TA cloning following manufacturer's instructions (Invitrogen Inc.). Each plasmid SEPT14 –M1, -M2 and –M3 was used with the TNT® Quick Coupled Transcription/Translation System (Promega) following manufacturer's instructions. Briefly, 0.5 ug of each plasmid was combined with 40ul TNT T7 Quick Master Mix, 1ul of Methionine 1mM, 1-2ul of Transcend™ Biotin-Lysyl-tRNA and nuclease-free water for a 50 ul reaction. The reaction was incubated at 30 °C for 90 minutes. SEPT14-M1 antisense plasmid was used as a negative control and a T7 promoter Luciferase plasmid was used as a positive control for the assay. Then, samples were analyzed by SDS-PAGE using a 4-15% Tris HCL acrylamide gel. Samples were transferred to a PVDF membrane using the Transblot SD Semidry blot system (BioRad) for 45 minutes. Then, the membrane was incubated for 1 hour with TBS+0.5% Tween® 20 (TBST), followed by a one hour incubation with a 1:10,000 dilution of Streptavidin-HRP conjugated in TBST. Then the membrane was washed 3 times with TBST and 3 times with water. To detect the products, 2.5 ml of Transcend™ Chemiluminescent Substrate A and 2.5ml of Substrate B were mixed and added to the PVDF membrane for one minute. The blot was exposed to Kodak X-Omat AR X-ray film for different exposure times. Finally, the film was developed in a Konika-Minolta SRX-101A developer.

Site-directed mutagenesis

SEPT9-M1 and –M2 methionines were mutated to leucines using QuickChange® XL Site-Directed Mutagenesis Kit (Stratagene®) following manufacturer's instructions. The following primers were used with the SEPT14-M1 plasmid to mutate M2 and M3 methionines: forward: 5'–GGCAGAAAGAACACTGGCTCTGCCCACACAAATACC-3' and reverse: 5'-GGTATTTGTGTGGGCAGAGCCAGAGCCAGTGTTCTTTCTGCC-3', and to mutate the –M3 methionine in the SEPT14-M2 plasmid the primers used were forward: 5'-

GGCAGAAAGAACAATGGCTCTGCCCACACAAATACC-3' and reverse: 5'-GGTATTTGTGTGGGCAGAGCCATTGTTCTTTCTGCC-3'. Briefly, 10 ng of each plasmid was combined with 5 μl of 10X reaction buffer, 125 ng of each primer, 1 μl of dNTP, 3 μl of Quick Solution, and 1 μl of Pfu Turbo DNA polymerase (2.5 U/μl) provided by the kit. The reactions were run in a thermocycler 95 °C for 1 min, (95 °C for 50 sec, 60 °C for 50 sec, 68 °C for 3.5 min) x 18 cycles and 68 °C for 7 minutes. Then, 1 μl of *Dpn* I restriction enzyme (10 U/μl) was added to each reaction and incubated for 1 hour at 37 °C. Finally, each reaction was transformed into XL10-Gold ultracompetent cells and screened for positive mutagenesis by DNA sequencing.

SEPT9 Yeast two-hybrid screening

Standard methods and media were used as described in the Yeast Protocols Handbook (BD Biosciences, San Diego, CA). pGBKT7 (TRP, Kan^R) constructs were transformed using lithium acetate into yeast strains AH109 (MATa, trp1-901, leu2-3, 112, ura3-52, his3-200, gal4Δ, gal80Δ, LYS2::$GAL1_{UAS}$-$GAL1_{TATA}$-HIS3, $GAL2_{UAS}$-$GAL2_{TATA}$-ADE2, URA3::$MEL1_{UAS}$-$MEL1_{TATA}$-lacZ) (BD Biosciences). Cultures were grown on SD-Met/-Ura, and transformants were selected on SD-Trp. Plasmid-derived protein expression was confirmed by Western analysis on total yeast lysate using fusion protein antibody c-Myc (BD Biosciences; pGBKT7 constructs). Full-length coding region MSF-A/SEPT9_v1-pGBKT7 was mated with a commercially available pretransformed human testis pACT2 cDNA library (LEU, Amp^R in Y187, BD Biosciences) in 2X YPDA overnight. The presence of zygotes was confirmed microscopically before plating the culture on 150 mm high stringency SD-Ade/-His/-Leu/-Trp plates containing 20 μg/mL X-α-gal. Blue colonies appearing after 7-14 days were used to inoculate SD-Ade/-His/-Leu/-Trp cultures from which plasmid DNA was isolated by lyticase/SDS lysis. DNA was electroporated into KC8 cells (BD Biosciences), and testis cDNA-pACT2 transformants were selected from MSF-

A/SEPT9_v1-pGBKT7 transformants by ampicillin resistance. DNA from subclones was purified using the Wizard Plus SV spin column (Promega Corporation) and sequenced.

Chromosomal map and genomic organization

Human Genome Blast (http://www.ncbi.nlm.nih.gov/BLAST) was applied to determine the chromosomal mapping. PCR against a human chromosomal mapping panel was used to confirm the mapping location. The exon/intron structure was modeled based on the complete sequence of BAC 419m24.

Phylogenetic analysis of the human septin family

Prior to this report, 13 human septins genes were reported. The amino acid sequences from the following accession numbers were used to create a phylogenetic tree using ClustalW (http://www.ebi.ac.uk/clustalw/): NM_052838 (SEPT1), NM_001008491 (SEPT2), BC111779 (SEPT3), NM_080415 (SEPT4), Y11593 (SEPT5), AF403061 (SEPT6), NM_001011553 (SEPT7), AF440762 (SEPT8), NM_006640 (SEPT9), AF146760 (SEPT10), NP_060713 (SEPT11), and NP_653206 (SEPT12). The SEPT13 partial predicted amino acid sequence is available in Hall et al. 2005.

Yeast two-hybrid with SEPT14 and septin family interactions

All plasmids and yeast strains were kindly provided by the lab of Roger Brent (140). All yeast two hybrid methods were performed as previously described (140-142), and interactions were assessed by the ability of diploid yeast to grow on selective media and to activate the LacZ reporter. Rat cDNAs for SEPT6 (GI 109512511) and SEPT11 (GI 109500352) were isolated from a rat brain cDNA library (Origene, Rockville, MD, USA). The following sequences were cloned into yeast expression vectors using EcoRI and/or XhoI sites, and constructs were confirmed by sequencing: human SEPT1 (GI 15082493); human SEPT2 (GI 56550108); rat SEPT3 (GI 9507084); human SEPT4 (GI 17986250); wildtype SEPT5 (28, 29); human SEPT7 (GI 19684120); human

SEPT8 (GI 1503987); human SEPT9_v1 (GI 34782782); human SEPT10 (GI 7688656); and rat SEPT12_v2 (GI 66911992). SEPT9_v1 also was subcloned into a pcDNA-Flag vector, analogous to that described elsewhere (Surka et al, 2002). pEGFPC1-SEPT14 was constructed by subcloning from PCR-XL-TOPO.

Northern analyses

Multi-tissue polyA+ Northern membranes (BD Biosciences Clontech) were hybridized as previously described (74) using the 3a-S1 and 3a-S2 *SEPT14* PCR products as a probe.

PCR

Reactions to amplify products for subcloning in TA and yeast two-hybrid vectors were performed using the Expand High Fidelity PCR System (Roche Molecular Biochemicals, Indianapolis, IN) per manufacturer's instructions. Reactions for 5' RACE were performed using the GeneRacer Kit (Invitrogen Corporation) with the Expand Long Template PCR System (Roche Molecular Biochemicals, Indianapolis, IN) and testis total RNA (BD Biosciences). All other PCR reactions were performed using *Taq* polymerase (Promega Corporation) as previously described (74).

To optimize semi-quantitative multiplex PCR, reactions using normal breast cDNA with actin (143) and septin primers initially at 0.8 μM each were sampled every two cycles from cycles 15-25. Products were analyzed on a 3% agarose gel to determine optimal cycle number for linear amplification of both bands. If necessary, reactions using the optimal cycle number were repeated adjusting actin or septin primer concentrations (0.1 to 3.2 μM) to generate products of equal intensity. Tissue-specific cDNA was generated from total RNA as previously described (144) or was commercially available (Human Immune Multitissue cDNA panel; BD Biosciences, San Diego, CA).

To generate products for TA subcloning, primer pairs MSF5-F and 311-F3 (1727 bp), 311atg-F2 and 311-F3 (1783 bp), and 311seq-P2 and 311-F3 (1312 bp) were used. To add *Nde*I and *Xma*I sites to PCR products for yeast vector subcloning, primer pairs MSFY2HNdeI-F and MSFxY2HxmaI-R (1715 bp), MSFaY2HNdeI-F and MSFxY2HXmaI-R (1779 bp), and MSFbY2HNdeI-F and MSFxY2HXmaI-R (1287 bp) were used. To amplify additional 5' sequences of SEPT14 by RACE, primers RACE1 and RACE2 were paired with commercially provided GeneRacer 5' and 5' nested primers respectively. To determine the chromosomal location of SEPT14 on a human chromosomal mapping panel (Coriell Institute for Medical Research panel 2/version 3) (145), primers 3a-F1 and 3a-R1 (142 bp) were used. To generate a SEPT14 hybridization product for Northern analysis, primers 3a-S1 and 3a-S2 (1077 bp) were used. To co-amplify septins with actin for semi-quantitative PCR, primer pairs MSF-F and 311-RACE4 (503 bp), 311atg-F2 and 311sljseq-R (129 bp), 311e3-R and 311-10R (1139 bp), and 3a-S3 and 3a-R1 (288 bp) were used.

Immunostaining and image acquisition

Cells were permeablized in 0.1% Triton X-100 in blocking solution (3% milk powder in PBS) for 2 minutes prior to staining. Cells were fixed, processed and imaged as previously described (Surka et al., 2002). Briefly, anti-SEPT9 polyclonal antibodies were used at a dilution of 1:2000, as previously described (Surka et al, 2002) and DNA was visualized with bisbenzimide (Sigma-Aldrich Canada Ltd) at a concentration of 5 μg/mL for 10 minutes. Rhodamine-conjugated secondary antibodies (Jackson ImmunoResearch Labs) were used as previously described (Surka et al., 2002). Imaging was done using a Quorum Spinning Disk Confocal Microscope and a Leica DMIRE2 inverted fluorescence microscope equipped with a Hamamatsu Back-Thinned EM-CCD camera and spinning disk confocal scan head, equipped with 4 separate diode-pumped solid state laser lines (Spectral Applied Research: 405nm, 491nm, 561nm, 652nm), an ASI motorized XY stage, an Improvision Piezo Focus Drive and a 1.5X magnification

lens (Spectral Applied Research). The equipment was driven by Volocity acquisition software and powered by an Apple Power Mac G5. Representative optical slices (captured at a Z-spacing of 0.2μm) are shown.

Co-immunoprecipitation studies

Sixty millimeter dishes of CHO cells (approximately 80% confluency) were cotransfected for 24 hours with Flag-SEPT9_v1 and GFP-SEPT14, using Fugene transfection reagent (Hoffman-La Roche Limited,). Upon lysis in 40 mM Tris, pH 8.0, 100 mM NaCl, 1% TritonX-100 and standard protease inhibitors, lysates were incubated with rotation for one hour at 4°C and clarified by high-speed centrifugation. Two micrograms of anti-FlagM2 monoclonal antibody (Sigma-Aldrich Canada, Ltd.) was used for immunoprecipitation, and controls were conducted with purified mouse IgG. Following the addition of antibodies, protein G-agarose was added (Invitrogen Canada Inc.), and samples were rotated for several more hours at 4°C. After extensive washing, samples were resolved by SDS-PAGE and transferred to PVDF membrane (Millipore Corp.), and Western blotting was performed using a standard protocol. Affinity-purified anti-GFP polyclonal antibody (Invitrogen Canada Inc.) was used at a dilution of 1:1000; anti-Flag monoclonal antibody (Sigma-Aldrich Canada, Ltd.) was used at a dilution of 1:1000, and HRP-conjugated secondary antibodies (BioRad Laboratories Ltd.) were used at a dilution of 1:5000. The signal was detected by ECL Western blotting Detection Reagent (GE Healthcare) and exposure to autoradiography film.

Mass Spectrometry

Immunoprecipitation was performed as described above, except 20 μg of anti-SEPT9 antibody was used; this antibody is described elsewhere (24). Rabbit IgG was used as a control. Briefly, one rat testicle (Harlan Laboratories, Indianapolis, IN, USA) was homogenized using a mortar and pestle, under liquid nitrogen; then resuspended and lysed in 40mM Tris, pH 8.0,

100mM NaCl, 1% TritonX-100, and standard protease inhibitors in a dounce mechanical homogenizer. After rotation for one hour at 4°C, followed by clarification by high-speed centrifugation, antibodies were added and rotation was continued. After approximately 4 hours, protein A-agarose beads were added (Invitrogen Inc.) and immunoprecipitation was conducted overnight. Following extensive washing in the above buffer, immunoprecipitated proteins were resolved by SDS-PAGE and bands of interest were excised. After standard trypsin digestion, bands were subjected to MALDI-TOF analysis. Unique peptide hits of greater than 95% accuracy were compared against public databases allowing for identification of corresponding proteins. Mass spectrometry was conducted by the Hospital for Sick Children Advanced Protein Technology Centre (Toronto, ON, Canada).

Identification of rat SEPT14

BLAST analysis was used to determine the sequence of the rat SEPT14 cDNA, using human SEPT14 ORF, human SEPT14 gene structure, and EST clones as templates. Alignments were performed with ClustalW and BLAST (NCBI).

Results

Identification and sequence analysis of human SEPT14

To begin to elucidate the functions of the members of the SEPT9 (MSF) subfamily of septins in normal cellular processes, we searched for interacting proteins. SEPT9_v1 (MSF-A) was chosen to initiate the analysis as this alternative transcript is ubiquitously expressed (74). We chose to screen against a testis-specific expression library, reasoning that this tissue exhibits a comprehensive transcript expression profile. Using a yeast two-hybrid GAL4 DNA interacting and binding domain coupled system, the development of blue diploid yeast colonies on high stringency SD-Ade/-His/-Leu/-Trp/+X-α-gal culture plates indicated the capture of a potential SEPT9_v1 (MSF-A) interacting partner. From one such colony, a testis library-derived, ampicillin resistant plasmid was isolated. BLAST sequence analysis determined that the 1658 bp insert encoded a partial sequence for an apparently novel septin that included the signature GTPase domain. Retransformation of this plasmid into the yeast Y187 haploid strain and subsequent mating with the original SEPT9_v1 (MSF-A)-expressing AH109 haploid strain produced blue diploid colonies under identical high stringency growth conditions, verifying this clone. In addition, mating of the recovered novel septin construct with GAL4 binding domain constructs expressing full-length SEPT9_v3 (MSF) or the SEPT9_v4 (MSF-B) isoforms also produced blue diploid yeast colonies under similar growth conditions (Fig. 4.1). Following the HUGO approved septin nomenclature system (81), we designated this novel septin SEPT14.

In addition to a GTPase domain, the captured *SEPT14* insert encoded in-frame amino acids ending in a predicted stop codon followed by a consensus polyadenylation signal and a polyA tract in a 3' untranslated region.

Table 4.1: SEPT14 genomic structure

Exon	Acceptor	Donor	Exon (bp)	Intron (Kb)
1	5′ UTR...	...ccctgggaaa**gt**aagttatt	68	0.677
2	aaatttcc**ag**ctcttttagt...	...TGGAGATACA**gt**taagtata	68	15.306
3	tttattta**ag**CAAAAAGAAA...	...CTCTGTGTGG**gt**aagtgtca	120	1.799
4	tctattac**ag**GGGAGACTGG...	...AAGAAGCCAG**gt**gagtgttt	195	1.395
5	tttttttt**ag**CTACCAACCA...	...TGACAGTAAG**gt**atgtttgg	186	8.356
6	ttcttcat**ag**GTGAATATTA...	...CTCAGTTAGT**gt**aagtttca	161	15.202
7	tgttttct**ag**GGGCTGTTAC...	...GTTTTGCAAG**gt**aaaaatga	96	11.869
8	tttttact**ag**TGGAAAATGA...	...AGCCAGTTAG**gt**gagtaaaa	168	1.7
9	ttctcttt**ag**TTTTCAAGAA...	...TGAAAAAGAG**gt**tagtactg	132	9.166
10	ggtttcac**ag**CTGCAGGACA...	...3′ UTR	629	

[a]Consensus ag/gt splice dinucleotides are in bold. Nucleotides in upper case flank coding exonic regions; nucleotides in lower case flank untranslated or intronic regions.

To complete the amino terminus coding sequence of *SEPT14*, RACE using a testis cDNA library was utilized to isolate additional 5' sequences that included a potential translational start methionine. Overlapping amplification products were assembled that added an additional 176 bp. Three potential translational start methionines (M1, M2, and M3) were found within 30 nucleotides of each other and downstream of a stop codon (Fig. 4.2). Proteins of 432 residues/50.0 kDa, 427 residues/49.4 kDa, and 425 residues/49.2 kDa were predicted originating from M1, M2, and M3 respectively (Fig. 4.2). Methionines M1 and M2 were preceded by more precise Kozak consensus sequences compared to M3, although all three were able to direct protein synthesis *in vitro* from constructs (Fig. 4.3).

SEPT14 was most similar to SEPT10 (67% identity/78% conservation), a septin on chromosome 8q11 (81), and showed only limited amino acid homology to MSF-A/SEPT9_v1 (39% identity, 61% conservation; Fig. 4.2). In addition to a GTPase domain, *in silico* modeling predicted a carboxy-terminus coiled-coiled domain, characteristic of Group II septins (19). A dendrogram generated with the ClustalW program confirmed these phylogenetic relationships (Fig. 4.4).

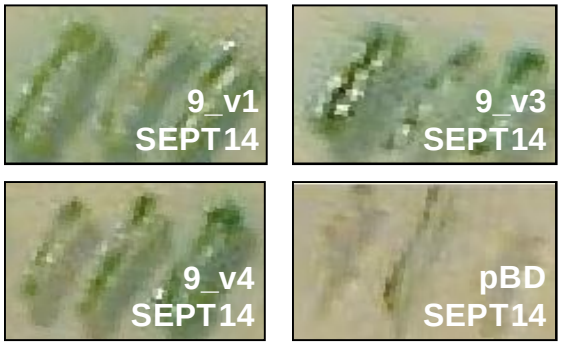

Fig 4.1: SEPT14 interacts with SEPT9 isoforms in a yeast-two hybrid assay

Formation of blue color by diploids grown on selective plates containing IPTG indicates a protein-protein interaction between full-length SEPT14 and SEPT9 _v1, _v3, and _v4. Mating pairs are indicated with the top haploid strain representing the yeast binding-domain GAL4 pGBKT7 construct or empty vector (pBD), and the bottom haploid strain representing the SEPT14 construct.

Fig 4.2: Alignment of human SEPT14 with SEPT10 and SEPT9

Amino acids identical to SEPT10 are shown with a gray background. The nine amino acids that are boxed in predict a GTP-binding site motif (AG)-X(4)-G-K-(ST), and sequences within a coiled-coil domain are shown in bold. Arrows indicate predicted start site methionines (M1, M2, and M3) for SEPT14.

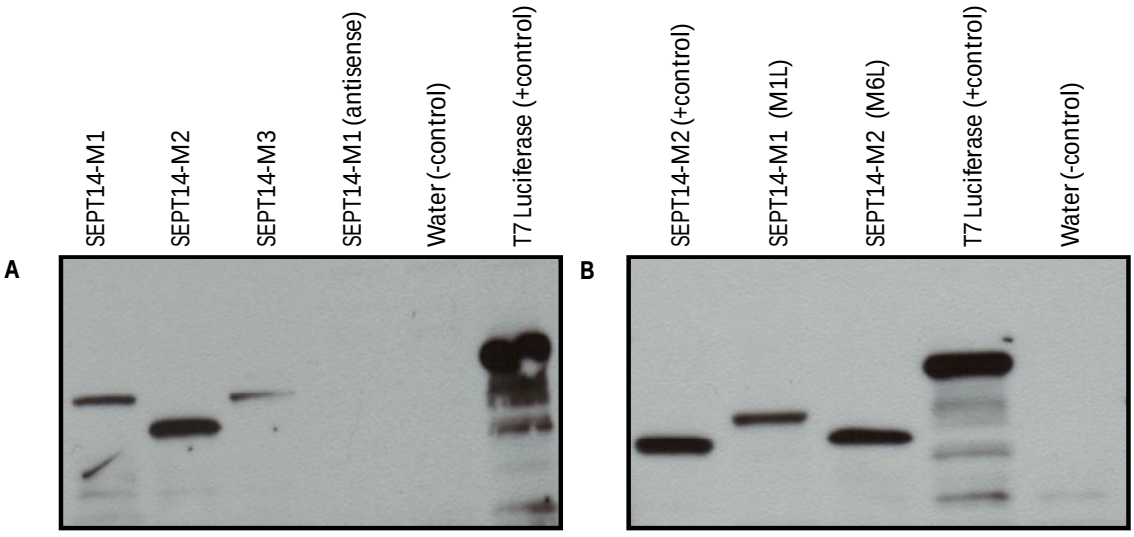

Fig 4.3: SEPT14 protein synthesis *in vitro* from three independent SEPT14 T7 plasmids with putative ORFs starting at methionines M1, M2 or M3 respectively

(A) SDS-Page showing protein synthesis of SEPT14-M1, -M2 or -M3 constructs made in (pCR-XL-TOPO) using the T7 TNT Transcription/Translation Assay. The SEPT14-M2 construct has a premature stop codon, producing a smaller band (~37 kDa) than –M1 and –M3 (~50 kDa). All three constructs were able to synthesize a peptide around 37-50 kDa. (B) M1 and M2 methionines were mutated to leucine by site-directed mutagenesis to try to discriminate which methionine is the translation start site. Construct SEPT14 –M1 (M1L) and –M2 (M6L) were able to synthesize a peptide with sizes 37-50 kDa similar to wild type constructs.

To determine the interaction specificity of SEPT14, haploid yeast containing human SEPT14 in the lexA bait vector were crossed with haploid yeast expressing each of the other mammalian septins (except SEPT13) in the prey vector, and interaction strength was determined by the degree of LacZ activation in the diploid yeast. Interestingly, SEPT14 interacted with all septins except those that are members of its family, namely SEPT6, 8, 10, and itself (Fig. 4.5).

BLAST analysis mapped SEPT14 to BAC RP11-419m24 (Genbank Accession No. AC092647) and chromosomal locus 7p11.2; PCR against a human chromosomal mapping panel confirmed localization to chromosome 7 (data not shown). The exon/intron structure of SEPT14 was modeled based on the complete sequence of 419m24 (Table 4.1). The gene spanned at least 65 kb, and all exon/intron boundaries followed the consensus GT/AG rule (146). Exon-specific primers were designed in flanking intronic sequences to confirm exon sizes.

Tissue expression pattern of human SEPT14

Multi-tissue Northern blot analysis showed only testis-specific expression of a single approximately 5.0 kb *SEPT14* transcript (Fig. 4.6A). Recognizing the sensitivity limitations of Northern blotting, expression of *SEPT14* and *SEPT9* alternative transcripts were further analyzed in multiple tissues by RT-PCR. Expression of *SEPT9_v1(MSF-A)*, originally used to pull out *SEPT14*, as well as *SEPT9_v3 (MSF)* and *SEPT9_v4** (*MSF-B),* also shown to interact by yeast two-hybrid, were detected in testis cDNA along with SEPT14 (Fig. 4.6B). SEPT14 expression profile was assayed by RT-PCR using cDNA from multiple fetal and adult tissues. SEPT14 was not expressed in fetal brain or fetal liver, two tissues generally known to have a broad expression profile, or in either of the normal or cancerous tissues of the breast, ovaries, prostate, bladder and kidney (Fig. 4.6B-C). In addition, testing for expression of SEPT14 in organs of the immune system, given the observations that several septins are implicated in leukemia as translocation

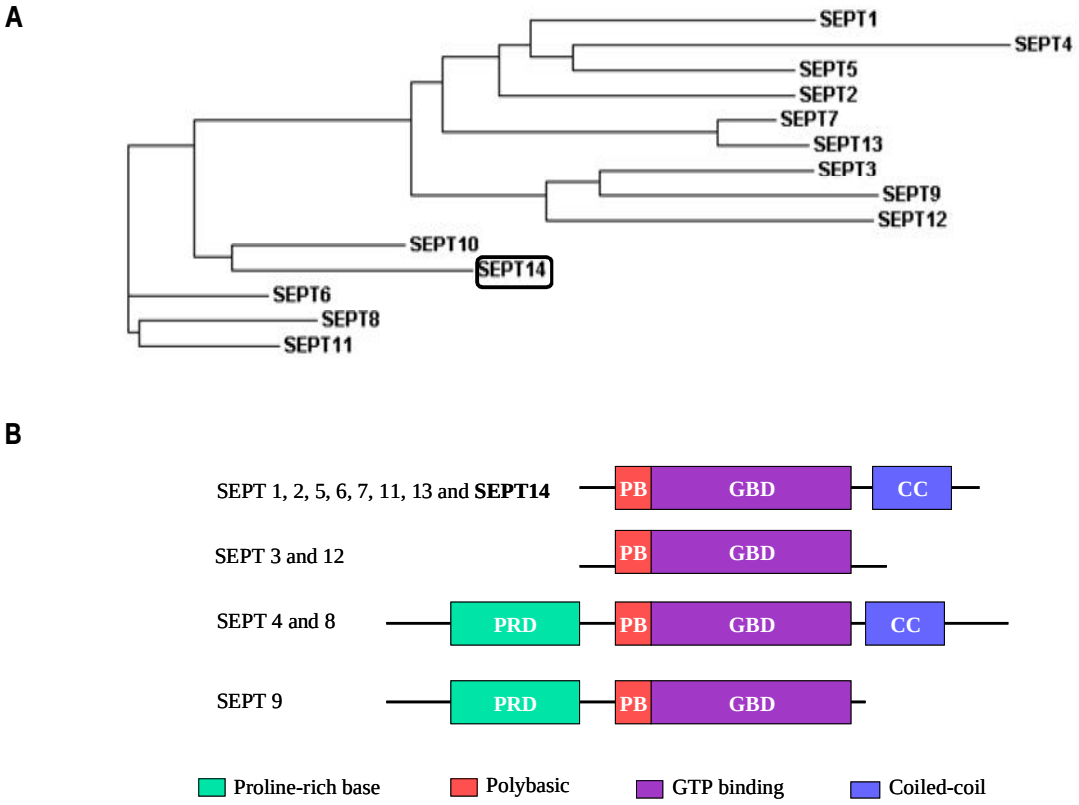

Fig 4.4: **Phylogenetic tree of the human septin family.**

(A) A dendrogram tree illustrates the phylogenetic relationship of SEPT14 with the other 13 human septin family members after ClustalW analysis (B) An Illustration showing the relationship of septin family members based on conserved domains.

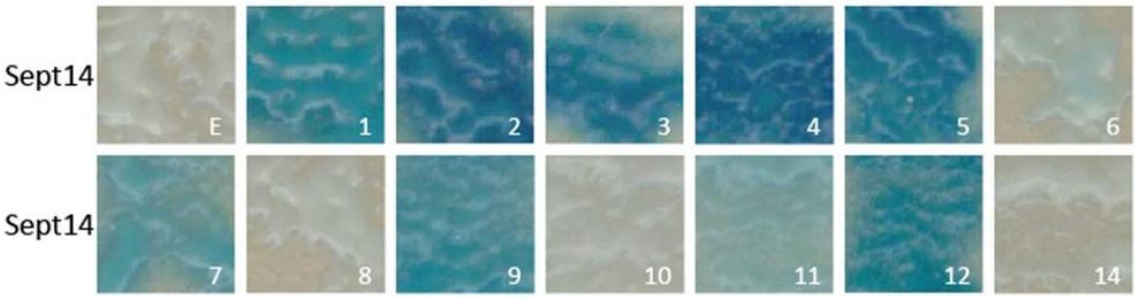

Fig 4.5: Yeast two-hybrid analysis indicates that SEPT14 interacts with other septin family members

Yeast mating intersections show SEPT14 interacts with 10 other septin family members. *S. cerevisiae* expressed human SEPT14 as bait and all other respective septins as prey. Intensity of blue color indicates strength of interaction as determined by the degree of LacZ activation. SEPT14 is capable of interacting with all septins except members of its own subgroup: SEPT6, 8, 10 and itself.

partners of MLL (65, 106), was negative (Fig 4.6D). Interestingly, even though SEPT14 was found to be expressed in normal testis cDNA by Northern blot and semi-quantitative RT-PCR, three testicular cancer cell lines were negative for SEPT14 expression by RT-PCR. (Fig. 4.6E).

To confirm SEPT14 and SEPT9 interact in a mammalian system, GFP-tagged SEPT14 and FLAG-tagged SEPT9_v4 were transiently transfected into CHO cells and after 24 hours the cells were fixed and processed for immunostaining. Only cells expressing both proteins at very low levels were imaged to eliminate artifacts of overexpression. In all cases, SEPT9 and SEPT14 were found to co-localize to stress fibers (Fig. 4.7). This is not surprising given that other septins, including SEPT9 variants, localize to these structures (24, 147).

To determine if the co-localized proteins interacted in the cells, lysates were prepared from transiently transfected CHO cells for immunoprecipitation. Monoclonal anti-FLAG or control mouse IgG antibodies were added to the lysates and immunoprecipitated on protein G-agarose beads. The immunoprecipitate was separated by SDS-PAGE and then blotted for the presence of GFP, fused to SEPT14. As shown in Figure 4.8, SEPT9 was capable of immunoprecipitating SEPT14, indicating that these proteins interact within mammalian cells. The presence of GFP-tagged SEPT14 in anti-FLAG immunoprecipitated lysates further confirmed the protein-protein interaction observed in the co-localization studies (Fig. 4.8A).

Since SEPT14 is not normally expressed in CHO cells (data not shown), we attempted to show that SEPT14 and SEPT9 interact in a more physiologically relevant context. As indicated above, SEPT14 expression is highest in the testes, and SEPT9 is expressed in testes as well (Kalikin *et al*. 2000; Surka *et al*, 2002), raising the possibility that these two proteins may interact in that tissue. Lysates were prepared from rat testes and SEPT9 was immunoprecipitated using antibodies specific for SEPT9. Immunoprecipitates were electrophoresed on SDS-PAGE gels and

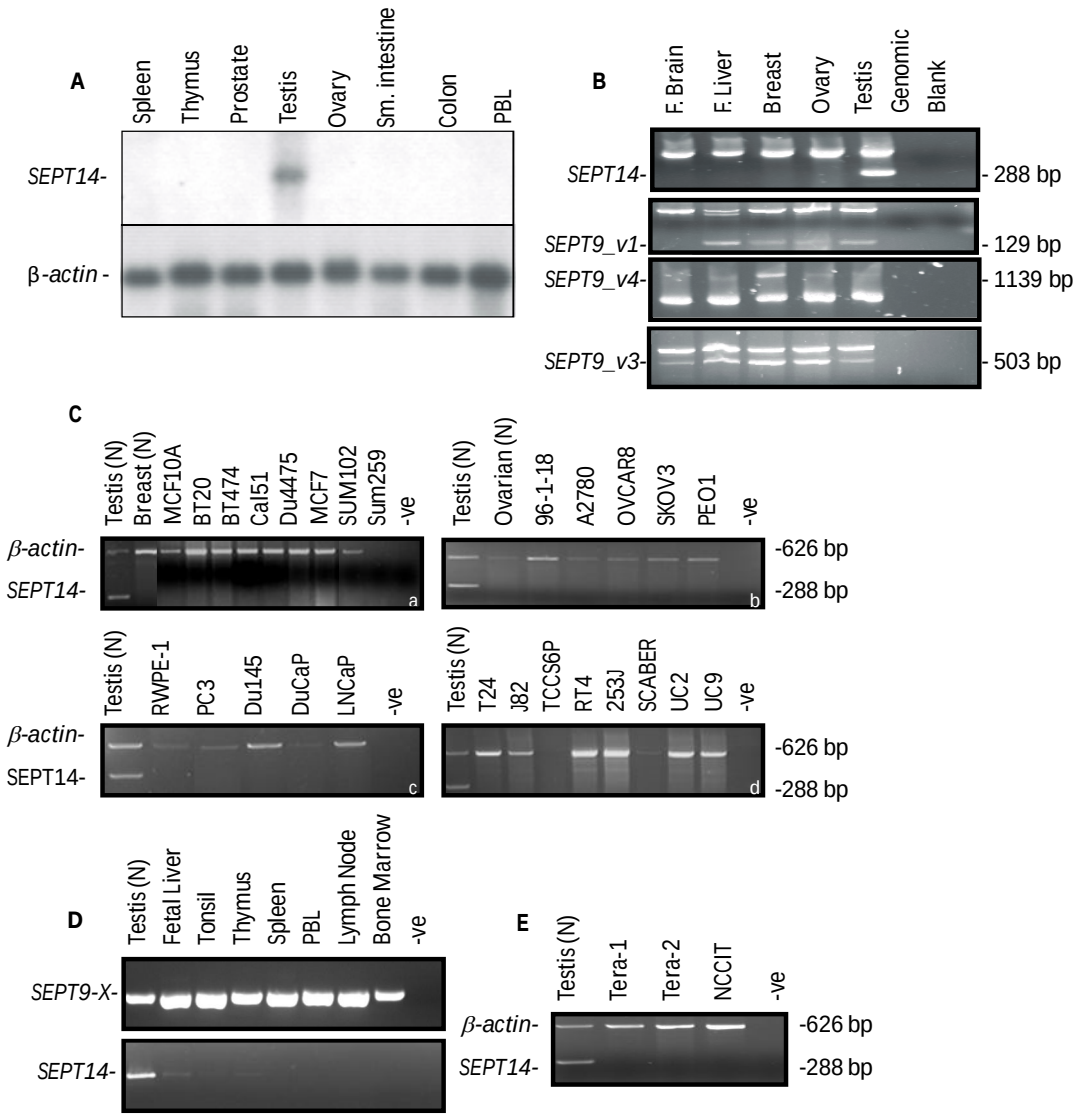

Fig 4.6: Characterization of SEPT14 expresssion by Northern blot and RT-PCR

(A-B) *SEPT14* expression by Northern blot (A) and semiquantitative duplex RT-PCR (sdRT-PCR) (B) is only detected in testis. Septin specific bands are indicated by product size; the other band is a 626bp *β-actin* product used as an internal control. (C) Relative expression of *SEPT14* (288 bp) in breast (a), ovarian (b), prostate (c) and bladder (d) cancer cell lines by sdRTPCR was performed. Testis cDNA was used as a positive control for expression. (D) Expression profile of SEPT9-X transcripts and *SEPT14* by standard RT-PCR using commercially available normalized immune tissue-derived cDNAs was performed. SEPT14 expression was barely detected or negative as compared to *SEPT9* expression. (E) *SEPT14* expression was absent in all the three testis teratoma cell lines.

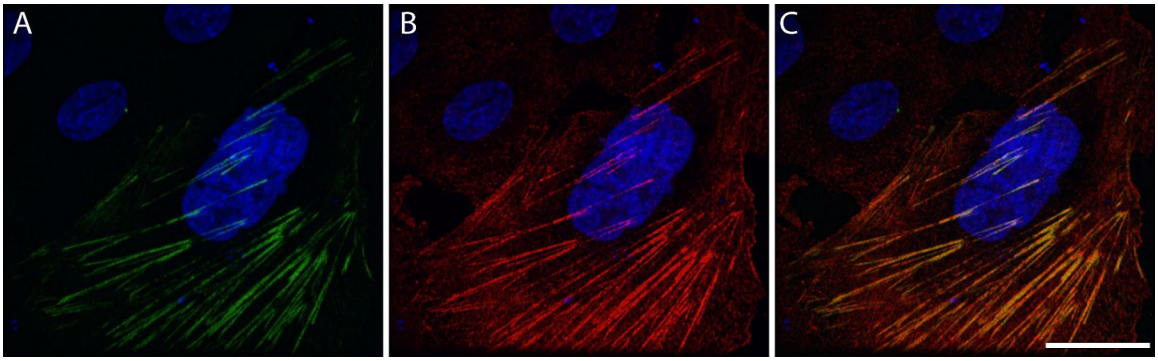

Fig 4.7: Over-expressed Flag-SEPT9 and GFP-SEPT14 colocalize to stress fibers in CHO cells.

CHO cells were transiently transfected with GFP-SEPT14 and Flag-SEPT9, fixed, and stained for GFP (green), Flag (red) and Dapi (blue). Cells expressing low levels of both proteins were analyzed for (A) GFP-SEPT14. (B) Flag-SEPT9 (C) Merge. Size bar = 2μm.

Coomassie staining revealed the presence of several bands in the SEPT9 immunoprecipitate that were absent from the control IgG lane (Fig. 4.8B). These bands were isolated, subjected to tryptic digestion and analyzed by MALDI-TOF mass spectrometry. The lower unique band (asterisk) contained several peptides specific for rat SEPT2, while the upper band (<) contained peptides for rat SEPT7, SEPT9 and SEPT14. The peptides identified for rat SEPT14 are shown highlighted on the sequence of rat SEPT14, which is shown in alignment with human SEPT14 (Fig. 4.8C).

Discussion

Septins have been characterized as proteins relevant in multiple cellular functions including cell division, membrane dynamics, cell signaling, cell cycle regulation, and apoptosis. Importantly they have been implicated in neurodevelopment and oncogenesis making them highly relevant to human disease. These biological functions of septins are intrinsically related in part to their ability to assemble into polymers, which serve as diffusion barriers in the cell membrane and form scaffolds for interacting proteins at specific intracellular locations(7, 138). Therefore, identifying new septin family members and novel interacting proteins is crucial to elucidating their cellular functions and their role in human diseases.

SEPT14 was identified by yeast-two hybrid as a novel septin family member and interacting protein of SEPT9 isoforms (SEPT9_v1-SEPT9_v4). The gene described here has previously been annotated in NCBI (Accession Number: NM_207366), but our findings describe additional 5' sequences that encode a highly conserved GTP-binding domain near the N-terminus in addition to the coiled-coil domain at the C-terminus, characteristic of the septin family. SEPT14 shares closest homology to SEPT10, a human dendritic septin on chromosome 8q11 (148), and shows limited homology with SEPT9 isoforms.

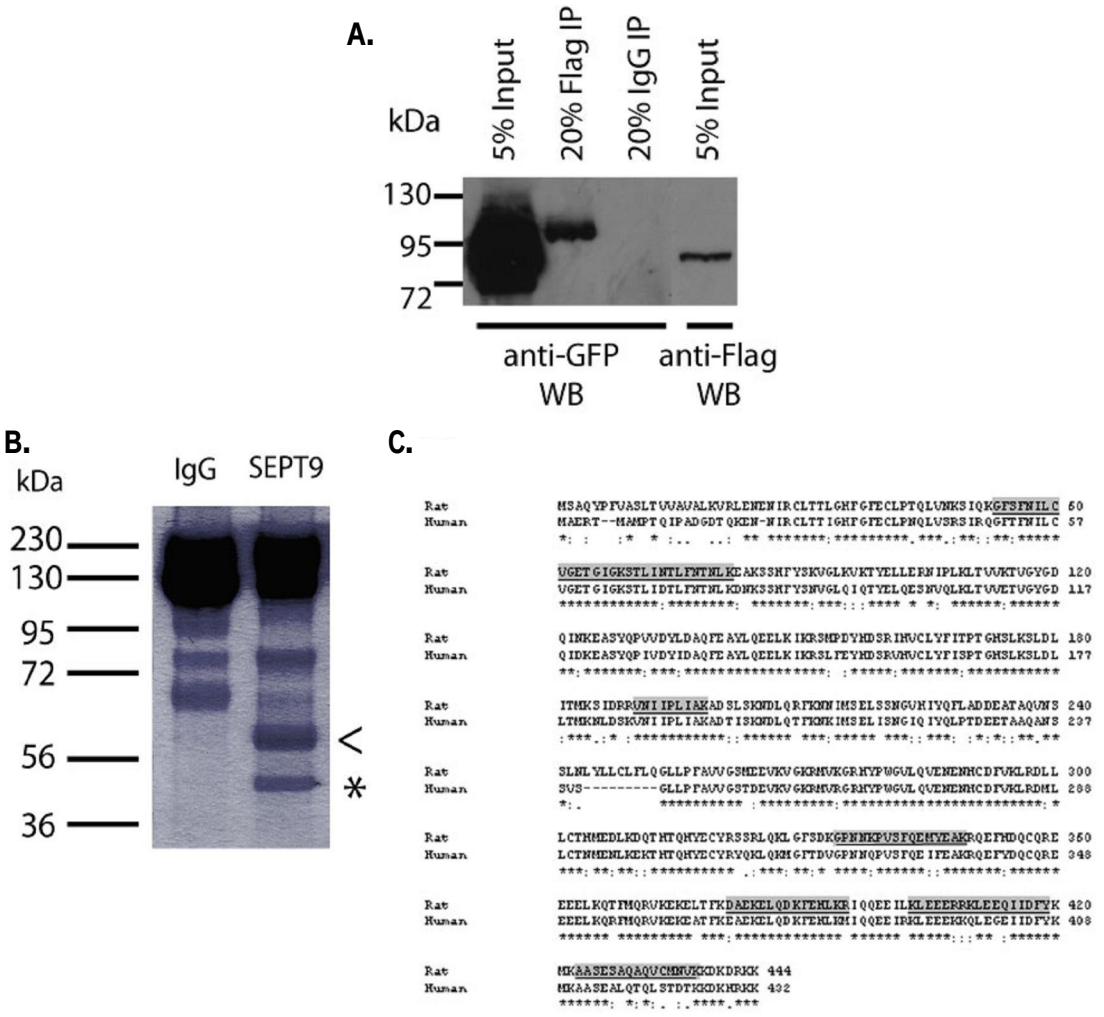

Fig 4.8: Coimmunoprecipitation of SEPT9 and SEPT14

(A) Co-immunoprecipitation of SEPT9 and SEPT14 following transfection. CHO cells were transiently transfected with GFP-SEPT14 and Flag-SEPT9, lysed, and subjected to immunoprecipitation with anti-Flag antibody. Twenty percent of the immunoprecipitated material was electrophoresed beside 5% of the initial cell lysate. Lane 2 shows that GFP-SEPT14 is able to co-immunoprecipitate with Flag-SEPT9, whereas this is not observed with non-specific rabbit IgG (lane 3). Lane 4 shows the expression of the Flag-SEPT9. (B) Co-immunoprecipitation of endogenous SEPT9 and SEPT14 from rat testis. Immunoprecipitation with anti-SEPT9 (second lane) from testis lysate revealed several bands on Coomassie stained SDS-PAGE gels not seen in control immunoprecipitate (<,*), C. Alignment of human and rat SEPT14 generated using ClustalW. Digestion and MALDI-TOF mass spectrometry of the region at approximately 50kDa (arrow) yielded several peptides unique to rat SEPT14 as well as peptides to SEPT7 and SEPT9, while a 42 kDa band contained peptides to SEPT2 (not shown). Peptides identified by MALDI-TOF are highlighted in light grey. An "*" means that the residues or nucleotides in that column are identical in all sequences in the alignment, a ":" indicates that conserved substitutions have been observed and a "." means that semi-conserved substitutions are identified.

Unlike *SEPT9,* which is ubiquitously expressed*, SEPT14* is specifically expressed in the normal testis, with a transcript size of approximately 5.0 kb. Thus, SEPT14 may not play a role in the pathobiology of breast and ovarian tumorigenesis for which SEPT9 has been implicated (74, 77, 78, 80, 94). However, interestingly, *SEPT14* was not expressed in testis teratoma cell lines by RT-PCR leading us to speculate that SEPT14 expression may be relevant in testis-specific cellular functions such as proper development and spermatogenesis and that SEPT14 expression may be associated with specific cell types within the testes.

In support of this, SEPT4 and other septins are expressed in post-meiotic male germ cells and associated with sperm terminal differentiation (149). Importantly, *Sept4* knockout mice lack a functional annulus structure and are sterile due to defective morphology and motility of the sperm flagellum. In addition, annulus ring disorganization has been noted in asthenospermia syndrome in humans. This has led to the suggestion that acortical organization based on circular assembly of the septin cytoskeleton is essential for the structural and mechanical integrity of mammalian spermatozoa (43). Finally, expression profiles of several other septins show differential expression in testis cancer tissues compared to normal controls (21, 83). To confirm this, further characterization of SEPT14 expression and functional analysis of its role in testis is fundamental.

Interestingly, SEPT14 can interact with nine other septins in addition to SEPT9, but does not strongly interact with SEPT8 or SEPT10, the septins within its branch on the phylogenetic tree. Moreover, SEPT14 co-localizes with SEPT9 in CHO cells and can co-immunoprecipitate with SEPT9 both following ectopic expression and from testes tissue. In testes, SEPT14 co-immunoprecipitated with SEPT2, 7, and 9. Septins form heterologous filaments, with each septin usually present in stoichiometric ratios, and studies by Versele and Thorner (2005), suggest a specific organization of the septins within yeast septin complexes (Versele and

Thorner, 2005). Based on available interaction data and limited sequence similarity, it was speculated that mammalian septins might assemble in similar ways with a member of each of the four major families taking each position in the complex. In support of this hypothesis, SEPT2, 7, 9 and 14 represent four different septin subgroups, suggesting that this is likely to be the septin subunit complex found in the testes.

In summary, we have identified and characterized SEPT14, a novel protein that interacts with several members of the human and rat septin family. Interestingly, the expression of this new septin appears to be unique to the testes, suggesting a role in the normal development and function of the testis and/or as a key player in the process of spermatogenesis. Further detailed studies of SEPT14 along with its interacting septin partners and related proteins may provide additional insight into its functional role in mammalian development.

Acknowledgments

This work was supported by the Department of Defense grant DAMD17-99-9295 to L.M. Kalikin, Canadian Institutes of Health Research to W.S. Trimble, NIH National Research Service Award #5-T32-GM07544 from the National Institute of General Medicine Sciences and NIH National Research Service Award F31 to Promote Diversity in Health Related Research #5-F31-CA123639-02 to E.A. Peterson, and NIH National Cancer Institute (NCI) grant RO1CA072877 to E.M. Petty. We want to thank A. Brenner and K. Kraft for technical assistance and L.M. Privette for critical reading of the manuscript.

Notes

This work was previously published in collaboration and co-authorship with the W.S. Trimble research group at the Department of Biochemistry, University of Toronto, Ontario, Canada as:

Peterson, E.A., Kalikin, L.M., Steels, J.D., Estey, M.P., Trimble, W.S., and Petty, E.M., "Characterization of a SEPT9 interacting protein, SEPT14, a novel testis-specific septin", *Mamm Genome.* 2007 Nov;18(11):796-807

CHAPTER V

CONCLUSIONS

Introduction

Breast cancer is a complex disease affecting millions of women and men worldwide. In the United States alone breast cancer accounts for 1 in 4 cancer diagnoses in women, excluding skin cancers. According to the American Cancer Society, a woman living in the US has a 12.3% (1 in 8) lifetime risk of developing breast cancer. Despite recent advances in the prevention, diagnosis and management of breast cancer, there are still gaps and limitations of current research into the pathophysiology, detection, treatment and prevention of this disease. Gaps in our knowledge still exist in the molecular genetics, mechanisms of initiation and progression, targeted therapies, prognostic markers and prevention of breast cancer (150). It is imperative that these gaps are closed to improve patients' treatment and outcomes.

Multiple genes of different penetrance are known to be involved in the predisposition to breast cancer (93). We still need to identify additional variants, effects, and interactions of low penetrance genes. This will help determine the relevance of somatic events to prognosis, response to therapy, development of new targeted therapies, and better genetic risk estimation. Understanding signaling pathways involved in breast architecture, apoptotic processes in mammary epithelial cells and the importance of the stroma, cell adhesion and extracellular matrix are crucial to identifying pre-invasive changes and their implications for patient-tailored therapies (150). Elucidating the complexity of additional molecular pathways

involved in the progression from DCIS to invasive disease including the processes of angiogenesis, metastasis, dormancy, reactivation of distant micrometastasis, and the influence of the tumor microenvironment, is also crucial (150). This understanding would facilitate the process of predicting therapeutic response with growth inhibitors, improve the selection of patients with ductal *in situ* carcinoma for adjuvant and endocrine therapies, and contribute to the development of new agents to target breast cancer progression (150). Finally, expanding our knowledge in biomarkers and compensatory signaling pathways responsible for drug resistance is an important challenge to conquer in order to improve prognostic indices, and the individualization, response and duration of therapy (150).

The efforts to identify additional high-penetrance susceptibility genes, such as BRCA1 and BRCA2, still continues, but as important is the identification and characterization of low penetrance genes and/or biomarkers with smaller effects that modulate cancer initiation, progression, chemotherapeutic response, aggressiveness and/or recurrence. Members of the human septin family are potential candidates for genes modulating cancer phenotypes. Several studies showed differential expression of these genes in various cancers including breast cancer. One of these, SEPT9, has become of great interest in the oncogenesis of many cancers. The effect of SEPT9 expression and its mechanism and relevance to breast cancer is still not well understood.

SEPT9_v1 expression is associated with breast cancer progression

SEPT9 was positionally cloned from a region of allelic imbalance in breast cancers (74). Subsequently, seven alternative transcripts were identified and their expression was assayed in a panel of breast cancer cell lines (BCCs) (20). SEPT9_v1 was preferentially over-expressed in 60% of BCCs as compared to immortalized human mammary epithelial cells (IHMECs). In addition, high SEPT9_v1 cytoplasmic staining was observed in tumor tissue as compared to

controls in 25 matched-control breast cancer samples (20). To tease out the role of SEPT9_v1 in mammary tumorigenesis, over-expression models in IHMECs were developed. Surprisingly, ectopic high SEPT9_v1 expression by retroviral transduction led to the development of several pro-oncogenic phenotypes, all characteristic of tumorigenesis (20). High SEPT9_v1 expression increased growth kinetics by accelerating cell proliferation and decreasing apoptotic response; both phenotypes are required for tumor growth (20). Another phenotype that confirmed the effect of SEPT9_v1 on cell proliferation was the increased mitotic index of SEPT9_v1- cells (20). SEPT9_v1 has been associated with increasing proliferative rates in prostate cancer and other septins, such as SEPT4/ARTS, have been implicated in mitochondria-mediated apoptosis (25, 26, 72).

Invasive disease and metastasis processes are still not completely understood. SEPT9_v1 expression seems to enhance motility and invasiveness in IHMECs, which is suggestive of a role in cancer progression to a more aggressive phenotype (20). Septins have been associated with cellular motility and polarity; both mechanisms are important for cancer cells to acquire the ability to invade and metastasize to other sites. Identifying novel interacting partners, especially with proteins involved in apical/basal polarity, cellular matrix, basement membrane, and pathways involved in invasion are crucial to understanding how deregulated SEPT9_v1 expression might lead to these phenotypes. In fact, SEPT9_v1-cells showed a change in morphology reminiscent of an epithelial to mesenchymal transition confirmed by an association of SEPT9_v1 with vimentin and the fact that cells showed increased vimentin staining, a phenotype tightly associated with cellular motility and invasion (20). Another possibility is the association of septins with cytoskeletal architecture and signaling, which is also important in cancer.

Another phenotype promoted by SEPT9_v1 was focus formation, indicating an effect on contact-contact growth inhibition, at least in Hs5787t, a breast cancer cell line with no endogenous SEPT9_v1 expression. This suggests that SEPT9_v1 acts in combination with other oncogenic mutations present in breast cancer cell lines to promote an oncogenic transformation. The future identification of possible genetic interactions of septins with breast cancer genes of major impact, for example HER2/neu, BRCA1 and/or BRCA2, will be relevant to identify the type of tumors in which SEPT9_v1 expression might affect the oncogenic process. For example, bioinformatics data annotated in GEO profiles at NCBI showed that SEPT9_v1 expression is up-regulated when BRCA1 is ablated by siRNA in MCF10A cell line studies. Hormone receptor-negative tumors are mainly associated with BRCA1 mutations (102, 105, 151, 152). Therefore, it was intriguing that high expression of SEPT9_v1 was found to be correlated with estrogen and progesterone receptor positive tumors. These potential correlations between SEPT9_v1 expression and either BRCA1 status and/or hormone receptor status showed the importantce to further study the role of SEPT9_v1 as a breast cancer biomarker for prognosis, clinical course of the disease and therapy. Looking at the expression of SEPT9_v1 protein on a BRCA1 and BRCA2 mutant tumor microarray will be extremely useful to confirm the possible association between BRCA status and SEPT9_v1 expression. In addition, the analysis showed that high SEPT9_v1 expression is correlated with grade 2 tumors and not with lymph node involvement. This may appear puzzling, given the fact that according to our cell culture model, SEPT9_v1 is associated with cancer progression and aggressiveness, but not necessarily with cancer initiation. One possibility is that SEPT9_v1 may drive or potentiate the development of invasive cancers but then might get lost during tumor progression to metastasis as a consequence of the increased in genomic instability or by a different mechanism that needs to

be determined. Still, further studies with more patient samples are imperative to confirm these correlations with SEPT9_v1 expression.

The observed oncogenic effects discussed seem to be specific for the SEPT9_v1 isoform; over-expression of SEPT9_v3 and SEPT9_v4 in IHMECs did not have as significant impact on oncogenic phenotypes. SEPT9_v3 expression had an opposite effect compared to SEPT9_v1 expression as proliferative rates of SEPT9_v3 transductants were significantly reduced. SEPT9_v1 differs from SEPT9_v3 only in the first 25 amino acids; this difference in protein structure might account for the different effects of these two isoforms in cells. These 25 amino acids might be important for distinct cellular localization and/or protein interactions relevant to specific roles of these two isoforms, as otherwise these two proteins are highly conserved in their central domains. For example, expression of SEPT9_v3, but not SEPT9_v1, inhibits the activation of Rho signaling pathway via its interaction with SA-RhoGEF in Hela and Cos7 cells (89, 90). This interaction could explain a different role for SEPT9_v3, especially because studies have showed that Rho proteins can activate the JNK signaling pathway (153). This connection between SEPT9_v3, Rho signaling, and JNK signaling could explain why SEPT9_v3 decreases cell proliferation in mammary epithelial cells. We can hypothesize that SEPT9_v3 inhibits Rho signaling pathway and this prevents the activation of the JNK signaling and its downstream genes involved in cell proliferation. This is in contrast to SEPT9_v1, which we have demonstrated up-regulates JNK signaling (154). SEPT9_v3 may also decrease cell proliferation by increasing the number of tetraploid cells, which may lower the mitotic index and increase apoptosis. Based on our data, one can argue that SEPT9_v1 also increases tetraploid cells, but the frequency is much lower than in SEPT9_v3 cells, so the downstream overall effect could be different. Future studies to elucidate the difference between SEPT9 isoforms and the potential

interactions between these will be important to understand the role of SEPT9 locus in tumorigenesis.

SEPT9_v1 expression regulates genomic stability

Genomic instability is common in many epithelial cancers. Septins have been implicated in cell division since the 1970's and are associated with filamentous proteins such as actin and myosin (1, 120, 121). Septins localize to the actomyosin ring and, when mutated, these proteins prevent cytokinesis (1, 24, 120, 121). To determine if the up-regulation of SEPT9 isoforms affects cell division and/or genomic stability, the ploidy status of SEPT9 transductants was assayed. When both SEPT9_v1 and SEPT9_v3 were independently over-expressed in IHMECs, an increase in the incidence of aneuploidy was shown. Interestingly, the degree of aneuploidy differs between the two isoforms; SEPT9_v1 cells showed a bimodal distribution with a generalized aneuploidy as well as an increase in the number of tetraploid cells. In contrast, the majority of SEPT9_v3-cells analyzed were tetraploid. It seems that SEPT9_v3 increases aneuploidy primarily by promoting cytokinesis failure which leads to tetraploidy. Conversely, SEPT9_v1 seems to promote both mitotic spindle defects and cytokinesis failure, two mechanisms by which SEPT9_v1 increases genomic instability (108, 109, 155). This seems to be mediated by SEPT9_v1's interaction with the cytoskeleton and microtubule proteins, including key components of the mitotic spindle such as α-tubulin and γ-tubulin. Interactions between SEPT9_v1 and other proteins important in the mitotic spindle checkpoint were not found, but other possible interactions and pathways need to be addressed, for example CENP-E, BUBR1, CDC20 and others. In addition, the effects of SEPT9_v1 expression on the activation of mitotic spindle checkpoint merits further study.

Increased genomic instability in cells could drive the development of other pro-oncogenic phenotypes due to the loss of tumor suppressors or gain of oncogenes. Analyzing the expression of SEPT9_v1 at different timepoints after transient transfection demonstrated that both aneuploidy and increased cell proliferation arise at the same time. More importantly, it suggested that these phenotypes are not an artifact of over-expression or multiple passages of cells in tissue culture. It also suggested that both phenotypes can arise independently and that there may be distinct mechanisms controlling both phenotypes. Further analyses will help differentiate the critical molecular pathways that give rise to SEPT9_v1-associated genomic instability and increased cell proliferation.

Novel SEPT9_v1 association with JNK signaling is relevant to cell proliferation

We found that up-regulation of SEPT9_v1 expression throughout the cell cycle, particularly in the G1 phase, significantly alters cell cycle progression via the JNK signaling pathway. We demonstrated a novel interaction between SEPT9_v1 and JNK1,2 kinases, which controls the activation of the transcription factor c-Jun by phosphorylation thereby resulting in the transcription of target cell cycle genes, such as *CCND1* (cyclin D1), with AP-1 sites in their promoters. Through its interaction with (and stabilization of) JNK1,2, SEPT9_v1 causes cells to progress at a faster rate through the cell cycle due to the increased expression of cyclin proteins, particularly cyclin D1 and cyclin B1, which are responsible for progression through the cell cycle. These findings shed new light on possible mechanisms by which SEPT9_v1 alters cellular proliferation and contributes to malignant progression in breast cancers.

Identification and characterization of SEPT14, a novel interacting partner

As cytoskeletal proteins, septins may interact with different proteins or form scaffolds to recruit proteins to specific compartments of the cell. Identifying interacting partners of septins has proven to be challenging due to the formation of complex heteroligomers with

themselves and other septin family members. The initial approach used in this study to try to identify novel interacting partners of SEPT9 isoforms was a highly stringent yeast-two hybrid assay using a human testis cDNA library as bait. A new septin, subsequently named SEPT14, was the only candidate captured by this method. One can speculate that the reason for this is the high stringency used in this method or possibly the disruption of structural conformation or protein complexes necessary for other protein interactions. SEPT14 was identified and characterized as a novel protein that interacts with several members of the human and rat septin family. Interestingly, the expression of this new septin appears to be unique to the testes, suggesting a role in the normal development and function of the testis and/or as a key player in the process of spermatogenesis. However, we can't exclude the possibility of very low levels of expression in other tissues and/or expression at different stages in development. We also analyzed the expression of SEPT14 in different cancer cell lines and did not find any expression. Further detailed studies of SEPT14, along with its interacting septin partners and related proteins may provide additional insight into its functional role in mammalian development and possibly testicular cancer.

SEPT9_v1 model of mammary tumorigenesis

This study showed that high expression of SEPT9_v1 in mammary epithelial cells impacts breast tumorigenesis through different mechanisms. The cellular processes affected, such as cell proliferation and genomic stability, are usually deregulated during cancer progression of different tumors. How the altered expression of SEPT9_v1 affects many of these processes is still puzzling. Septins form complex filaments with two molecules of each individual septin which tend to localize along cytoskeletal components such as microtubules and actin stress fibers (7). The importance of the formation of these complexes is being studied at present, but

we cannot discard the possibility that these proteins can also have distinct functions independent of the formation of these highly ordered filaments.

SEPT9_v1 interacts with several proteins such as tubulins and JNK. The dynamics of these associations might dictate the effect of SEPT9_v1 in normal and cancer cells. One hypothesis states that septins are cytoskeletal proteins acting as scaffolds mediating the localization of other proteins in specific sites of the cell and/or the interaction between specific proteins (18). Another possibility is that septins act as signaling GTPases modulating specific signaling pathways. SEPT9_v1 has proven to have a role as cytoskeletal protein important in cell division by interacting with tubulins. High expression impacts alpha-tubulin filaments and mitotic spindle function which might be indicative of a structural function of SEPT9_v1 in the cell cytoskeleton. High SEPT9_v1 expression might be inhibiting microtubule dynamics by either affecting their assembly or disassembly, which would prevent the proper function of the mitotic spindle during mitosis, causing chromosome mis-segregation. SEPT9_v1 also increases the frequency of cytokinesis failure. To understand this, future studies to determine SEPT9_v1 protein interactions with components of the cytokinesis machinery, cleavage furrow, and midbody are essential to see if altered expression of SEPT9_v1 affects their localization and/or expression. For example, it has been shown anillin, an organizer of the cytokinesis machinery, interacts with septins and that SEPT9_v1 is localized to the midbody and cleavage furrow during completion of telophase and cytokinesis. Additional studies to explore the functional consequences of this interaction are needed.

Changes in morphology, such as the epithelial to mesenchymal transition, increased cellular motility and invasiveness also support the hypothesis of SEPT9_v1 as a structural protein as cytoskeleton dynamics are crucial for the regulation of these phenotypes. This might not be the only way SEPT9_v1 functions in the cell. By identifying the interaction of SEPT9_v1 with the

JNK signaling pathway, in which it stabilized the JNK protein products and increased JNK kinase activity as well as transcriptional activation, we showed that SEPT9_v1 could actively regulate JNK. In fact, this interaction is dependent on the GTPase domain, which might be involved in the activation of this pathway. We cannot discard, however, the possibility that SEPT9_v1 might be sequestering JNK and preventing its degradation, which could lead to overall enhanced activity of the JNK pathway and its downstream targets that might be indicative of the scaffolding properties of SEPT9_v1.

One important observation is that our preliminary data suggests that SEPT9_v1 contains a bipartite nuclear localization signal located within the first 25 amino acids. SEPT9_v1 was also found to be localized to the nucleus, in addition to the cytoplasm in breast cancer cell lines and cells retrovirally expressing high levels of SEPT9_v1. The role of nuclear SEPT9_v1 remains to be determined, but one can hypothesize that it might be important in the transport of other proteins to the nucleus or it may exert its own specific cellular function. The first aspect to tease out is to determine if SEPT9_v1 normally shuttles between the cytoplasm and the nucleus and then examine how this affects the phenotypes described here. Another hypothesis is that when SEPT9_v1 is highly expressed in cells it might be sequestered in the nucleus preventing its function as a cytoskeletal component, or, at the same time, promoting the mis-localization of its interacting proteins. This might explain how the high expression of SEPT9_v1 can give rise to similar phenotypes as SEPT9 knockdown experiments described in other studies (20, 23, 24, 37). Nuclear localization of SEPT9_v1 could be similar to not having the protein available in the cytoplasm during essential cellular processes.

Our model for oncogenic SEPT9_v1 in mammary epithelial cells demonstrates that, by some unknown mechanism, SEPT9_v1 becomes amplified and over-expressed during cancer initiation or progression and that this altered expression causes critical changes in different

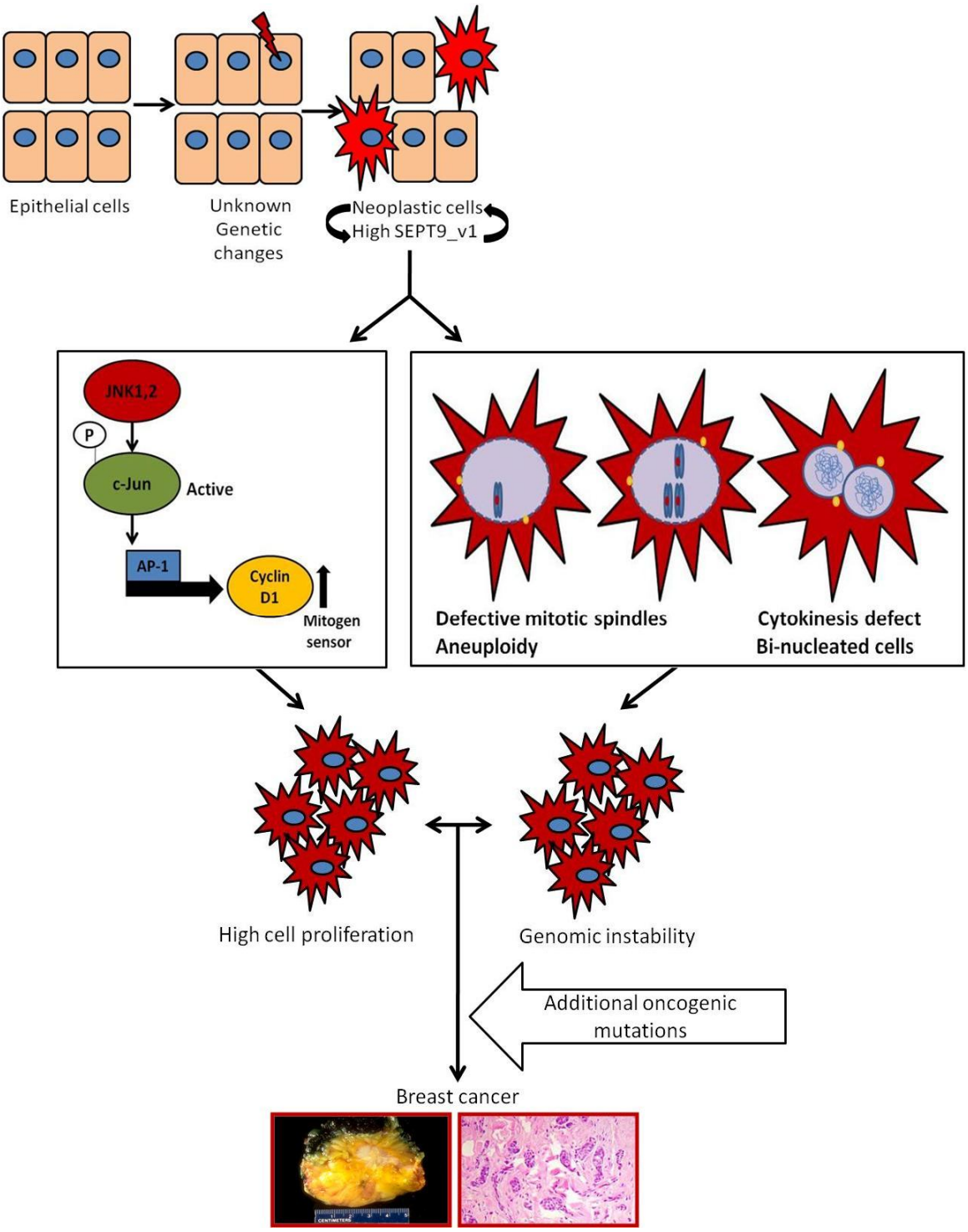

Fig 5.1: SEPT9_v1 working model of mammary tumorigenesis

essential cellular processes as dictated by SEPT9_v1 specific interactions. During mitosis, we have demonstrated that SEPT9_v1 affects mitotic spindle formation by impacting microtubule organization, assembly, or disassembly, which increases genomic instability, a hallmark characteristic of many cancers. We have also shown that SEPT9_v1 increases proliferation rates by modulating the JNK signaling pathway important in cell cycle progression. Together, these SEPT9_v1 associated cellular processes drive malignant progression in mammary epithelial cells (Fig 5.2).

Future Directions

This study answered many questions and provided several novel insights about the cellular roles of septins in general and, more specifically, about the multiple roles of SEPT9_v1 in mammary tumorigenesis. However, many other aspects of SEPT9 biology still need to be elucidated. The SEPT9 expression model used here was determined by highly expressing SEPT9 isoforms under the CMV promoter. The threshold where the expression level is not transforming was not determined given that all the lines produced for our studies had comparable protein expression to breast cancer cell lines with high endogenous SEPT9. To explore expression levels more comprehensively, development and analysis of an inducible system will be ideal to control SEPT9_v1 expression levels and to determine how expression is important to promote transformation. Another approach will be to select and expand monoclonal stable cell lines with different expression levels of SEPT9_v1 and examine them for the development of pro-oncogenic phenotypes. The data acquired from these experiments will complement the knockdown of SEPT9 by RNAi experiments described in Chapter 2 to get a more complete profile of SEPT9_v1 expression and its ability to transform cells. We described that high expression of SEPT9_v1 promotes pro-oncogenic phenotypes, but the breadth of molecular mechanisms responsible for these changes remains elusive. To study this, a cDNA microarray

analysis should be performed after transient transfection of SEPT9_v1 to help determine if there are changes in downstream messages that will give us a clue as to the specific molecular mechanism of SEPT9_v1 transformation. In addition, ongoing correlation studies using tissue microarrays may be helpful in identifying important gene associations.

Analysis of deletion constructs encompassing the different conserved domains are crucial to understanding further the role of each domain in the development of pro-oncogenic phenotypes. A deletion construct of the GTPase domain will be especially useful to study the aneuploidy and mitotic spindle defect phenotypes. The GTPase domain has proven essential for the interaction of SEPT9_v1 and microtubules (23, 24), therefore expression of a GTPase deletion construct should provide insights into the relevant functional dynamics of this interaction. For example, expression of the GTPase deletion construct might abrogate the mitotic spindle defects and chromosome mis-segregation by inhibiting SEPT9_v1's interaction with tubulins. In addition, co-expression of this construct with full length SEPT9_v1 will be important to see if the GTPase deletion acts as a dominant negative by inhibiting the interaction of full length SEPT9_v1 with tubulin or by decreasing or enhancing aneuploidy and mitotic spindle defects.

The difference between SEPT9_v1 and SEPT9_v3 effects on several cellular processes and in oncogenesis might be associated with their difference in protein sequence, specifically with the distinct 25 amino acids at the N-terminus of SEPT9_v1. A deletion construct of these 25 amino acids will be useful to determine its relevance to the acquisition of the different oncogenic phenotypes in cells with high SEPT9_v1 expression. Novel protein interactions mediated by these 25 amino acids will be of extreme importance to understand better the differences between these two isoforms, their relationships with different functional

mechanisms, and to understand why SEPT9_v1 acts as an oncogene while SEPT9_v3 does not seem to have similar properties.

Further discovery of novel protein interactions relevant to the distinct functional roles of SEPT9_v1 in mammary epithelial cells is crucial to further understand its role in oncogenesis. The potential interactions of SEPT9_v1 with other components of the mitotic spindle and the mitotic spindle checkpoint will be addressed by immunoprecipitation analyses. Some of the candidates that will be tested are CENP-E, BUBR1, CDC20, and Aurora A. In addition it will be useful to include proteins important to cytokinesis, given the role of SEPT9_v1 in this process. Due to the possible complexity of these interactions, multiple methods may be used, including GST pull downs, yeast-two hybrid analysis, and if necessary, analysis of interactions in live cells using fluorescent resonance energy transfer (FRET).

Finally, tumorigenicity studies in SCID mice are ongoing. Human mammary epithelial cells (MCF10A) expressing SEPT9_v1 constructs have been injected into mammary fat pads of female SCID mice to monitor tumor formation. Results from these experiments will be crucial to determine if high expression of SEPT9_v1 is sufficient to induce transformation of cells and, therefore, the development of tumorigenesis in an *in vivo* model. If over-expression of SEPT9_v1 is not sufficient to promote tumor development, a cancer cell line, Hs578t, with high ectopic SEPT9_v1 expression will be used for analysis. This approach will help determine if, instead of promoting the initiation of tumorigenesis, SEPT9_v1 is a modulator of cancer aggressiveness by promoting the development of tumors earlier than vector controls or by increasing the metastatic potential of the tumors. It will also help determine what other molecular factors are needed to work in concert with SEPT9_v1 expression to drive tumorigenesis.

Transgenic mouse models expressing SEPT9_v1 and a SEPT9_v1 knockout mouse will be essential to further analyze multiple aspects of the biological roles of SEPT9_v1. A SEPT9_v1 transgene, under the control of a specific mammary promoter (e.g. MMTV), will be essential to pinpoint the biological role of SEPT9_v1 in the initiation and/or progression of mammary tumorigenesis. This animal model will be also important to determine if SEPT9_v1 expression is important for proper mammary gland development. This aspect is important because cancer development and progression are intrinsically dependent on the tumor microenvironment as well as changes in tissue development and remodeling. In addition, crosses between SEPT9_v1 transgenic mice and other mouse model of oncogenes (e.g. Her2/neu, BRCA1) will be important to study potential associations of SEPT9_v1 with pathways and genes known to be important in breast cancer. The knockout mouse will shed additonal light on the various functional roles in which SEPT9_v1 is important. It is already known that a conventional knockout of SEPT9 is embryonic lethal at E9 with increased apoptosis (Füchtbauer, E-M., personal communication), so the use of a conditional or inducible system will be needed to analyze this.

Summary

This study has characterized the relevance of SEPT9_v1 as a modulator of mammary tumorigenesis. We showed that SEPT9_v1 is a multi-functional protein that impacts cell proliferation and genomic instability (20, 154). SEPT9_v1 is associated with these phenotypes by interacting with cytoskeletal proteins and its association with the JNK signaling pathway (Figure 5.1) (154). These data in combination with other published studies, highlight SEPT9_v1 as a potential prognostic tool and/or biomarker for breast cancer therapy options, given the preliminary correlation with hormone negative-receptor tumors and an interaction with microtubules. These data open new and important directions of exploration in the area of breast cancer research. The discovery and characterization of new proteins, such as SEPT9_v1,

that may be important in the oncogenesis process is crucial to advance this field. The pathogenesis of breast cancer is complex and the identification of new molecular pathways and interactions leading to better diagnosis, prognosis and treatment for patients is the goal of further characterizing genes such as *SEPT9*_v1.

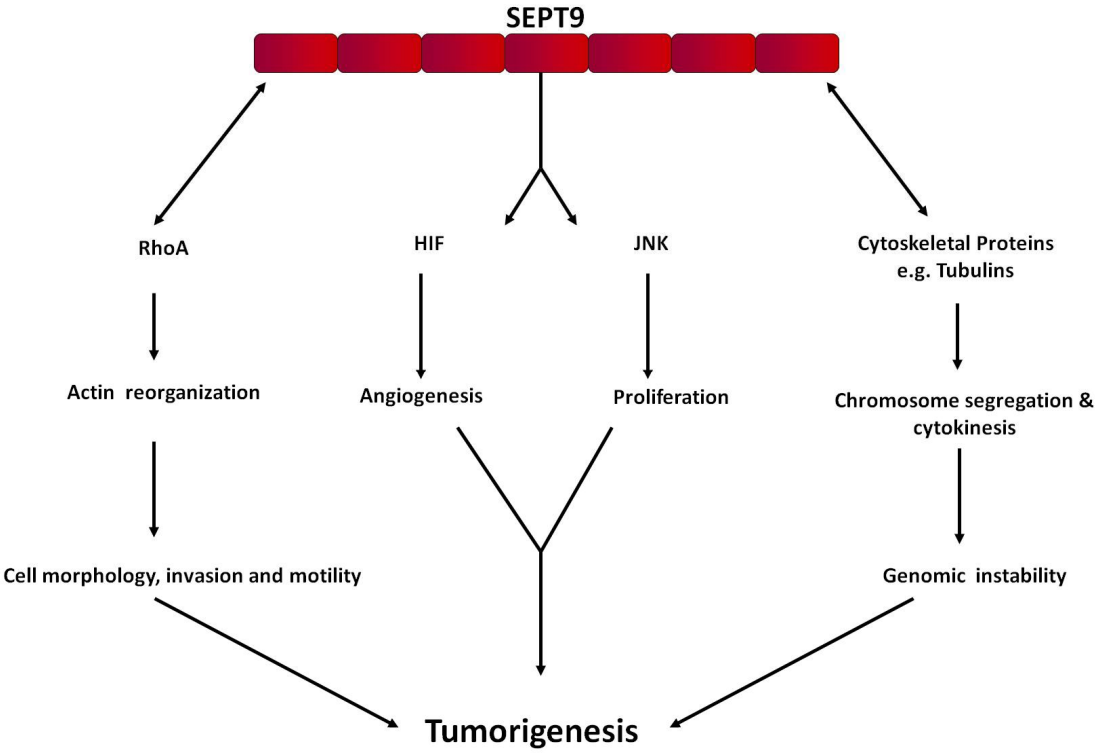

Fig 5.2: The impact of SEPT9 on different molecular pathways and cellular processes important in tumorigenesis

REFERENCES

1. Hartwell, L. H. Genetic control of the cell division cycle in yeast. IV. Genes controlling bud emergence and cytokinesis. Exp Cell Res, *69:* 265-276, 1971.

2. Cao, L., Ding, X., Yu, W., Yang, X., Shen, S., and Yu, L. Phylogenetic and evolutionary analysis of the septin protein family in metazoan. FEBS Lett, *581:* 5526-5532, 2007.

3. Feng, S., Chen, J. K., Yu, H., Simon, J. A., and Schreiber, S. L. Two binding orientations for peptides to the Src SH3 domain: development of a general model for SH3-ligand interactions. Science, *266:* 1241-1247, 1994.

4. Lim, W. A. and Richards, F. M. Critical residues in an SH3 domain from Sem-5 suggest a mechanism for proline-rich peptide recognition. Nat Struct Biol, *1:* 221-225, 1994.

5. Garcia, W., de Araujo, A. P., Neto Mde, O., Ballestero, M. R., Polikarpov, I., Tanaka, M., Tanaka, T., and Garratt, R. C. Dissection of a human septin: definition and characterization of distinct domains within human SEPT4. Biochemistry, *45:* 13918-13931, 2006.

6. Low, C. and Macara, I. G. Structural analysis of septin 2, 6, and 7 complexes. J Biol Chem, *281:* 30697-30706, 2006.

7. Sirajuddin, M., Farkasovsky, M., Hauer, F., Kuhlmann, D., Macara, I. G., Weyand, M., Stark, H., and Wittinghofer, A. Structural insight into filament formation by mammalian septins. Nature, *449:* 311-315, 2007.

8. Johnson, E. S. and Gupta, A. A. An E3-like factor that promotes SUMO conjugation to the yeast septins. Cell, *106:* 735-744, 2001.

9. She, Y. M., Huang, Y. W., Zhang, L., and Trimble, W. S. Septin 2 phosphorylation: theoretical and mass spectrometric evidence for the existence of a single phosphorylation site in vivo. Rapid Commun Mass Spectrom, *18:* 1123-1130, 2004.

10. Xue, J., Milburn, P. J., Hanna, B. T., Graham, M. E., Rostas, J. A., and Robinson, P. J. Phosphorylation of septin 3 on Ser-91 by cGMP-dependent protein kinase-I in nerve terminals. Biochem J, *381:* 753-760, 2004.

11. Xue, J., Wang, X., Malladi, C. S., Kinoshita, M., Milburn, P. J., Lengyel, I., Rostas, J. A., and Robinson, P. J. Phosphorylation of a new brain-specific septin, G-septin, by cGMP-dependent protein kinase. J Biol Chem, *275:* 10047-10056, 2000.

12. Qi, M., Yu, W., Liu, S., Jia, H., Tang, L., Shen, M., Yan, X., Saiyin, H., Lang, Q., Wan, B., Zhao, S., and Yu, L. Septin1, a new interaction partner for human serine/threonine kinase aurora-B. Biochem Biophys Res Commun, *336:* 994-1000, 2005.

13. Sanders, S. L. and Field, C. M. Cell division. Septins in common? Curr Biol, *4:* 907-910, 1994.

14. Kinoshita, M., Kumar, S., Mizoguchi, A., Ide, C., Kinoshita, A., Haraguchi, T., Hiraoka, Y., and Noda, M. Nedd5, a mammalian septin, is a novel cytoskeletal component interacting with actin-based structures. Genes Dev, *11:* 1535-1547, 1997.

15. Neufeld, T. P. and Rubin, G. M. The Drosophila peanut gene is required for cytokinesis and encodes a protein similar to yeast putative bud neck filament proteins. Cell, *77:* 371-379, 1994.

16. Nguyen, T. Q., Sawa, H., Okano, H., and White, J. G. The C. elegans septin genes, unc-59 and unc-61, are required for normal postembryonic cytokineses and morphogenesis but have no essential function in embryogenesis. J Cell Sci, *113 Pt 21:* 3825-3837, 2000.

17. Zhang, J., Kong, C., Xie, H., McPherson, P. S., Grinstein, S., and Trimble, W. S. Phosphatidylinositol polyphosphate binding to the mammalian septin H5 is modulated by GTP. Curr Biol, *9:* 1458-1467, 1999.

18. Field, C. M. and Kellogg, D. Septins: cytoskeletal polymers or signalling GTPases? Trends Cell Biol, *9:* 387-394, 1999.

19. Kartmann, B. and Roth, D. Novel roles for mammalian septins: from vesicle trafficking to oncogenesis. J Cell Sci, *114:* 839-844, 2001.

20. Gonzalez, M. E., Peterson, E. A., Privette, L. M., Loffreda-Wren, J. L., Kalikin, L. M., and Petty, E. M. High SEPT9_v1 expression in human breast cancer cells is associated with oncogenic phenotypes. Cancer Res, *67:* 8554-8564, 2007.

21. Hall, P. A., Jung, K., Hillan, K. J., and Russell, S. E. Expression profiling the human septin gene family. J Pathol, *206:* 269-278, 2005.

22. Kremer, B. E., Haystead, T., and Macara, I. G. Mammalian septins regulate microtubule stability through interaction with the microtubule-binding protein MAP4. Mol Biol Cell, *16:* 4648-4659, 2005.

23. Nagata, K., Kawajiri, A., Matsui, S., Takagishi, M., Shiromizu, T., Saitoh, N., Izawa, I., Kiyono, T., Itoh, T. J., Hotani, H., and Inagaki, M. Filament formation of MSF-A, a mammalian septin, in human mammary epithelial cells depends on interactions with microtubules. J Biol Chem, *278:* 18538-18543, 2003.

24. Surka, M. C., Tsang, C. W., and Trimble, W. S. The mammalian septin MSF localizes with microtubules and is required for completion of cytokinesis. Mol Biol Cell, *13:* 3532-3545, 2002.

25. Gottfried, Y., Rotem, A., Lotan, R., Steller, H., and Larisch, S. The mitochondrial ARTS protein promotes apoptosis through targeting XIAP. Embo J, *23:* 1627-1635, 2004.

26. Larisch, S. The ARTS connection: role of ARTS in apoptosis and cancer. Cell Cycle, *3:* 1021-1023, 2004.

27. Larisch, S., Yi, Y., Lotan, R., Kerner, H., Eimerl, S., Tony Parks, W., Gottfried, Y., Birkey Reffey, S., de Caestecker, M. P., Danielpour, D., Book-Melamed, N., Timberg, R., Duckett, C. S., Lechleider, R. J., Steller, H., Orly, J., Kim, S. J., and Roberts, A. B. A novel

mitochondrial septin-like protein, ARTS, mediates apoptosis dependent on its P-loop motif. Nat Cell Biol, *2:* 915-921, 2000.

28. Beites, C. L., Campbell, K. A., and Trimble, W. S. The septin Sept5/CDCrel-1 competes with alpha-SNAP for binding to the SNARE complex. Biochem J, *385:* 347-353, 2005.

29. Beites, C. L., Xie, H., Bowser, R., and Trimble, W. S. The septin CDCrel-1 binds syntaxin and inhibits exocytosis. Nat Neurosci, *2:* 434-439, 1999.

30. Hsu, S. C., Hazuka, C. D., Roth, R., Foletti, D. L., Heuser, J., and Scheller, R. H. Subunit composition, protein interactions, and structures of the mammalian brain sec6/8 complex and septin filaments. Neuron, *20:* 1111-1122, 1998.

31. Huang, Y. W., Yan, M., Collins, R. F., Diciccio, J. E., Grinstein, S., and Trimble, W. S. Mammalian septins are required for phagosome formation. Mol Biol Cell, *19:* 1717-1726, 2008.

32. Blaser, S., Horn, J., Wurmell, P., Bauer, H., Strumpell, S., Nurden, P., Pagenstecher, A., Busse, A., Wunderle, D., Hainmann, I., and Zieger, B. The novel human platelet septin SEPT8 is an interaction partner of SEPT4. Thromb Haemost, *91:* 959-966, 2004.

33. Blaser, S., Roseler, S., Rempp, H., Bartsch, I., Bauer, H., Lieber, M., Lessmann, E., Weingarten, L., Busse, A., Huber, M., and Zieger, B. Human endothelial cell septins: SEPT11 is an interaction partner of SEPT5. J Pathol, *210:* 103-110, 2006.

34. Dent, J., Kato, K., Peng, X. R., Martinez, C., Cattaneo, M., Poujol, C., Nurden, P., Nurden, A., Trimble, W. S., and Ware, J. A prototypic platelet septin and its participation in secretion. Proc Natl Acad Sci U S A, *99:* 3064-3069, 2002.

35. Martinez, C., Corral, J., Dent, J. A., Sesma, L., Vicente, V., and Ware, J. Platelet septin complexes form rings and associate with the microtubular network. J Thromb Haemost, *4:* 1388-1395, 2006.

36. Ahuja, P., Perriard, E., Trimble, W., Perriard, J. C., and Ehler, E. Probing the role of septins in cardiomyocytes. Exp Cell Res, *312:* 1598-1609, 2006.

37. Spiliotis, E. T., Kinoshita, M., and Nelson, W. J. A mitotic septin scaffold required for Mammalian chromosome congression and segregation. Science, *307:* 1781-1785, 2005.

38. Spiliotis, E. T., Hunt, S. J., Hu, Q., Kinoshita, M., and Nelson, W. J. Epithelial polarity requires septin coupling of vesicle transport to polyglutamylated microtubules. J Cell Biol, *180:* 295-303, 2008.

39. Kremer, B. E., Adang, L. A., and Macara, I. G. Septins regulate actin organization and cell-cycle arrest through nuclear accumulation of NCK mediated by SOCS7. Cell, *130:* 837-850, 2007.

40. Lin, Y. H., Lin, Y. M., Wang, Y. Y., Yu, I. S., Lin, Y. W., Wang, Y. H., Wu, C. M., Pan, H. A., Chao, S. C., Yen, P. H., Lin, S. W., and Kuo, P. L. The expression level of septin12 is critical for spermiogenesis. Am J Pathol, *174:* 1857-1868, 2009.

41. Steels, J. D., Estey, M. P., Froese, C. D., Reynaud, D., Pace-Asciak, C., and Trimble, W. S. Sept12 is a component of the mammalian sperm tail annulus. Cell Motil Cytoskeleton, *64:* 794-807, 2007.

42. Sugino, Y., Ichioka, K., Soda, T., Ihara, M., Kinoshita, M., Ogawa, O., and Nishiyama, H. Septins as diagnostic markers for a subset of human asthenozoospermia. J Urol, *180:* 2706-2709, 2008.

43. Ihara, M., Kinoshita, A., Yamada, S., Tanaka, H., Tanigaki, A., Kitano, A., Goto, M., Okubo, K., Nishiyama, H., Ogawa, O., Takahashi, C., Itohara, S., Nishimune, Y., Noda, M., and Kinoshita, M. Cortical organization by the septin cytoskeleton is essential for structural and mechanical integrity of mammalian spermatozoa. Dev Cell, *8:* 343-352, 2005.

44. Mostowy, S. and Cossart, P. Cytoskeleton rearrangements during Listeria infection: Clathrin and septins as new players in the game. Cell Motil Cytoskeleton, 2009.

45. Mostowy, S., Danckaert, A., Tham, T. N., Machu, C., Guadagnini, S., Pizarro-Cerda, J., and Cossart, P. Septin 11 restricts InlB-mediated invasion by Listeria. J Biol Chem, *284:* 11613-11621, 2009.

46. Mostowy, S., Nam Tham, T., Danckaert, A., Guadagnini, S., Boisson-Dupuis, S., Pizarro-Cerda, J., and Cossart, P. Septins regulate bacterial entry into host cells. PLoS ONE, *4:* e4196, 2009.

47. Zhu, M., Wang, F., Yan, F., Yao, P. Y., Du, J., Gao, X., Wang, X., Wu, Q., Ward, T., Li, J., Kioko, S., Hu, R., Xie, W., Ding, X., and Yao, X. Septin 7 interacts with centromere-associated protein E and is required for its kinetochore localization. J Biol Chem, *283:* 18916-18925, 2008.

48. Kinoshita, A., Kinoshita, M., Akiyama, H., Tomimoto, H., Akiguchi, I., Kumar, S., Noda, M., and Kimura, J. Identification of septins in neurofibrillary tangles in Alzheimer's disease. Am J Pathol, *153:* 1551-1560, 1998.

49. Choi, P., Snyder, H., Petrucelli, L., Theisler, C., Chong, M., Zhang, Y., Lim, K., Chung, K. K., Kehoe, K., D'Adamio, L., Lee, J. M., Cochran, E., Bowser, R., Dawson, T. M., and Wolozin, B. SEPT5_v2 is a parkin-binding protein. Brain Res Mol Brain Res, *117:* 179-189, 2003.

50. Zhang, Y., Gao, J., Chung, K. K., Huang, H., Dawson, V. L., and Dawson, T. M. Parkin functions as an E2-dependent ubiquitin- protein ligase and promotes the degradation of the synaptic vesicle-associated protein, CDCrel-1. Proc Natl Acad Sci U S A, *97:* 13354-13359, 2000.

51. Ihara, M., Tomimoto, H., Kitayama, H., Morioka, Y., Akiguchi, I., Shibasaki, H., Noda, M., and Kinoshita, M. Association of the cytoskeletal GTP-binding protein Sept4/H5 with cytoplasmic inclusions found in Parkinson's disease and other synucleinopathies. J Biol Chem, *278:* 24095-24102, 2003.

52. Fujishima, K., Kiyonari, H., Kurisu, J., Hirano, T., and Kengaku, M. Targeted disruption of Sept3, a heteromeric assembly partner of Sept5 and Sept7 in axons, has no effect on developing CNS neurons. J Neurochem, *102:* 77-92, 2007.

53. Xue, J., Tsang, C. W., Gai, W. P., Malladi, C. S., Trimble, W. S., Rostas, J. A., and Robinson, P. J. Septin 3 (G-septin) is a developmentally regulated phosphoprotein enriched in presynaptic nerve terminals. J Neurochem, *91:* 579-590, 2004.

54. Ito, H., Atsuzawa, K., Morishita, R., Usuda, N., Sudo, K., Iwamoto, I., Mizutani, K., Katoh-Semba, R., Nozawa, Y., Asano, T., and Nagata, K. Sept8 controls the binding of vesicle-associated membrane protein 2 to synaptophysin. J Neurochem, *108:* 867-880, 2009.

55. Kinoshita, N., Kimura, K., Matsumoto, N., Watanabe, M., Fukaya, M., and Ide, C. Mammalian septin Sept2 modulates the activity of GLAST, a glutamate transporter in astrocytes. Genes Cells, *9:* 1-14, 2004.

56. Buser, A. M., Erne, B., Werner, H. B., Nave, K. A., and Schaeren-Wiemers, N. The septin cytoskeleton in myelinating glia. Mol Cell Neurosci, *40:* 156-166, 2009.

57. Hannibal, M. C., Ruzzo, E. K., Miller, L. R., Betz, B., Buchan, J. G., Knutzen, D. M., Barnett, K., Landsverk, M. L., Brice, A., LeGuern, E., Bedford, H. M., Worrall, B. B., Lovitt, S., Appel, S. H., Andermann, E., Bird, T. D., and Chance, P. F. SEPT9 gene sequencing analysis reveals recurrent mutations in hereditary neuralgic amyotrophy. Neurology, *72:* 1755-1759, 2009.

58. Kuhlenbaumer, G., Hannibal, M. C., Nelis, E., Schirmacher, A., Verpoorten, N., Meuleman, J., Watts, G. D., De Vriendt, E., Young, P., Stogbauer, F., Halfter, H., Irobi, J., Goossens, D., Del-Favero, J., Betz, B. G., Hor, H., Kurlemann, G., Bird, T. D., Airaksinen, E., Mononen, T., Serradell, A. P., Prats, J. M., Van Broeckhoven, C., De Jonghe, P., Timmerman, V., Ringelstein, E. B., and Chance, P. F. Mutations in SEPT9 cause hereditary neuralgic amyotrophy. Nat Genet, *37:* 1044-1046, 2005.

59. Landsverk, M. L., Ruzzo, E. K., Mefford, H. C., Buysse, K., Buchan, J. G., Eichler, E. E., Petty, E. M., Peterson, E. A., Knutzen, D. M., Barnett, K., Farlow, M. R., Caress, J., Parry, G. J., Quan, D., Gardner, K. L., Hong, M., Simmons, Z., Bird, T. D., Chance, P. F., and Hannibal, M. C. Duplication within the SEPT9 gene associated with a founder effect in North American families with hereditary neuralgic amyotrophy. Hum Mol Genet, *18:* 1200-1208, 2009.

60. McDade, S. S., Hall, P. A., and Russell, S. E. Translational control of SEPT9 isoforms is perturbed in disease. Hum Mol Genet, *16:* 742-752, 2007.

61. Megonigal, M. D., Rappaport, E. F., Jones, D. H., Williams, T. M., Lovett, B. D., Kelly, K. M., Lerou, P. H., Moulton, T., Budarf, M. L., and Felix, C. A. t(11;22)(q23;q11.2) In acute myeloid leukemia of infant twins fuses MLL with hCDCrel, a cell division cycle gene in the genomic region of deletion in DiGeorge and velocardiofacial syndromes. Proc Natl Acad Sci U S A, *95:* 6413-6418, 1998.

62. Borkhardt, A., Teigler-Schlegel, A., Fuchs, U., Keller, C., Konig, M., Harbott, J., and Haas, O. A. An ins(X;11)(q24;q23) fuses the MLL and the Septin 6/KIAA0128 gene in an infant with AML-M2. Genes Chromosomes Cancer, *32:* 82-88, 2001.

63. Cerveira, N., Correia, C., Bizarro, S., Pinto, C., Lisboa, S., Mariz, J. M., Marques, M., and Teixeira, M. R. SEPT2 is a new fusion partner of MLL in acute myeloid leukemia with t(2;11)(q37;q23). Oncogene, 2006.

64. Kojima, K., Sakai, I., Hasegawa, A., Niiya, H., Azuma, T., Matsuo, Y., Fujii, N., Tanimoto, M., and Fujita, S. FLJ10849, a septin family gene, fuses MLL in a novel leukemia cell line CNLBC1 derived from chronic neutrophilic leukemia in transformation with t(4;11)(q21;q23). Leukemia, *18:* 998-1005, 2004.

65. Osaka, M., Rowley, J. D., and Zeleznik-Le, N. J. MSF (MLL septin-like fusion), a fusion partner gene of MLL, in a therapy-related acute myeloid leukemia with a t(11;17)(q23;q25). Proc Natl Acad Sci U S A, *96:* 6428-6433, 1999.

66. Meyer, C., Schneider, B., Jakob, S., Strehl, S., Attarbaschi, A., Schnittger, S., Schoch, C., Jansen, M. W., van Dongen, J. J., den Boer, M. L., Pieters, R., Ennas, M. G., Angelucci, E., Koehl, U., Greil, J., Griesinger, F., Zur Stadt, U., Eckert, C., Szczepanski, T., Niggli, F. K., Schafer, B. W., Kempski, H., Brady, H. J., Zuna, J., Trka, J., Nigro, L. L., Biondi, A., Delabesse, E., Macintyre, E., Stanulla, M., Schrappe, M., Haas, O. A., Burmeister, T., Dingermann, T., Klingebiel, T., and Marschalek, R. The MLL recombinome of acute leukemias. Leukemia, *20:* 777-784, 2006.

67. Ernst, P., Wang, J., and Korsmeyer, S. J. The role of MLL in hematopoiesis and leukemia. Curr Opin Hematol, *9:* 282-287, 2002.

68. Capurso, G., Crnogorac-Jurcevic, T., Milione, M., Panzuto, F., Campanini, N., Dowen, S. E., Di Florio, A., Sette, C., Bordi, C., Lemoine, N. R., and Delle Fave, G. Peanut-like 1 (septin 5) gene expression in normal and neoplastic human endocrine pancreas. Neuroendocrinology, *81:* 311-321, 2005.

69. Kim, D. S., Hubbard, S. L., Peraud, A., Salhia, B., Sakai, K., and Rutka, J. T. Analysis of mammalian septin expression in human malignant brain tumors. Neoplasia, *6:* 168-178, 2004.

70. Tanaka, M., Kijima, H., Itoh, J., Matsuda, T., and Tanaka, T. Impaired expression of a human septin family gene Bradeion inhibits the growth and tumorigenesis of colorectal cancer in vitro and in vivo. Cancer Gene Ther, *9:* 483-488, 2002.

71. Yu, W., Ding, X., Chen, F., Liu, M., Shen, S., Gu, X., and Yu, L. The phosphorylation of SEPT2 on Ser218 by casein kinase 2 is important to hepatoma carcinoma cell proliferation. Mol Cell Biochem, *325:* 61-67, 2009.

72. Amir, S., Wang, R., Matzkin, H., Simons, J. W., and Mabjeesh, N. J. MSF-A interacts with hypoxia-inducible factor-1alpha and augments hypoxia-inducible factor transcriptional activation to affect tumorigenicity and angiogenesis. Cancer Res, *66:* 856-866, 2006.

73. Burrows, J. F., Chanduloy, S., McIlhatton, M. A., Nagar, H., Yeates, K., Donaghy, P., Price, J., Godwin, A. K., Johnston, P. G., and Russell, S. E. Altered expression of the septin gene, SEPT9, in ovarian neoplasia. J Pathol, *201:* 581-588, 2003.

74. Kalikin, L. M., Sims, H. L., and Petty, E. M. Genomic and expression analyses of alternatively spliced transcripts of the MLL septin-like fusion gene (MSF) that map to a 17q25 region of loss in breast and ovarian tumors. Genomics, *63:* 165-172, 2000.

75. Montagna, C., Lyu, M. S., Hunter, K., Lukes, L., Lowther, W., Reppert, T., Hissong, B., Weaver, Z., and Ried, T. The Septin 9 (MSF) gene is amplified and overexpressed in mouse mammary gland adenocarcinomas and human breast cancer cell lines. Cancer Res, *63:* 2179-2187, 2003.

76. Scott, M., Hyland, P. L., McGregor, G., Hillan, K. J., Russell, S. E., and Hall, P. A. Multimodality expression profiling shows SEPT9 to be overexpressed in a wide range of human tumours. Oncogene, *24:* 4688-4700, 2005.

77. Scott, M., McCluggage, W. G., Hillan, K. J., Hall, P. A., and Russell, S. E. Altered patterns of transcription of the septin gene, SEPT9, in ovarian tumorigenesis. Int J Cancer, *118:* 1325-1329, 2006.

78. Kalikin, L. M., Frank, T. S., Svoboda-Newman, S. M., Wetzel, J. C., Cooney, K. A., and Petty, E. M. A region of interstitial 17q25 allelic loss in ovarian tumors coincides with a defined region of loss in breast tumors. Oncogene, *14:* 1991-1994, 1997.

79. Kalikin, L. M., Qu, X., Frank, T. S., Caduff, R. F., Svoboda, S. M., Law, D. J., and Petty, E. M. Detailed deletion analysis of sporadic breast tumors defines an interstitial region of allelic loss on 17q25. Genes Chromosomes Cancer, *17:* 64-68, 1996.

80. Russell, S. E., McIlhatton, M. A., Burrows, J. F., Donaghy, P. G., Chanduloy, S., Petty, E. M., Kalikin, L. M., Church, S. W., McIlroy, S., Harkin, D. P., Keilty, G. W., Cranston, A. N., Weissenbach, J., Hickey, I., and Johnston, P. G. Isolation and mapping of a human septin gene to a region on chromosome 17q, commonly deleted in sporadic epithelial ovarian tumors. Cancer Res, *60:* 4729-4734, 2000.

81. Macara, I. G., Baldarelli, R., Field, C. M., Glotzer, M., Hayashi, Y., Hsu, S. C., Kennedy, M. B., Kinoshita, M., Longtine, M., Low, C., Maltais, L. J., McKenzie, L., Mitchison, T. J., Nishikawa, T., Noda, M., Petty, E. M., Peifer, M., Pringle, J. R., Robinson, P. J., Roth, D., Russell, S. E., Stuhlmann, H., Tanaka, M., Tanaka, T., Trimble, W. S., Ware, J., Zeleznik-Le, N. J., and Zieger, B. Mammalian septins nomenclature. Mol Biol Cell, *13:* 4111-4113, 2002.

82. Sorensen, A. B., Lund, A. H., Ethelberg, S., Copeland, N. G., Jenkins, N. A., and Pedersen, F. S. Sint1, a common integration site in SL3-3-induced T-cell lymphomas, harbors a putative proto-oncogene with homology to the septin gene family. J Virol, *74:* 2161-2168, 2000.

83. Hall, P. A. and Russell, S. E. The pathobiology of the septin gene family. J Pathol, *204:* 489-505, 2004.

84. McIlhatton, M. A., Burrows, J. F., Donaghy, P. G., Chanduloy, S., Johnston, P. G., and Russell, S. E. Genomic organization, complex splicing pattern and expression of a human septin gene on chromosome 17q25.3. Oncogene, *20:* 5930-5939, 2001.

85. Bennett, K. L., Karpenko, M., Lin, M. T., Claus, R., Arab, K., Dyckhoff, G., Plinkert, P., Herpel, E., Smiraglia, D., and Plass, C. Frequently methylated tumor suppressor genes in head and neck squamous cell carcinoma. Cancer Res, *68:* 4494-4499, 2008.

86. Devos, T., Tetzner, R., Model, F., Weiss, G., Schuster, M., Distler, J., Steiger, K. V., Grutzmann, R., Pilarsky, C., Habermann, J. K., Fleshner, P. R., Oubre, B. M., Day, R., Sledziewski, A. Z., and Lofton-Day, C. Circulating Methylated SEPT9 DNA in Plasma Is a Biomarker for Colorectal Cancer. Clin Chem, 2009.

87. Grutzmann, R., Molnar, B., Pilarsky, C., Habermann, J. K., Schlag, P. M., Saeger, H. D., Miehlke, S., Stolz, T., Model, F., Roblick, U. J., Bruch, H. P., Koch, R., Liebenberg, V., Devos, T., Song, X., Day, R. H., Sledziewski, A. Z., and Lofton-Day, C. Sensitive detection of colorectal cancer in peripheral blood by septin 9 DNA methylation assay. PLoS ONE, *3:* e3759, 2008.

88. Amir, S. and Mabjeesh, N. J. SEPT9_V1 protein expression is associated with human cancer cell resistance to microtubule-disrupting agents. Cancer Biol Ther, *6:* 1926-1931, 2007.

89. Ito, H., Iwamoto, I., Morishita, R., Nozawa, Y., Narumiya, S., Asano, T., and Nagata, K. Possible role of Rho/Rhotekin signaling in mammalian septin organization. Oncogene, *24:* 7064-7072, 2005.

90. Nagata, K. and Inagaki, M. Cytoskeletal modification of Rho guanine nucleotide exchange factor activity: identification of a Rho guanine nucleotide exchange factor as a binding partner for Sept9b, a mammalian septin. Oncogene, *24:* 65-76, 2005.

91. Veronesi, U., Boyle, P., Goldhirsch, A., Orecchia, R., and Viale, G. Breast cancer. Lancet, *365:* 1727-1741, 2005.

92. Cleator, S. and Ashworth, A. Molecular profiling of breast cancer: clinical implications. Br J Cancer, *90:* 1120-1124, 2004.

93. Nathanson, K. L., Wooster, R., and Weber, B. L. Breast cancer genetics: what we know and what we need. Nat Med, *7:* 552-556, 2001.

94. Russell, S. E. and Hall, P. A. Do septins have a role in cancer? Br J Cancer, *93:* 499-503, 2005.

95. Lofton-Day, C., Model, F., Devos, T., Tetzner, R., Distler, J., Schuster, M., Song, X., Lesche, R., Liebenberg, V., Ebert, M., Molnar, B., Grutzmann, R., Pilarsky, C., and Sledziewski, A. DNA methylation biomarkers for blood-based colorectal cancer screening. Clin Chem, *54:* 414-423, 2008.

96. Hanahan, D. and Weinberg, R. A. The hallmarks of cancer. Cell, *100:* 57-70, 2000.

97. Kleer, C. G., Cao, Q., Varambally, S., Shen, R., Ota, I., Tomlins, S. A., Ghosh, D., Sewalt, R. G., Otte, A. P., Hayes, D. F., Sabel, M. S., Livant, D., Weiss, S. J., Rubin, M. A., and Chinnaiyan, A. M. EZH2 is a marker of aggressive breast cancer and promotes neoplastic transformation of breast epithelial cells. Proc Natl Acad Sci U S A, *100:* 11606-11611, 2003.

98. Erson, A. E., Niell, B. L., DeMers, S. K., Rouillard, J. M., Hanash, S. M., and Petty, E. M. Overexpressed genes/ESTs and characterization of distinct amplicons on 17q23 in breast cancer cells. Neoplasia, *3:* 521-526, 2001.

99. Christiansen, J. J. and Rajasekaran, A. K. Reassessing epithelial to mesenchymal transition as a prerequisite for carcinoma invasion and metastasis. Cancer Res, *66:* 8319-8326, 2006.

100. Lacroix, M. and Leclercq, G. Relevance of breast cancer cell lines as models for breast tumours: an update. Breast Cancer Res Treat, *83:* 249-289, 2004.

101. Higgins, M. J. and Stearns, V. Understanding resistance to tamoxifen in hormone receptor-positive breast cancer. Clin Chem, *55:* 1453-1455, 2009.

102. Lakhani, S. R., Reis-Filho, J. S., Fulford, L., Penault-Llorca, F., van der Vijver, M., Parry, S., Bishop, T., Benitez, J., Rivas, C., Bignon, Y. J., Chang-Claude, J., Hamann, U., Cornelisse, C. J., Devilee, P., Beckmann, M. W., Nestle-Kramling, C., Daly, P. A., Haites, N., Varley, J., Lalloo, F., Evans, G., Maugard, C., Meijers-Heijboer, H., Klijn, J. G., Olah, E., Gusterson, B. A., Pilotti, S., Radice, P., Scherneck, S., Sobol, H., Jacquemier, J., Wagner, T., Peto, J., Stratton, M. R., McGuffog, L., and Easton, D. F. Prediction of BRCA1 status in patients with breast cancer using estrogen receptor and basal phenotype. Clin Cancer Res, *11:* 5175-5180, 2005.

103. Howell, A. The endocrine prevention of breast cancer. Best Pract Res Clin Endocrinol Metab, *22:* 615-623, 2008.

104. Rugo, H. S. The breast cancer continuum in hormone-receptor-positive breast cancer in postmenopausal women: evolving management options focusing on aromatase inhibitors. Ann Oncol, *19:* 16-27, 2008.

105. Putti, T. C., El-Rehim, D. M., Rakha, E. A., Paish, C. E., Lee, A. H., Pinder, S. E., and Ellis, I. O. Estrogen receptor-negative breast carcinomas: a review of morphology and immunophenotypical analysis. Mod Pathol, *18:* 26-35, 2005.

106. Taki, T., Ohnishi, H., Shinohara, K., Sako, M., Bessho, F., Yanagisawa, M., and Hayashi, Y. AF17q25, a putative septin family gene, fuses the MLL gene in acute myeloid leukemia with t(11;17)(q23;q25). Cancer Res, *59:* 4261-4265, 1999.

107. Turhan, N., Yurur-Kutlay, N., Topcuoglu, P., Sayki, M., Yuksel, M., Gurman, G., and Tukun, A. Translocation (13;17)(q14;q25) as a novel chromosomal abnormality in acute myeloid leukemia-M4. Leuk Res, *30:* 903-905, 2006.

108. Charames, G. S. and Bapat, B. Genomic instability and cancer. Curr Mol Med, *3:* 589-596, 2003.

109. Dey, P. Aneuploidy and malignancy: an unsolved equation. J Clin Pathol, *57:* 1245-1249, 2004.

110. Musacchio, A. and Salmon, E. D. The spindle-assembly checkpoint in space and time. Nat Rev Mol Cell Biol, *8:* 379-393, 2007.

111. Storchova, Z. and Kuffer, C. The consequences of tetraploidy and aneuploidy. J Cell Sci, *121:* 3859-3866, 2008.

112. Duensing, S. and Munger, K. Centrosome abnormalities, genomic instability and carcinogenic progression. Biochim Biophys Acta, *1471:* M81-88, 2001.

113. Perez de Castro, I., de Carcer, G., and Malumbres, M. A census of mitotic cancer genes: new insights into tumor cell biology and cancer therapy. Carcinogenesis, *28:* 899-912, 2007.

114. Glotzer, M. The molecular requirements for cytokinesis. Science, *307:* 1735-1739, 2005.

115. Shackney, S. E., Smith, C. A., Miller, B. W., Burholt, D. R., Murtha, K., Giles, H. R., Ketterer, D. M., and Pollice, A. A. Model for the genetic evolution of human solid tumors. Cancer Res, *49:* 3344-3354, 1989.

116. Hermsen, M., Postma, C., Baak, J., Weiss, M., Rapallo, A., Sciutto, A., Roemen, G., Arends, J. W., Williams, R., Giaretti, W., De Goeij, A., and Meijer, G. Colorectal adenoma to carcinoma progression follows multiple pathways of chromosomal instability. Gastroenterology, *123:* 1109-1119, 2002.

117. Duesberg, P., Rausch, C., Rasnick, D., and Hehlmann, R. Genetic instability of cancer cells is proportional to their degree of aneuploidy. Proc Natl Acad Sci U S A, *95:* 13692-13697, 1998.

118. Baretton, G., Vogt, T., Valina, C., Schneiderbanger, K., and Lohrs, U. [Prostate cancers and potential precancerous conditions: DNA cytometric investigations and interphase cytogenetics]. Verh Dtsch Ges Pathol, *77:* 86-92, 1993.

119. Rubin, E. M., DeRose, P. B., and Cohen, C. Comparative image cytometric DNA ploidy of liver cell dysplasia and hepatocellular carcinoma. Mod Pathol, *7:* 677-680, 1994.

120. Versele, M., Gullbrand, B., Shulewitz, M. J., Cid, V. J., Bahmanyar, S., Chen, R. E., Barth, P., Alber, T., and Thorner, J. Protein-protein interactions governing septin heteropentamer assembly and septin filament organization in Saccharomyces cerevisiae. Mol Biol Cell, *15:* 4568-4583, 2004.

121. Versele, M. and Thorner, J. Some assembly required: yeast septins provide the instruction manual. Trends Cell Biol, *15:* 414-424, 2005.

122. Douglas, L. M., Alvarez, F. J., McCreary, C., and Konopka, J. B. Septin function in yeast model systems and pathogenic fungi. Eukaryot Cell, *4:* 1503-1512, 2005.

123. Sisson, J. C., Field, C., Ventura, R., Royou, A., and Sullivan, W. Lava lamp, a novel peripheral golgi protein, is required for Drosophila melanogaster cellularization. J Cell Biol, *151:* 905-918, 2000.

124. Escuin, D., Kline, E. R., and Giannakakou, P. Both microtubule-stabilizing and microtubule-destabilizing drugs inhibit hypoxia-inducible factor-1alpha accumulation and activity by disrupting microtubule function. Cancer Res, *65:* 9021-9028, 2005.

125. Mabjeesh, N. J., Escuin, D., LaVallee, T. M., Pribluda, V. S., Swartz, G. M., Johnson, M. S., Willard, M. T., Zhong, H., Simons, J. W., and Giannakakou, P. 2ME2 inhibits tumor growth and angiogenesis by disrupting microtubules and dysregulating HIF. Cancer Cell, *3:* 363-375, 2003.

126. Hall, P. A., Todd, C. B., Hyland, P. L., McDade, S. S., Grabsch, H., Dattani, M., Hillan, K. J., and Russell, S. E. The septin-binding protein anillin is overexpressed in diverse human tumors. Clin Cancer Res, *11:* 6780-6786, 2005.

127. Joo, E., Surka, M. C., and Trimble, W. S. Mammalian SEPT2 is required for scaffolding nonmuscle myosin II and its kinases. Dev Cell, *13:* 677-690, 2007.

128. Derijard, B., Hibi, M., Wu, I. H., Barrett, T., Su, B., Deng, T., Karin, M., and Davis, R. J. JNK1: a protein kinase stimulated by UV light and Ha-Ras that binds and phosphorylates the c-Jun activation domain. Cell, *76:* 1025-1037, 1994.

129. Fan, M., Du, L., Stone, A. A., Gilbert, K. M., and Chambers, T. C. Modulation of mitogen-activated protein kinases and phosphorylation of Bcl-2 by vinblastine represent persistent forms of normal fluctuations at G2-M1. Cancer Res, *60:* 6403-6407, 2000.

130. Schwabe, R. F., Bradham, C. A., Uehara, T., Hatano, E., Bennett, B. L., Schoonhoven, R., and Brenner, D. A. c-Jun-N-terminal kinase drives cyclin D1 expression and proliferation during liver regeneration. Hepatology, *37:* 824-832, 2003.

131. Wisdom, R., Johnson, R. S., and Moore, C. c-Jun regulates cell cycle progression and apoptosis by distinct mechanisms. Embo J, *18:* 188-197, 1999.

132. Albanese, C., Johnson, J., Watanabe, G., Eklund, N., Vu, D., Arnold, A., and Pestell, R. G. Transforming p21ras mutants and c-Ets-2 activate the cyclin D1 promoter through distinguishable regions. J Biol Chem, *270:* 23589-23597, 1995.

133. Nelsen, C. J., Rickheim, D. G., Timchenko, N. A., Stanley, M. W., and Albrecht, J. H. Transient expression of cyclin D1 is sufficient to promote hepatocyte replication and liver growth in vivo. Cancer Res, *61:* 8564-8568, 2001.

134. Yang, K., Hitomi, M., and Stacey, D. W. Variations in cyclin D1 levels through the cell cycle determine the proliferative fate of a cell. Cell Div, *1:* 32, 2006.

135. Martin, L. G., Demers, G. W., and Galloway, D. A. Disruption of the G1/S transition in human papillomavirus type 16 E7-expressing human cells is associated with altered regulation of cyclin E. J Virol, *72:* 975-985, 1998.

136. Wulf, G. M., Ryo, A., Wulf, G. G., Lee, S. W., Niu, T., Petkova, V., and Lu, K. P. Pin1 is overexpressed in breast cancer and cooperates with Ras signaling in increasing the transcriptional activity of c-Jun towards cyclin D1. Embo J, *20:* 3459-3472, 2001.

137. Fu, M., Wang, C., Li, Z., Sakamaki, T., and Pestell, R. G. Minireview: Cyclin D1: normal and abnormal functions. Endocrinology, *145:* 5439-5447, 2004.

138. Spiliotis, E. T. and Nelson, W. J. Here come the septins: novel polymers that coordinate intracellular functions and organization. J Cell Sci, *119:* 4-10, 2006.

139. Nagata, K., Asano, T., Nozawa, Y., and Inagaki, M. Biochemical and cell biological analyses of a mammalian septin complex, Sept7/9b/11. J Biol Chem, *279:* 55895-55904, 2004.

140. Finley, R. L., Jr. and Brent, R. Interaction mating reveals binary and ternary connections between Drosophila cell cycle regulators. Proc Natl Acad Sci U S A, *91:* 12980-12984, 1994.

141. Gietz, R. D. and Schiestl, R. H. Applications of high efficiency lithium acetate transformation of intact yeast cells using single-stranded nucleic acids as carrier. Yeast, *7:* 253-263, 1991.

142. Gietz, R. D., Schiestl, R. H., Willems, A. R., and Woods, R. A. Studies on the transformation of intact yeast cells by the LiAc/SS-DNA/PEG procedure. Yeast, *11:* 355-360, 1995.

143. Raff, T., van der Giet, M., Endemann, D., Wiederholt, T., and Paul, M. Design and testing of beta-actin primers for RT-PCR that do not co-amplify processed pseudogenes. Biotechniques, *23:* 456-460, 1997.

144. Kalikin, L. M., George, R. A., Keller, M. P., Bort, S., Bowler, N. S., Law, D. J., Chance, P. F., and Petty, E. M. An integrated physical and gene map of human distal chromosome 17q24-proximal 17q25 encompassing multiple disease loci. Genomics, *57:* 36-42, 1999.

145. Drwinga, H. L., Toji, L. H., Kim, C. H., Greene, A. E., and Mulivor, R. A. NIGMS human/rodent somatic cell hybrid mapping panels 1 and 2. Genomics, *16:* 311-314, 1993.

146. Senapathy, P., Shapiro, M. B., and Harris, N. L. Splice junctions, branch point sites, and exons: sequence statistics, identification, and applications to genome project. Methods Enzymol, *183:* 252-278, 1990.

147. Kinoshita, M., Field, C. M., Coughlin, M. L., Straight, A. F., and Mitchison, T. J. Self- and actin-templated assembly of Mammalian septins. Dev Cell, *3:* 791-802, 2002.

148. Sui, L., Zhang, W., Liu, Q., Chen, T., Li, N., Wan, T., Yu, M., and Cao, X. Cloning and functional characterization of human septin 10, a novel member of septin family cloned from dendritic cells. Biochem Biophys Res Commun, *304:* 393-398, 2003.

149. Kissel, H., Georgescu, M. M., Larisch, S., Manova, K., Hunnicutt, G. R., and Steller, H. The Sept4 septin locus is required for sperm terminal differentiation in mice. Dev Cell, *8:* 353-364, 2005.

150. Thompson, A., Brennan, K., Cox, A., Gee, J., Harcourt, D., Harris, A., Harvie, M., Holen, I., Howell, A., Nicholson, R., Steel, M., and Streuli, C. Evaluation of the current knowledge limitations in breast cancer research: a gap analysis. Breast Cancer Res, *10:* R26, 2008.

151. Loman, N., Johannsson, O., Bendahl, P. O., Borg, A., Ferno, M., and Olsson, H. Steroid receptors in hereditary breast carcinomas associated with BRCA1 or BRCA2 mutations or unknown susceptibility genes. Cancer, *83:* 310-319, 1998.

152. Putti, T. C., Pinder, S. E., Elston, C. W., Lee, A. H., and Ellis, I. O. Breast pathology practice: most common problems in a consultation service. Histopathology, *47:* 445-457, 2005.

153. Teramoto, H., Crespo, P., Coso, O. A., Igishi, T., Xu, N., and Gutkind, J. S. The small GTP-binding protein rho activates c-Jun N-terminal kinases/stress-activated protein kinases in human kidney 293T cells. Evidence for a Pak-independent signaling pathway. J Biol Chem, *271:* 25731-25734, 1996.

154. Gonzalez, M. E., Makarova, O., Peterson, E. A., Privette, L. M., and Petty, E. M. Up-regulation of SEPT9_v1 stabilizes c-Jun-N-terminal kinase and contributes to its pro-proliferative activity in mammary epithelial cells. Cell Signal, *21:* 477-487, 2009.

155. Ganem, N. J., Storchova, Z., and Pellman, D. Tetraploidy, aneuploidy and cancer. Curr Opin Genet Dev, *17:* 157-162, 2007.